Alma Mater Studiorum - Università di Bologna

Wireless Networks for Body-Centric Communications

Tesi di:

Flavia Martelli

Coordinatore:

Chiar.mo Prof. Ing. **Alessandro Vanelli-Coralli**

Relatori:

Chiar.mo Prof. Ing. **Oreste Andrisano**

Chiar.mo Prof. Ing. **Roberto Verdone**

"If we knew what it was we were doing,
it would not be called research, would it?"
[Albert Einstein]

"Think, Believe, Dream, and Dare."
[Walt Disney]

Table of Contents

Contents

Abstract

Progress in miniaturization of electronic components and design of wireless systems paved the way towards ubiquitous and pervasive communications, enabling anywhere and anytime connectivity. Wireless devices present on, inside, around the human body are becoming commonly used, leading to the class of body-centric communications. The presence of the body with all its peculiar characteristics has to be properly taken into account in the development and design of wireless networks in this context.

This thesis addresses various aspects of body-centric communications, with the aim of investigating network performance achievable in different scenarios. The main original contributions pertain to the performance evaluation for Wireless Body Area Networks (WBANs) at the Medium Access Control layer: the application of Link Adaptation to these networks is proposed, Carrier Sense Multiple Access with Collision Avoidance algorithms used for WBAN are extensively investigated, coexistence with other wireless systems is examined. Then, an analytical model for interference in wireless access network is developed, which can be applied to the study of communication between devices located on humans and fixed nodes of an external infrastructure. Finally, results on experimental activities regarding the investigation of human mobility and sociality are presented.

Chapter 1

Introduction

This introductory chapter gives an overview of body-centric communications, being the central topic of the thesis. A particular focus is dedicated to Wireless Body Area Networks (WBANs), with the description of their main reference standards and of a related research project. Finally, the structure and main contributions of the work are outlined.

1.1 Body-Centric Communications

Wireless communication systems have become in the past two decades so widespread that nowadays they can be considered as part of everyday life in different contexts, such as homes, offices, factories, transports, schools, entertainment places. Thanks to advances in electronics, portable devices are becoming smaller and/or more powerful every day and they are carried around by people in every situation, leading to almost seamless and ubiquitous connectivity.

Research on Wireless Personal Area Networks (WPANs) began around the end of the last century, and the first applications considered were to replace the cables connecting electronic devices, such as the mouse with the Personal Computer (PC)

or the headset with the mobile phone. WPAN focus on the Personal Operating Space (POS), that is the space around a person or an object that typically extends up to 10 meters in all directions and envelops the person/object whether stationary or in motion [1]. Devices belonging to a POS may be worn, carried, or located near the human body; this class of devices includes, for example, laptop computers, cellular phones, Personal Digital Assistants (PDAs), handheld personal computers, microphones, headsets, bar code readers, sensors, and pagers.

The advent of miniaturized sensors and actuators for monitoring, diagnostic, and therapeutic functions, together with advances in wireless systems, paved the way towards WBANs [2], where the network scope is even more focused on the vicinity to the human body. The increasing attention that has been devoted to WBAN in the past years is certainly related to the potential impact that such a technology can have on our society, in supporting new medical and healthcare services, as well as a variety of applications in various fields, such as fitness and training, gaming, entertainment [3].

The general topic of the thesis are *body-centric communications*, also referred to as body or human-focused communications [4], which include all those communication processes between devices located in the proximity of the human body, and of which WBANs represent an important big subset. Therefore, the defining element of body-centric communications is the presence of the human body, where at least one of the devices involved in the communication has to be located. In the thesis, the human body will be considered in the totality of its distinctive aspects that may affect the communication processes, such as its effect on the propagation medium, the mobility of the subject, his or her social behaviour, even if not all the aspects will be always

taken into account simultaneously.

With respect to the position of the communicating devices, the following classification, graphically depicted in Fig. 1.1, can be drawn:

- *on-body communications*: all the devices are located on the body of the same person, most of the radio channel is on the surface of the body;

- *in-body communications*: at least one of the end-points of the communication link is implanted in the body, a significant part of the channel is thus inside the body (a further distinction could be made between *in-in* and *in-on* communications, if both devices, or only one of them, are situated inside the body);

- *off-body communications*: one of the devices is placed on the body, while the other one is located outside it, being an external device, such as a router or a gateway;

- *body-to-body communications*: the communication takes place between devices placed on the body of at least two different subjects.
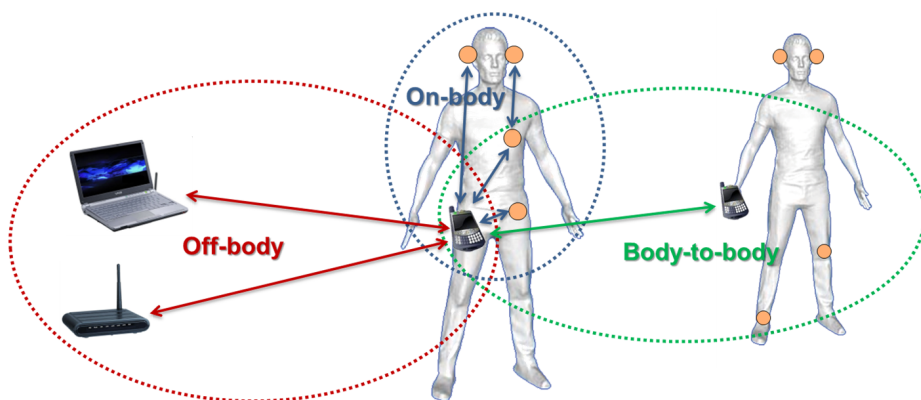
Figure 1.1: Body-centric communications.

The first three cases can be included in WBAN scope, as defined and specified by the IEEE 802.15 Task Group (TG) 6 [5], and the attention of the research community has been greatly devoted to them in the past years, from different perspectives. Focusing on the communication viewpoint, propagation issues have been extensively examined (e.g. [6,7]) and several Physical layer (PHY), Medium Access Control (MAC), and network layer solutions have been proposed and evaluated [8].

Body-to-body (B2B) communications, on the other hand, represent a quite recent research direction, which has received limited contributions so far, mainly with regard to the propagation channel [9,10]. B2B networks may be used to complement and extend existing infrastructure networks (e.g., cellular networks) by supporting capacity and improving achievable data rates. Besides, they allow the realisation of innovative services and applications that involve human users. In both cases, outcomes on forwarding and routing, coming from research on Delay Tolerant Networks (DTNs) and opportunistic techniques [11], could be fruitfully merged with the above mentioned studies to develop this kind of networks.

In the following subsections, a general overview on WBANs will be given, going into more details about its scope, definition, applications, requirements, and open issues. The reference standard air interface solutions, mainly IEEE 802.15.4 and IEEE 802.15.6, will also be thoroughly described. Finally, an outline of the Integrating Project (IP) WiserBAN will be presented, as a practical example of WBAN employment and since a significant part of the research of the thesis has been carried out in its framework.

1.1.1   Wireless Body Area Network Overview

A WBAN can be defined as a collection of low-power, miniaturized, invasive or non-invasive, lightweight devices with wireless communication capabilities that operate in the proximity of a human body [8]. These devices are often wireless sensor nodes that can monitor the human body functions and characteristics from the surrounding environment.

Wireless Body Sensor Network (WBSN) and Wireless Body Area Sensor Network (WBASN) are sometimes used as WBAN synonyms, to underline the presence of sensor nodes in the network.

On one hand, WBANs enable new applications and thus new possible markets with respect to WPANs and Wireless Sensor Networks (WSNs); on the other hand, the design is affected by several constraints that call for new paradigms and protocols. In some works from the literature, there is no strict distinction between WPANs and WBANs [3]. Actually, WBANs complement WPANs, target diverse applications and are limited to a shorter range (typically around 2 or 3 meters from a person) [12], while WPANs could extend up to 10 meters for high data rate applications and even to several tens of meters for low rate cases [13]. WPANs do not meet medical guidelines due to the proximity to human tissues and are not able to fully support Quality of Service (QoS) for the wide variety of applications WBANs are supposed to enable [14]. With respect to WSNs, the presence of the human body affects the radio wave propagation, leading to a specific and peculiar radio channel, which has to be properly accounted for in the design of the protocols [15]. The diversity of envisioned applications, which span from the medical field (vital signs monitoring, automatic drug delivery) to the entertainment, gaming, and ambient intelligence sectors, creates

a set of technical requirements with a wide variation in terms of expected performance metrics (e.g., throughput or delay) [16]. Therefore, scalable and flexible architectures and protocols are needed.

As already mentioned, the ability to deploy wireless devices on the human body leads to the opportunity of developing a large number of applications in several fields, which could be summarised as follows.

1) *Healthcare and medical services* – At a first glance, this could be the most promising field of application for a WBAN. Several non-intrusive sensors deployed in the human body allow the patients and the doctors to sample continuous waveform of biomedical signals in a remote and continuous way [17]. Events that require prompt assistance, like heart attack and epileptic seizure, can be detected and even foreseen thanks to the continued monitoring of the heart and brain activity respectively. WBANs can not only detect fatal events and anomalies, they can also improve the life style of hearing and visually impaired people, by means of earing aids or cochlear implants and artificial retina, respectively [18–20]. A non-exhaustive list of medical applications that can benefit from WBAN usage is: Electrocardiogram (ECG), Electroencephalogram (EEG), Electromyogram (EMG), drugs delivery, post operative monitoring, monitoring of vital parameters or body functions, such as temperature, respiration rate, glucose level, oxygen saturation, toxins, blood pressure [21, 22].

2) *Sport and fitness* – A real-time log of vital parameters like blood pressure, heart beat, blood oximetry, and posture can improve fitness and sport experience [23]. In this way the users can gather information concerning their sport activity and use them to prevent injuries and to plan future training to improve their performance.

Moreover, the central network controller (e.g., a smartphone) can be used to stream music to a pair of wireless headphones thus eliminating the wires, which are very annoying when performing physical activity.

3) *Entertainment and gaming* – WBANs can bring more realism in the user experience in the field of entertainment. Motion capturing techniques allow the tracking of the position of different body parts by means of a set of gyroscopes and accelerometers wirelessly connected to a central node and worn by the user. The real-time information about motion makes possible for the user the direct employment of his body as a controller in videogames. Moreover, film industry takes advantage of motion capture along with post production techniques to realise highly realistic digital movies where actors play the role of non-human subjects [24].

4) *Emergency services* – In the domain of public safety, WBANs can be used by firefighters, policemen, or rescue teams [14]. Police uniforms could for example incorporate vital signs, audiovisual communications and positioning functionality in the textiles. In addition to these functions, firefighters suits could also incorporate environmental sensors to measure parameters such as external temperature, carbon monoxide, and carbon dioxide levels, in order to warn if a life threatening situation is detected. Paramedics uniforms would also be able to discover and query patient WBANs and link BAN data with the electronic medical record. Audio-visual communications integrated into the paramedic uniforms would enable telepresence and augmented reality experience of the scene for hospital staff. Similarly, disaster coordinators could benefit from remote viewing of the scene using the same technology [25].

5) *Military and Defence* – Network-Enabled Capability is the name of the NATO long term program aimed to achieve enhanced military effect through the use of information systems [26]. New capabilities added by a WBAN will improve the performance of soldiers engaged in military operations at both individual and squad levels. At individual level, a set of sensors can monitor vital parameters and provide information about the surrounding environment in order to avoid threats, whereas information taken at squad level will make the commander able to better coordinate the squad actions and tasks. Spatial localization techniques and communications between different WBANs play an important role in this field, as well as security in order to prevent sensitive information from being caught by the enemies [27].

6) *Industrial* – In the industrial framework WBANs can improve the safety conditions of workers, for example monitoring their movements and the surrounding environment in order to prevent the exposure to toxic gasses and radiations, or checking the shocks and vibrations human machine operators are subject to [28]. The deployment of WBANs is not limited to human subjects, robotics arms can also be equipped with wireless nodes whose primary goal is to track their fine grained movements. Interaction between machines and workers can as well be improved by the exploitation of inter-WBAN communication.

7) *Lifestyle applications* – In this last domain several applications could be envisioned, such as emotion detection, ambient intelligence, smart keys, identification and authentication. For instance, WBANs can be used to monitor people vital signs as a basis to develop systems that adapt the surrounding environment depending on the user condition and emotional status (music, lights, heating/cooling).

A secure authentication system could use both physiological and behavioral biometrics schemes collected by a WBAN, like facial patterns, finger prints and iris recognition.

Due to this broad range of possible applications, developing WBAN technologies is a challenging task. Main WBAN requirements are detailed hereafter, following [16] guidelines.

1) *Range and Topology* – The communication range should not be larger than few meters ($3 \div 6$ m) for most of the applications. Thus, a simple star topology is usually enough; however, the human body can represent an obstacle for the radio propagation especially for the implanted nodes. In this case, a multihop communication must be established. The number of nodes forming the WBAN may range from two (e.g., glucose meter) to few hundreds (e.g., accelerometers and gyroscopes on a robotic arm) and can vary at run time. Therefore the network should implement reliable association and disassociation procedures to allow nodes to take part and leave the WBAN as needed by the application.

2) *Bit rate* – The bit rate requirement varies on a very broad range depending on the application and the type of data to be transmitted. It goes from less than 1 kbit/s (e.g., temperature monitoring) to 10 Mbit/s (e.g., video streaming).

3) *Quality of Service* – High level of QoS should be guaranteed in medical and military applications. The critical factor is the reliability of the transmission, meaning that appropriate error detection and correction methods, interference avoidance methods, or any other suitable technique should be implemented at MAC and PHY layers. QoS provisions should be flexible so that they can be tailored to suit

9

specific application needs.

4) *Time constraints* – Real time communication is required for some applications. Reliability, latency, and jitter (variation of one-way transmission delay) shall be supported for applications that need them. The latency in medical applications should be less than 125 ms [16]. The latency in non-medical applications should be less than 250 ms and jitter should be less than 50 ms [16]. Capability of providing fast (< 1 s) and reliable reaction in emergency situations and for alarm messages, which have higher priority than others, shall be provided after the network has been set up.

5) *Coexistence* – Coexistence between WBANs, coexistence between WBAN and other wireless technologies, and coexistence of WBAN in medical environments shall be addressed. The devices must be able to operate in high noise, high multi-path and dynamic environment. In particular, implantable and wearable WBANs should gracefully coexist in-and-around the body. Medical applications may be given higher priority than others when bandwidth is scarce.

6) *Form Factor* – Size constraints can be stringent; the most critical aspect in this regard is to fit the antenna and the battery into a very tight case while providing good radiation property and lifetime. This is obviously true for implantable devices; on the other hand, when a WBAN node is designed to be worn, flexibility and stretchability may be more relevant in order to be comfortable for the user, especially in sport and fitness applications.

7) *Antenna* – As already stated, antenna design can be very critical. This holds not only because of the size constraints, but also due to the presence of the human

body, which represents an obstacle for the radio wave propagation and affects antenna radiation properties.

8) *Security* – Security and privacy are of primary importance especially for what concerns medical and military applications. Secure authentication processes (e.g. biometric identification based mechanism) and data encryption mechanisms should always be implemented. The latter usually requires high computational resources and storage, thus, an energy efficient and lightweight implementation is essential. The inability of the user to provide key information when needed must be taken into account (devices, for example, should be accessible to paramedics/medics in a trauma condition; however, in such situations, the unconscious user may not be able to provide authentication information).

9) *Power Consumption* – The power consumption requirement depends on the nature of the application. However, WBAN devices are generally battery powered and the battery lifetime is required to be in the order of years for implanted devices (e.g., pacemakers require at least five years). Ultra-low power design for radio transceivers is essential, as well as power-wise MAC design.

In order to meet these technical requirements, a lot of research effort has been carried out in the last years from different perspectives, but some design issues still remain open or to be fully solved. The first five aspects underlined above certainly guided the development of protocols for PHY, MAC, and network layers. Several proposals and studies can be found in the literature, as it will be more detailed in Chapter 2.

Advances in integrated circuit design and miniaturization of components strive

to realise devices with proper form factors to be implanted or comfortably worn. Similarly, researches on miniature antennas are leading to more efficient solutions [29].

Security has to be addressed in terms of privacy, confidentiality, authentication, authorisation, and integrity [2]. Since conventional mechanisms are not suitable for WBANs, due to several reasons (limited processing power, memory, energy, etc.), novel lightweight and resource-efficient methods are being developed [30, 31]. A promising solution in this context is the use of biometrics [32].

As far as power consumption is concerned, it is a requirement that has to be accounted for in the design of all WBAN aspects. On one side, proper design of circuits and transceivers is needed to ensure low current consumption. On the other side, protocols have to be energy-efficient. A common technique for the latter aim, which may come at the expense of end-to-end delay, is the duty cycling of the devices. In this way, devices are allowed to be in sleep mode (transceiver and CPU shut down) for most of the time. This is effective for applications that require infrequent transmissions; however, a proper trade-off between delay and power consumption should be found. Energy scavenging or harvesting could also be an interesting option to prolong nodes lifetime. In the WBAN context, indeed, energy scavenging from body sources such as heat [33] and movements [34] seems very well suited.

Besides these technical requirements, some social challenges and economic concerns should also be overcome to allow practical WBAN widespread adoption [35]. Value and ease of use perceived by the users are of foremost importance: WBAN must improve quality of life being unobtrusive, ergonomic, easy to put on, and even stylish. Once developed, WBAN systems will likely involve numerous stakeholders (users, caregivers, researchers, etc.), creating complex relationships, which can raise

ownership and liability issues. Questions such as "who will pay for WBAN systems?", "who will own WBAN data?", "who is liable for damages involving WBAN?" should be answered to protect all interests and to promote WBAN adoption and diffusion.

1.1.2 Reference Standards

IEEE 802.15.4

IEEE 802.15.4 wireless technology [36] is a short-range communication system intended to provide applications with relaxed throughput and latency requirements in WPAN. The key features of IEEE 802.15.4 wireless technology are low complexity, low cost, low power consumption, low data rate transmissions, to be supported by either fixed or moving cheap devices. The main field of application of this technology is the implementation of WSNs. The IEEE 802.15 TG 4 [37] focuses on the standardization of the bottom two layers of the International Organization for Standardization (ISO)/Open System Interconnection (OSI) reference protocol stack, namely the PHY and MAC layers. As for the upper layers, one of the most used solution is the ZigBee protocol stack, specified by the industrial consortium ZigBee Alliance [38]. A different possible approach, aiming at using 802.15.4 standard in IP-based networks, has been specified by the Internet Engineering Task Force (IETF) as 6LowPAN (IPv6 over Low power WPAN).

The IEEE 802.15.4 PHY operates in three different unlicensed bands (with different modalities) according to the geographical area where the system is deployed. However, Direct Sequence Spread Spectrum (DSSS) is mandatory to reduce the interference level in shared unlicensed bands.

The PHY provides the interface with the physical medium. It is in charge of

radio transceiver activation and deactivation, energy detection, link quality, clear channel assessment, channel selection, and transmission and reception of the message packets. Moreover, it is responsible for establishment of the Radio Frequency (RF) link between two devices, bit modulation and demodulation, synchronisation between the transmitter and the receiver, and, finally, for packet level synchronisation.
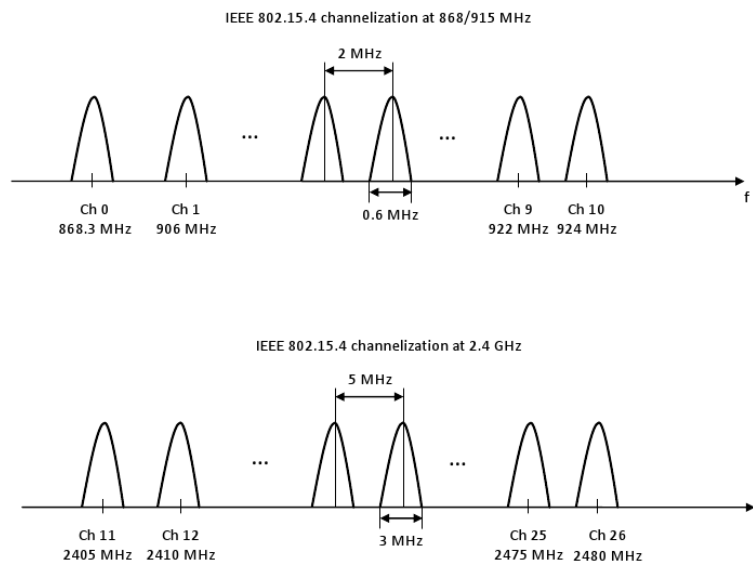
Figure 1.2: IEEE 802.15.4 standard channelization.

The standard specifies a total of 27 half-duplex channels across the three frequency bands, whose channelization is depicted in Fig. 1.2 and is organized as follows:

- The 868 MHz band, ranging from 868.0 to 868.6 MHz and used in the European area, implements a raised-cosine-shaped Binary Phase Shift Keying (BPSK) modulation format, with DSSS at a chip-rate of 300 kchip/s (a pseudo-random sequence of 15 chips transmitted in a 25 μs symbol period). Only a single channel with a data rate of 20 kbit/s is available.

- The 915 MHz band, ranging between 902 and 928 MHz and used in the North American and Pacific area, implements a raised-cosine-shaped BPSK modulation format, with DSSS at a chip-rate equal to 600 kchip/s (a pseudo-random sequence of 15 chips is transmitted in a 50 μs symbol period). Ten channels with rate of 40 kbit/s are available.

- The 2.45 GHz Industrial, Scientific, and Medical (ISM) band, which extends from 2400 to 2483.5 MHz and is used worldwide, implements a half-sine-shaped Offset Quadrature Phase Shift Keying (O-QPSK) modulation format, with DSSS at 2 Mchip/s (a pseudo-random sequence of 32 chips is transmitted in a 16 μs symbol period). Sixteen channels with data rate equal to 250 kbit/s are available, whose center frequencies are defined by $f_c = 2405 + 5 \cdot (k-11)$ [MHz], $k = \{11, \ldots, 26\}$ [36].

Focusing on the latter band, which will be the reference one in the rest of the thesis, the process to convert bits to the final signal is represented in Fig. 1.3. A 16-ary quasi-orthogonal modulation technique is applied: during each data symbol period, four information bits are used to select one of 16 nearly orthogonal 32-chip long pseudo-random sequences to be transmitted. The sequences for successive symbols are concatenated, and the resulting chip sequence is modulated onto the carrier using O-QPSK with half-sine pulse shaping, which is equivalent to Minimum Shift Keying (MSK) modulation [39].

According to the standard, transmission is organized in frames, which can differ according to the relevant purpose. In particular, there are four frame structures, each designated as a Physical layer Protocol Data Unit (PPDU): a beacon frame, a data frame, an acknowledgment (ACK) frame, and a MAC command frame. As
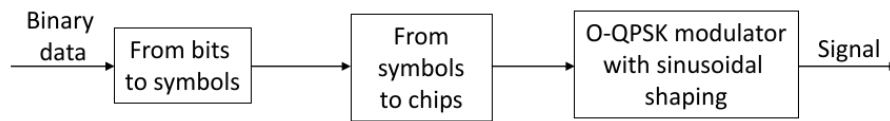
Figure 1.3: IEEE 802.15.4 modulation and spreading functional block diagram for the 2.45 GHz band.

shown in Fig. 1.4, they are all structured with the Synchronization Header (SHR), which allows a receiving device to synchronise and lock onto the bit stream, the Physical Header (PHR), which contains frame length information, and the Physical Service Data Unit (PSDU), which carries the MAC Payload Data Unit (MPDU). The latter is constructed with the MAC Header (MHR), which comprises frame control, sequence number, address information, and security related data, the MAC Footer (MFR), which contains a frame check sequence (FCS), and the MAC Service Data Unit (MSDU), which contains information specific to the frame type, except for the ACK frame, which does not contain an MSDU.

The beacons are used by the WPAN coordinator to synchronise the attached devices, to identify the WPAN, and to describe the structure of the superframes, which are used to access the channel, as will be explained below. The data frames are used to transmit application data, while the ACK frame is optionally used for confirming successful frame reception. The command frame is used for handling all MAC control transfers.

The MAC layer provides access control to a shared channel and reliable data delivery. IEEE 802.15.4 uses a protocol based on a Carrier Sense Multiple Access with Collision Avoidance (CSMA/CA) algorithm, which requires listening to the channel

2 bytes	1 bytes	variable (0-20 bytes)	variable (0-14 bytes)	variable length	2 bytes
Frame control	Sequence number	Addressing fields	Auxiliary security header	MAC Payload	FCS
MHR				MSDU	MFR
MPDU					

4 bytes	1 byte	1 byte	variable length (5-127 bytes)
Preamble	SFD	Frame length	PHY Payload
SHR		PHR	PSDU
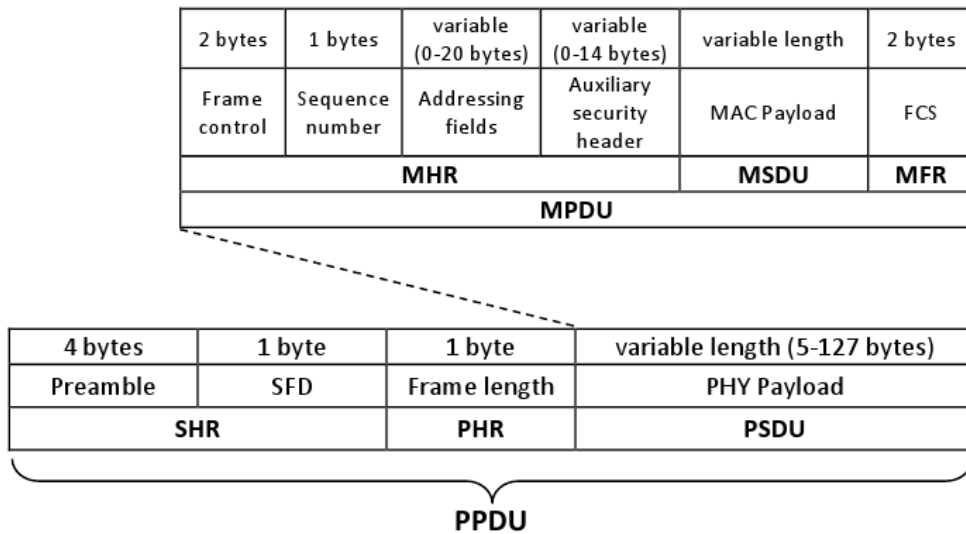
PPDU

Figure 1.4: IEEE 802.15.4 PPDU format.

before transmitting to reduce the probability of collisions with other ongoing transmissions.

The main functions performed by the MAC layer are: association and disassociation, security control, optional star network topology functions, such as beacon generation and Guaranteed Time Slots (GTSs) management, generation of ACK frames (if used), and, finally, application support for the two possible network topologies described in the standard, that are the star topology and the peer-to-peer one.

IEEE 802.15.4 defines two different operational modes, namely beacon-enabled and non beacon-enabled, which correspond to two different channel access mechanisms. In the beacon-enabled case, the access to the channel is managed through a superframe, starting with the beacon packet, transmitted by the network coordinator. The superframe is subdivided into three parts: a Contention Access Period (CAP),

17

during which nodes use a slotted CSMA/CA, a Contention Free Period (CFP), containing a number of GTSs, that can be allocated by the coordinator to specific nodes with stringent requirements, and an inactive part. The coordinator may allocate up to seven GTSs, but a sufficient portion of the CAP must remain for contention-based access. The minimum CAP duration is equal to 440 T_s, being T_s the symbol time (its duration depends on the band used). An example of superframe structure is shown in Fig. 1.5.
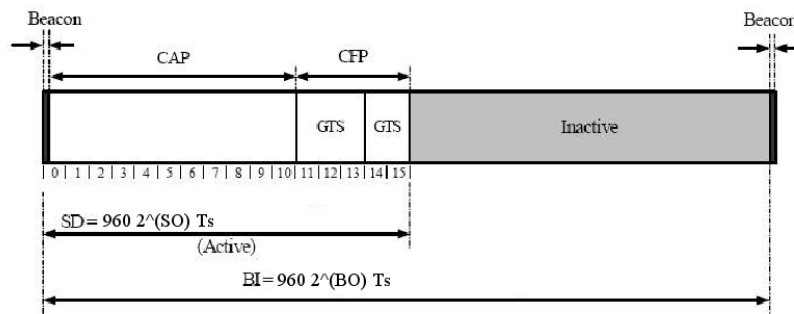
Figure 1.5: Example of IEEE 802.15.4 superframe structure [36].

The duration of the active part of the superframe, containing CAP and CFP, is called superframe duration (SD), and it can be expressed as $SD = 960 \cdot 2^{SO} \cdot T_s$, where SO is the superframe order, an integer parameter ranging from 0 to 14. The duration of the whole superframe, i.e. the interval of time between two successive beacons, is called beacon interval (BI), and it can be expressed as $BI = 960 \cdot 2^{BO} \cdot T_s$, where BO is the beacon order, an integer parameter ranging from 0 to 14. Note that BO must not be smaller than SO.

The CSMA/CA algorithm used in the CAP portion of the superframe is implemented using units of time called backoff periods: a backoff period has a duration of

320 μs.

Each device shall maintain three variables for each transmission attempt: NB, CW, and BE. NB is the number of times the algorithm was required to backoff while attempting the current transmission; it is initialized to zero before each new transmission attempt and its maximum value is NB_{max}. CW is the contention window length, defining the number of backoff periods that need to be clear of channel activity before the transmission can start; its initial value is equal to 2. BE is the backoff exponent, which is related to how many backoff periods a device shall wait before attempting to assess the channel; its initial value is BE_{min} and its maximum value is BE_{max}.

Fig. 1.6 illustrates the steps of the CSMA/CA algorithm. When using slotted CSMA/CA, the MAC layer shall first initialize NB, CW, and BE, and then locate the boundary of the next backoff period [step (1)]. Any activity is delayed (backoff state) for a random number of backoff periods in the range $[0, 2^{BE} - 1]$ [step (2)]. Then, channel sensing is performed for one backoff period [step (3)]. If the channel is assessed to be busy [step (4)], CW is reset to 2, while NB and BE are incremented by one, ensuring that BE is not larger than BE_{max}. If the value of NB is less than or equal to NB_{max}, the algorithm shall return to step (2). Otherwise, the algorithm will unsuccessfully terminate, meaning that the node does not succeed in accessing the channel. If the channel is assessed to be idle [step (5)], the CW is decremented by one. If $CW > 0$, the algorithm shall return to step (3), otherwise the transmission of the frame may start on the boundary of the next backoff period.

In the non beacon-enabled mode, on the other hand, nodes use an unslotted
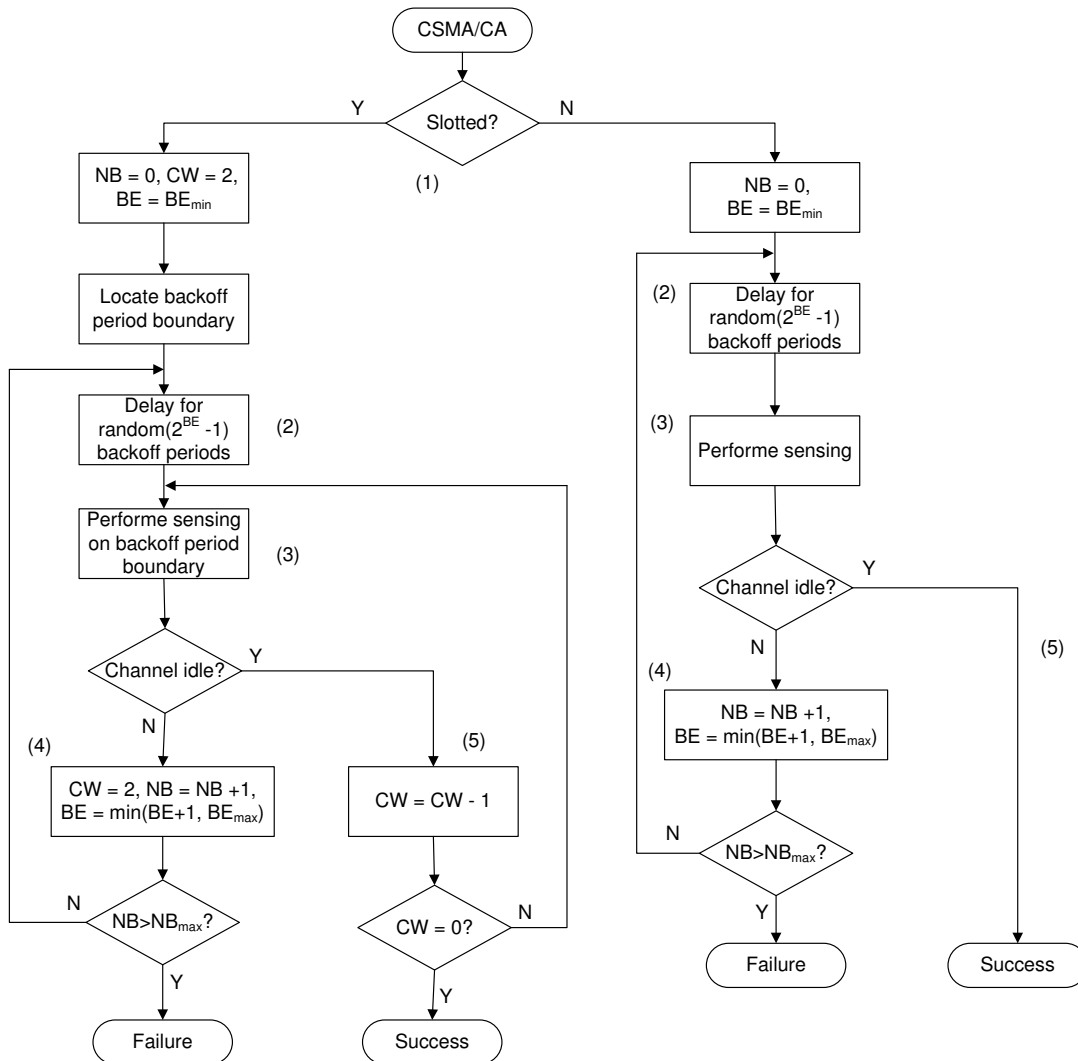
Figure 1.6: IEEE 802.15.4 CSMA/CA algorithm [36].

CSMA/CA protocol to access the channel and transmit their packets and no super-frame structure is defined. Its steps are also shown in Fig. 1.6. The main differences between the slotted algorithm and the unslotted one are that in the latter only one sensing phase should be performed, and that the backoff periods of devices are not related in time to each other. In the former, instead, all backoff periods are aligned with the superframe slot boundaries, i.e., the start of the first backoff period of each device is aligned with the start of the beacon transmission, and transmissions may start only at the beginning of backoff boundaries.

The description given above refers to IEEE 802.15.4 standard as defined in its 2006 version [36]. During these last years, several amendments have been issued to complement and enhance its applicability, as briefly summarised in Table 1.1.

Among these amendments, it is worth mentioning IEEE 802.15.4e [40], which presents new MAC layer behaviors to better support industrial markets. Timeslotted Channel Hopping (TSCH), targeting application domains such as process automation (oil and gas industry, food, beverage, chemical, pharmaceutical products, water treatments, green energy production, climate control), uses time synchronised communication and channel hopping to provide network robustness through spectral and temporal redundancy. Instead of using superframes, communication resources are broken up into timeslots that are organized into repeating slotframes. According to Low Latency Deterministic Networks (LLDN), designed for factory automation application domains (automotive manufacturing, robots, overhead cranes, milling machines, automated dispensers, airport logistics, automated packaging), where very low latency (transmission of sensor data in 10 ms) and many sensors per PAN coordinator (in the order of hundreds) are strongly required, a fine granular

Table 1.1: IEEE 802.15.4 amendments [37].

TG	Aim	Amendment		Status
		PHY	**MAC**	
15.4a	Alternative PHYs (IR-UWB and CSS) supporting high throughput, ultra low power consumption, high precision ranging and location	✓	✓	802.15.4a-2007 Amendment
15.4c	Chinese regulatory changes for WPAN channels (314-316, 430-434, and 779-787 MHz)	✓		802.15.4c-2009 Amendment
15.4d	New frequency allocation (950-956 MHz) in Japan	✓		802.15.4d-2009 Amendment
15.4e	Better support to industrial markets and compatibility with Chinese WPAN		✓	802.15.4e-2012 Amendment
15.4f	Active RFID system	✓	✓	802.15.4f-2012 Amendment
15.4g	Smart metering utility network	✓	✓	802.15.4g-2012 Amendment
15.4j	Medical BAN band (2360-2400 MHz)	✓		802.15.4j-2012 Amendment
15.4k	Critical infrastructure monitoring devices	✓		Latest draft in January 2013
15.4m	Operation in the available TV white spaces	✓	✓	First draft in November 2012
15.4n	Medical bands in China (174-216, 407-425, and 608-630 MHz)	✓	✓	TG approved in March 2012
15.4p	Applications specific to rail and rail transit	✓	✓	TG approved in April 2012

deterministic Time Division Multiple Access (TDMA) is used to access the channel, through an enhanced superframe specification. For general industrial and commercial application domains cited by Chinese WPAN regulations (process and factory automation, smart metering, home automation, smart building, entertainment, healthcare monitoring, telemedicine), Deterministic and Synchronous Multi-channel Extension (DSME) has been defined: GTSs use has been extended towards a multi-channel, multi-superframe, mesh mechanism for deterministic latency, flexibility, and scalability. Two channel diversity modes (channel adaptation and channel hopping) have also been introduced for robustness and reliability in dynamic channel conditions.

Moreover, a low-energy protocol has been specified [40], which is suitable for all application domains, to allow very low duty cycle devices to send ad hoc data using minimal amounts of energy. Two possible mechanisms are described: coordinated sampled listening, suitable for applications with relatively low latency requirements (i.e. $< 1\,\mathrm{s}$), and receiver initiated transmissions, applicable to situations where a high latency (e.g., tens of seconds) is tolerated.

IEEE 802.15.6

IEEE 802.15 TG 6 was established in November 2007 to realise a standard specifically designed for WBAN, namely Standard IEEE 802.15.6, whose final version was released in February 2012 [41].

The standard defines PHY and MAC layers optimised for short range transmissions in, on, or around the human body. The purpose is to support a low complexity, low cost, ultra-low power, and high reliable wireless communication for use in close

proximity to, or inside, a human body (but not limited to humans), to serve a variety of applications both in the medical/healthcare and in the non medical fields.

The broad range of possible application fields in which WBANs could be used leads to an equally wide variety of system requirements that have to be met. Hence, the definition of a unique PHY layer solution could not be appropriate, and three different alternatives are then proposed in the standard [41] (see Fig. 1.7):

I) *Narrowband PHY:* A compliant device shall be able to support transmission and reception in at least one of the following optional frequency bands:

- 402-405 MHz: Medical Implant Communication System (MICS) band, it is widely accepted although the possible bandwidth is limited;

- 420-450 MHz: Wireless Medical Telemetry System (WMTS) band, available in Japan;

- 863-870 MHz: WMTS band, available in Europe;

- 902-928 MHz: ISM band, it is available to be used without licence in North America, Australia, and New Zealand;

- 950-958 MHz: available in Japan;

- 2360-2400 MHz: newly proposed band to be used for WBANs applications;

- 2400-2483.5 MHz: ISM band, it is available worldwide, but there could be issues of coexistence with other wireless systems that use the same band.

II) *Ultra Wideband (UWB) PHY:* UWB band is divided into two frequency groups: low band (3.25-4.75 GHz) and high band (6.6-10.25 GHz), both of them are subdivided into operating channels of 500 MHz bandwidth each. The low power

levels used in UWB make this particular band very appealing to be used in WBAN applications, where the human safety and the coexistence aspects with other communication systems are primary issues to deal with. UWB PHY is then specifically designed to offer robust performance for high quality, low complexity, and ultra low power operations.

III) *Human Body Communications (HBC) PHY:* this PHY solution uses the human body as communication media. The band of operation is centred at 21 MHz with a bandwidth of 5.25 MHz.
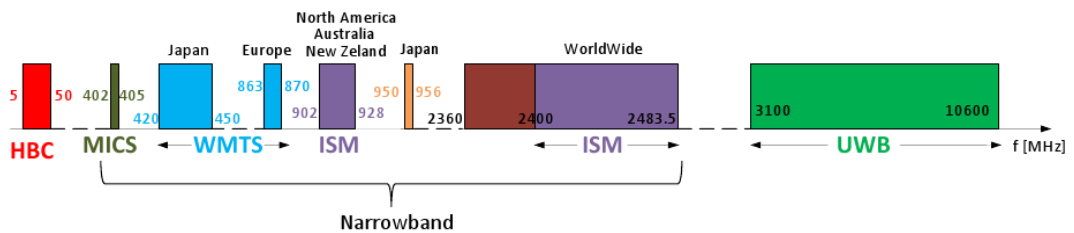
Figure 1.7: IEEE 802.15.6 possible bands of operation.

In the 2.45 GHz band, which will be the reference band in the following of the thesis, 79 RF channels are defined, with a bandwidth of 1 MHz each. Four possible information data rates are specified, which are obtained as combinations of different modulations (from the Differential Phase Shift Keying (DPSK) family), coding, and spreading. Details are reported in Table 1.2. Either Differential Binary Phase Shift Keying (DBPSK) or Differential Quadrature Phase Shift Keying (DQPSK) modulations are used, with BCH code, and a square root raised cosine (SRRC) pulse shape.

IEEE 802.15.6 PPDU is composed of three main components, as illustrated in

Table 1.2: IEEE 802.15.6 modulation parameters for the 2.45 GHz band [41].

Packet component	Modulation	Symbol rate	Code rate	Spreading factor	Information data rate
PLCP header	$\pi/2$-DBPSK	600 ksymb/s	19/31	4	91.9 kbit/s
PSDU	$\pi/2$-DBPSK	600 ksymb/s	51/63	4	121.4 kbit/s
PSDU	$\pi/2$-DBPSK	600 ksymb/s	51/63	2	242.9 kbit/s
PSDU	$\pi/2$-DBPSK	600 ksymb/s	51/63	1	485.7 kbit/s
PSDU	$\pi/4$-DQPSK	600 ksymb/s	51/63	1	971.4 kbit/s

Fig. 1.8: the Physical Layer Convergence Protocol (PLCP) preamble, with the purpose to aid the receiver in packet detection, timing synchronisation and carrier-offset recovery, the PLCP header, used to convey information about PHY and MAC parameters needed to decode the PSDU, and the PSDU itself. The PSDU is formed by concatenating the MAC header with the MAC payload and the FCS.

MAC Header	MAC Frame Payload	FCS
7 bytes	0 − 255 bytes	2 bytes

PLCP Preamble	PLCP Header	PSDU
90 bits	31 bits	Variable length
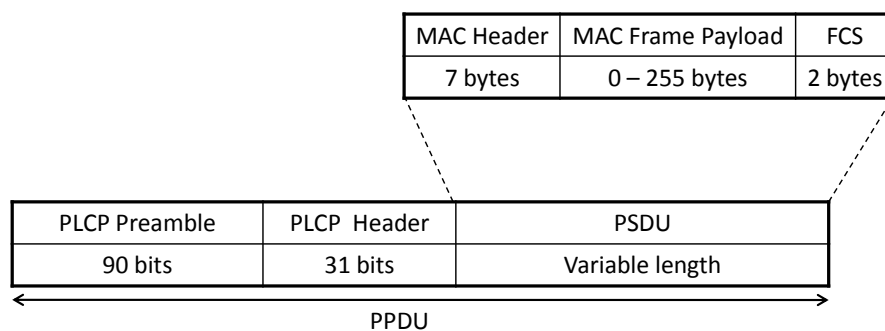
PPDU

Figure 1.8: IEEE 802.15.6 PPDU format [41].

The PLCP is transmitted at a specific header data rate, while the PSDU is transmitted using one of the four possible information data rates, as reported in Table 1.2.

Three frame types are defined: management, control, and data. The first includes beacons and frames used for association and security procedures. The second comprises ACKs and poll frames, while the last type is used to transmit application data.

Even if different PHYs are proposed in the standard, just a single MAC protocol is specified. In order to support different applications and data flow types (i.e. continuous, periodic, non-periodic, and burst), each one characterised by specific performance requirements, the MAC protocol should be as versatile as possible, combining both contention-based and time division-based access techniques [42].

The standard provides several priority values in order to diversify and prioritise the medium access of data and management type frames, according to the payload type contained (e.g., background data, video traffic, medical data, or emergency traffic; for more details refer to the standard [41]).

A WBAN coordinator could decide whether to operate in one of the following three access modes:

a) *Beacon mode with beacon periods (superframes)*: the coordinator establishes a common time base by sending beacon packets that define the beginning of an active beacon period. It shall also divide each active superframe into applicable access phases, ordering them as shown in Fig. 1.9, and defining their specific duration. The length of any phase may be set to zero, except for Random Access Phase (RAP) 1, which must have a minimum guaranteed duration. The coordinator may also maintain inactive superframes where it transmits no beacons and provides no

access phases, if there are no allocation intervals scheduled in those superframes.
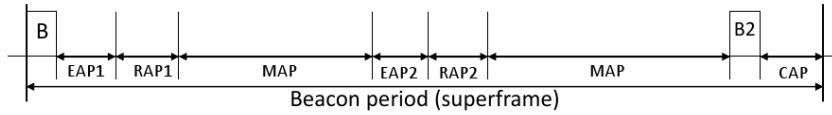
Figure 1.9: IEEE 802.15.6 superframe structure for beacon mode access [41].

During the Managed Access Phase (MAP), the coordinator may arrange scheduled uplink, downlink, and bilink allocation intervals, or it may provide unscheduled bilink allocation intervals or even improvise immediate polled and posted allocation intervals. A poll indicates a control frame sent by the WBAN coordinator to grant an immediate polled allocation (non recurring time interval for uplink traffic), or to inform a node of a future poll or post. A post, instead, is a management or data type frame sent by the coordinator to a node to inform of a posted allocation, which is a non recurring time interval that the coordinator grants to itself for downlink traffic exchange. Further details on polled and posted allocation techniques can be found in [41].

In Exclusive Access Phase (EAP) 1 and EAP2, RAP1 and RAP2, and CAP, the allocation process may take place only by contention between nodes, using CSMA/CA or Slotted ALOHA based random access methods.

In CSMA/CA, time is divided into slots, whose duration is equal to 145 μs. When a node has data to be sent, it randomly chooses a backoff counter (BC) in the interval $[1, \text{CW}]$, where $\text{CW} \in [\text{CW}_{\min}, \text{CW}_{\max}]$. The values of $\text{CW}_{\min}$ and $\text{CW}_{\max}$ depend on the user priority. If the channel has been sensed as idle for a Short Inter Frame Spacing ($pSIFS = 75\,\mu$s), the node decrements its BC by one for each idle

slot that follows. Once the BC has reached zero, the node can transmit its frame. The CW is doubled every two failures, ensuring that it does not become larger than CW_{max}. If the channel is found busy, the BC is locked until the channel becomes idle again for *pSIFS*.

As for the Slotted ALOHA technique, time is divided into slots whose duration should be set depending on the length of the frames that have to be transmitted. Each node wishing to transmit a frame obtains a contended allocation in the current slot if $z \leq CP$, where z is a random value in the interval $[0, 1]$, newly drawn for every attempt, and CP is the Contention Probability, set according to the following strategy. If the node did not obtain any contended allocation previously or succeeded in the last contended allocation it had obtained, it shall set the CP to CP_{max} (parameter that depends on the user priority). If the node transmitted a frame requiring no ACK, or the ACK was received at the end of its last contended allocation, it shall keep the CP unchanged. If the node failed in the last contended allocation it had obtained, it shall halve the CP value every two failed attempts, ensuring that it does not become smaller than CP_{min}.

b) *Non-beacon mode with superframes*: In this mode a coordinator may have only a MAP access phase in any superframe, and it may organise the access to the medium as explained above for the MAP phases.

c) *Non-beacon mode without superframes*: A WBAN coordinator may provide unscheduled bilink allocation interval. After determining that the next frame exchange will take place in non-beacon mode without superframe, a node shall treat any time interval as a portion of EAP1 or RAP1 and employ CSMA/CA based

random access to obtain a contended allocation [41].

Other Candidate Technologies

A brief overview of Bluetooth, low-power Wi-Fi, and ANT systems is given in this section, since they can be considered candidate technologies for WBAN applications in the 2.45 GHz band [2].

Bluetooth wireless technology is a short-range communications system intended to replace the cable(s) connecting portable and/or fixed electronic devices. The key features of Bluetooth are robustness, low power consumption, and low cost [43]. There are two main core configurations of Bluetooth technology systems: Basic Rate (BR), with optional Enhanced Data Rate (EDR), and Low Energy (LE). BR is the 'classic' Bluetooth, which allows a bit rate up to 3 Mbit/s with EDR. The LE system includes features designed to realise products characterised by lower current consumption, lower complexity, and lower cost than BR/EDR. The LE system is also designed for use cases and applications with lower data rates and duty cycles. LE aims at small and cheap devices, powered by button-cell batteries, such as wireless sensor devices, for several applications: sports and fitness (sport equipment and monitoring devices, speedometer, heart rate meter, pedometer), healthcare and illness treatment (weight scale, blood pressure monitor, glucose meter, pulse oximeter), home automation and entertainment (remote controls, home sensors and switches), automotive (tyre pressure monitoring, parking assistant, keyless entry), watch/wrist wearable devices (music players and mobile phones remote controls, proximity detection).

Bluetooth LE specifications regard the whole protocol stack. Only star topologies are possible. Two implementation options are defined: a single-mode (stand-alone)

implementation, targeted at applications requiring low power consumption and small size (typically button cell battery powered devices), and a dual-mode implementation, an extension to the classic Bluetooth radio, targeted at mobile phones and PCs.

Bluetooth LE operates at the 2.45 GHz ISM band, in the frequency range of 2400-2483.5 MHz, where forty 2 MHz RF channels are defined. The modulation is Gaussian Frequency Shift Keying (GFSK) and the supported bit rate is equal to 1 Mbit/s.

At the Link Layer (LL), the RF channels are allocated into two different types: advertising physical channels and data physical channels. The three advertising channels are used for discovering devices, initiating a connection, and broadcasting data. The thirty-seven data physical channels are used for communication between connected devices during normal operation. In both cases, channels are sub-divided into time units known as events: advertising events and connection events, respectively. On data channels, the communication is managed by a master node, which defines the timings of transmissions and channel hopping procedures.

Being Bluetooth a well-known and widespread technology, it could be a good option for WBANs. The most recent mobile phones and tablets come with dual-mode Bluetooth radio, and some monitoring devices equipped with LE can already be found on the market (e.g., heart rate belts) [44]. The main drawbacks of Bluetooth LE are the lack of multihop communication and the limited scalability.

Low-power Wi-Fi refers to the optimisation of standard Wi-Fi chips targeting low power consumption, in order to meet sensor applications requirements [45]. Wi-Fi is the commercial brand for products and networks based on the IEEE 802.11 standard [46], as certified by the Wi-Fi Alliance [47]. IEEE published the first 802.11 standard

in 1997, to specify PHY and MAC layers for Wireless Local Area Network (WLAN), and several amendments were released aftewards to improve performance, for example in terms of achievable data rate, QoS, or covered range. For many years, Wi-Fi technology has not been considered as an option for low-power wireless applications because it was not designed for energy efficiency. However, multiple companies have recently developed power-efficient Wi-Fi components with appropriate system design and usage models (e.g., G2 Microsystems [48]).

Low-power Wi-Fi devices have the advantages of easy integration with existing infrastructure, built-in IP-network compatibility, and having known protocols and management tools. Low-power Wi-Fi operation uses duty cycling technique to increase battery lifetime, and, on top of it, such systems employ fast network access, low sleep current, and battery power management in order to meet multiple years battery lifetime. Recent studies have claimed that low-power Wi-Fi devices have power consumption comparable with sensors based on 6LowPAN (i.e. IEEE 802.15.4) [45]. Low-power Wi-Fi targets application domains such as smart-grid utilities, healthcare, home and building automation, transportation, and, given the current penetration of Wi-Fi technology, it could be another viable option to be considered for body-centric communications.

ANT is a proprietary wireless sensor network protocol running in the 2.45 GHz ISM band [49]. It is designed for ultra-low power, ease of use, efficiency and scalability and it allows to handle different network topologies: peer-to-peer, star, tree, and mesh. The ANT protocol provides reliable data communications and flexible and adaptive network operation. The protocol stack is extremely compact; it is based on a Nordic 2.45 GHz Radio PHY, and it includes Data Link, Network, and Transport layers.

The implementation of the upper layers is left to the user.

The access is managed through a TDMA-like adaptive scheme. Frequency Agility is introduced to improve coexistence with other wireless devices operating in the same band: the channel is monitored and the operating frequency is changed in case of a significant degradation in the performance. A network data rate of 20 kbit/s can be achieved (the over-the-air bit-rate is equal to 1 Mbit/s). The ultra-low power consumption is obtained through duty cycling (nodes spend most of their time in an ultra-low power sleep mode) and the use of very short packets (minimizing the time spent in transmitting or receiving modes). A battery life (with coin-cell batteries) of up to 3 years is possible.

ANT+ is an open alliance of over 100 member companies that defines health and fitness device profiles, such as Heart Rate Monitor, Stride-Based Speed and Distance Monitor (footpod), Bicycle Speed and Cadence, and Bicycle Power [2].

1.1.3   WiserBAN Project

The WiserBAN (Smart miniature low-power wireless microsystem for Body Area Networks) project [50] is a large-scale Integrating Project, funded by the European Commission through the Seventh Framework Programme, started in September 2010 and with a duration of three years. The aim of the project is to create an ultra-miniature and ultra low-power RF microsystem for WBANs, targeting primarily wearable and implanted devices for healthcare and biomedical applications. The WiserBAN microsystem will be fifty times smaller than today's radio modules for WBANs and will implement flexible communication protocols.

Four industrial-driven use cases are specifically addressed: *Hearing Instruments*

(DE-SAT use case), *Cochlear Implants* (MEDEL use case), *Cardiac Implants* (SORIN use case) and *Insulin Pump* (DEBIOTECH use case).

As for the first two cases, illustrated in Fig. 1.10, wireless connectivity is central for the performance and comfort of modern hearing systems. A wireless communication module for hearing systems and cochlear implants needs to be extremely low power, while allowing the transmission of different kind of traffics, both streaming and non streaming. Communication among the hearing instruments and an external Remote Control (RC), together with bidirectional ear-to-ear communication, should be allowed.

<center>(a)   (b)</center>
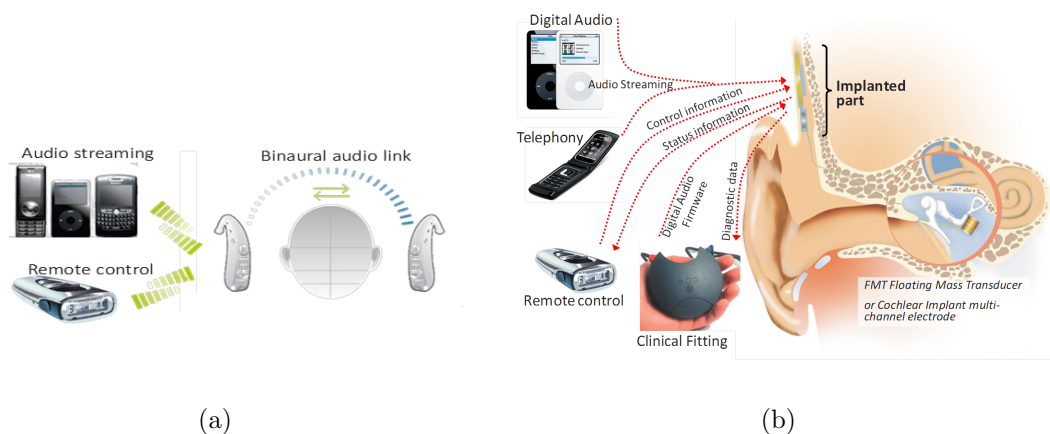
Figure 1.10: WiserBAN use cases: (a) hearing instruments, DE-SAT, (b) cochlear implants, Medel.

The cardiac implants use case concerns people carrying a cardiac implant in the context of enabling remote monitoring of the patient at home, see Fig. 1.11. The reduction of the power consumption of these implantable devices will allow to decrease the size of the battery and hence of the implant, leading to more comfort for the patient. In this case, the communication between the implanted device and the RC

should be allowed.
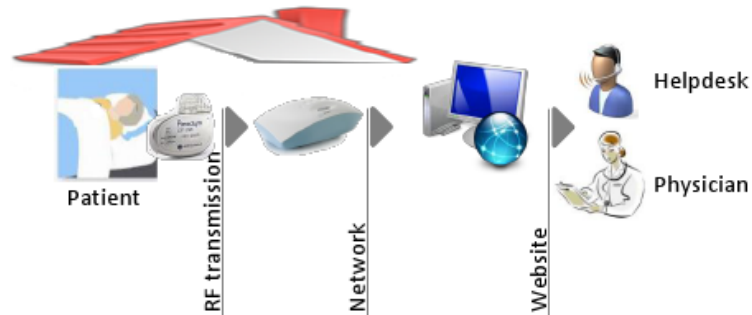
Figure 1.11: WiserBAN cardiac implant (Sorin) use case.

In the case of the insulin pump, shown in Fig. 1.12, a patch pump is applied on the patient's skin, concealed under his clothes, for medication delivery. In order to interact with the pump, the patient uses the RC. The weight and the size of the pump, as well as the power consumption, are critical issues for this application.
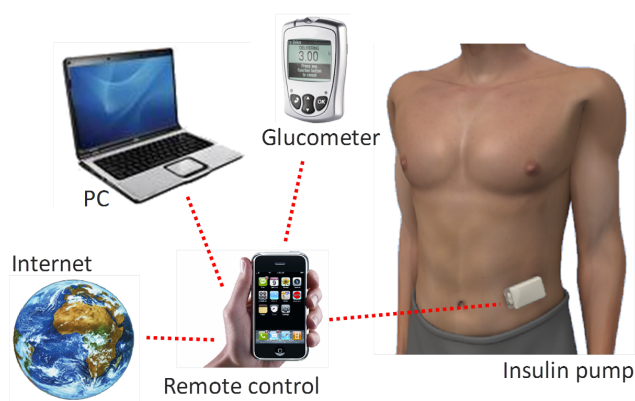
Figure 1.12: WiserBAN insulin pump (Debiotech) use case.

Besides the reference primary use cases described above, the WiserBAN technology differentiators, i.e. ultra low-power and miniature radio microsystems, may be leveraged in complementary applicative areas such as ambient intelligence, home automation, motion capture and gaming, sports and wellness, rehabilitation, smart clothing, and other applications related to WBANs and WSNs in general.

According to the differences among the use cases and the different kind of traffics generated in each of them (streaming or non streaming traffic, large amount or small amount of application data to be transferred), a huge set of requirements, in terms of expected battery lifetime, maximum delays, and Packet Loss Rate (PLR) has been defined. Therefore, a flexible protocol solution has been designed, not only to properly take into account these requirements, but also to allow possible future extensions or different end-user applications.

WiserBAN is thus developing a dedicated protocol communication stack, shown in Fig. 1.13. In the vertical layer, energy management and time synchronisation functions are implemented. The former is fundamental for all WiserBAN envisioned applications, while time synchronisation will be used only by some of the applications (where streaming traffic is envisioned or when needed at the application layer).

Energy Management

According to WiserBAN use cases, the traffic generated in the network will be aperiodic and loose. Thanks to this, a duty-cycled protocol may be implemented, in order to save energy. Preamble sampling, also referred to as Low Power Listening (LPL), is a key technique to enable duty-cycled operations. Two main approaches have been proposed in the literature, based on the transmission of a single long preamble [51]
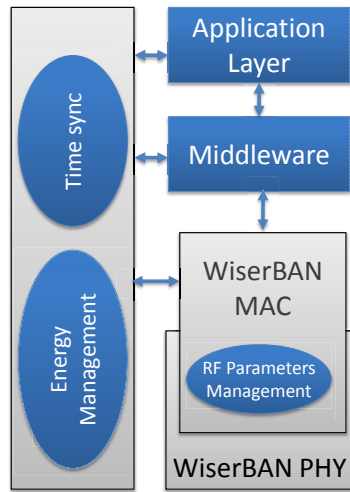
Figure 1.13: WiserBAN protocol stack.

or on the transmission of a burst of short preambles [52]. The latter solution has been chosen in WiserBAN, since it is more energy efficient, better preventing the overhearing problem.

The LPL mechanism is depicted in Fig. 1.14. Devices in the network alternate sleeping and active phases, which durations are T_w and T_{on}, respectively. Each node wishing to send data to a given receiver, or a set of receivers, will transmit a burst of short preambles, separated by an interval of time T_1 for the reception of the ACK. Once the preambles, which contain the addresses of all the intended receivers, are sent, the transmitter will wait for the ACK from all these devices. Before the transmission of the first preamble, the node will sense the channel for T_{on}, in order to check that no other device is already transmitting, and to avoid preambles collision. To be sure that the intended destination node receives at least one preamble, the transmitter has to send preambles for at least the duration of the sleep period of the destination node. When a node wakes up and receives a preamble packet, it looks at the target node

address that is included in the packet: if the node is not the intended recipient, it returns to sleep immediately and continues its duty cycling as if the medium had been idle; if the node is the intended recipient, instead, it sends an ACK to the transmitter and it remains awake for the subsequent data packet.
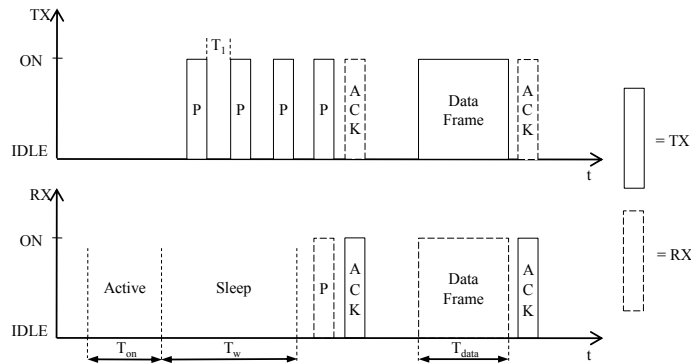
Figure 1.14: Description of the LPL mechanism.

In WiserBAN networks, depending on the number of nodes in the network and on the type of traffic that has to be exchanged, after the preamble procedures, the communication could take place directly as explained above, or through the establishment of a superframe when needed. Details can be found in [53].

Physical Layer

At the WiserBAN PHY, three different modulation options have been specified:

- *PHY 1*: IEEE 802.15.4-compliant PHY, that is MSK modulation with spreading, with a bit-rate of 250 kbit/s;

- *PHY 2*: in this case MSK modulation is used, derived starting from PHY 1 and removing the spreading, with a bit-rate of 2 Mbit/s;

- *PHY 3*: Bluetooth Low Energy-compliant PHY, i.e. Gaussian Minimum Shift Keying (GMSK) modulation, with a bit-rate of 1 Mbit/s.

Medium Access Control Layer

The MAC layer is responsible for the association and disassociation of devices to the network (network formation), the maintenance of the network, and the management of the access to the radio channel. As for network formation and maintenance, procedures similar to the ones proposed in IEEE 802.15.4 standard have been specified (see [53] for details). Hereafter, the channel access mechanisms will be described.

When more than one device (apart from the coordinator) are present in the network, the access to the channel is managed by the coordinator, through the establishment of a superframe. When the RC is in the range of the other network devices, it will always act as WiserBAN coordinator. When, instead, it is out of the range (i.e., it cannot reach the devices), whatever a node in the network may take the role of coordinator. In particular, such a node will be the first node having a packet to be transmitted after the disconnection of the RC.

To establish and maintain the superframe, the coordinator periodically broadcasts beacon frames, containing management information. The period between two consecutive beacons defines the superframe structure. The superframe may have an active portion and an inactive part; during the latter, nodes can go into a stand-by state, in order to reduce the energy consumption. The durations of the superframe and of the different parts composing it are set according to the application requirements. As shown in Fig. 1.15, the active portion is composed of different parts:

- *Beacon portion*, reserved for the transmission of the beacon by the coordinator;

- *Indicators portion*, where nodes have reserved mini-slots to send an ACK to the coordinator in case the beacon has been successfully received;

- *Contention Free Period (CFP)*, where the access is TDMA based: a certain number of time slots is allocated to nodes with stringent requirements;

- *Contention Access Period (CAP)*, where the access to the channel is contention based, according to a CSMA/CA or a Slotted ALOHA algorithm;

- *ACK portion*, where mini-slots are assigned to the nodes to communicate if the transactions in the superframe were successful or not.

In particular, three different protocols were proposed to be used in the CAP portion: the CSMA/CA protocol in the two different versions considered respectively in the IEEE 802.15.4 and 802.15.6 standards, and the Slotted ALOHA algorithm as defined in IEEE 802.15.6.
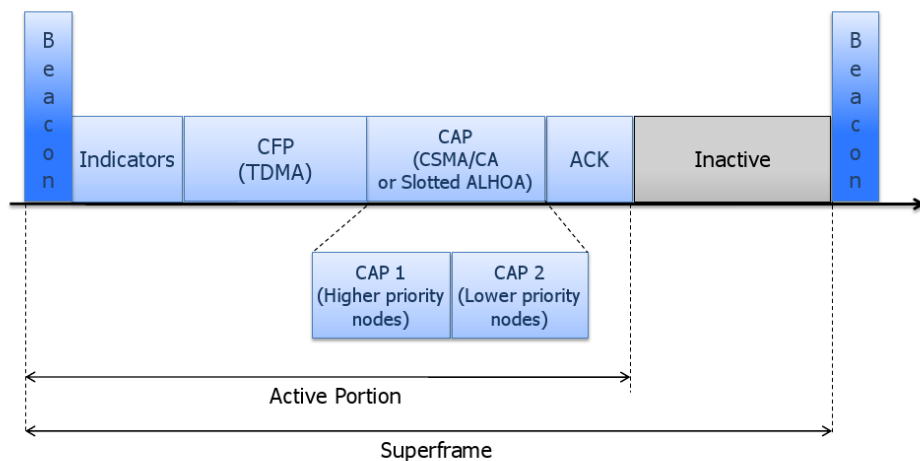
Figure 1.15: WiserBAN superframe structure.

The CAP should always be present in a superframe, at least to handle slots requests. If no other traffic needs to be managed in it, its duration will be set to the minimum.

If there will be the need to assign different priorities to the nodes in the access to the channel, two possible solutions are envisaged. One approach is to split the CAP into different parts, allowing the access in one part or in another one depending on the priority of the data to be transmitted; this splitting is shown in Fig. 1.15 as CAP 1 and CAP 2 phases. The second solution is based on the assignment of different parameters values for the algorithm used in the CAP (e.g., sensing duration, contention window, and backoff exponent for CSMA/CA, contention probability for Slotted ALOHA) to the nodes according to their priorities.

1.2   Structure and Contributions of the Thesis

Various aspects of body-centric communications are explored in this thesis. Following the classification mentioned above regarding nodes position with respect to the body, Chapter 2 is mostly dedicated to *on-body communications*, Chapter 3 is related to *off-body communications*, while Chapter 4 deals mainly with *body-to-body communications*.

The focus of most of the described research is on the characterisation of the access to the channel; network performance is in fact evaluated at the MAC layer, always taking into account electromagnetic propagation aspects and PHY layer features properly in order to attain realistic results.

In Chapter 2 the performance of WBAN is investigated under three different perspectives. The main tool used for this purpose is simulation. In this way it is in fact

possible to consider in details all the significant aspects of the system under examination even for complex scenarios. First, Link Adaptation (LA) is applied to a WBAN with the aim of decreasing packet losses. Two different strategies are presented and demonstrated to improve performance. The novel contribution of this activity lies in the proposal of LA application to a new context (i.e. WBANs) and with a different goal (decreasing packet loss rate in query-based applications, instead of increasing throughput as usually considered in most LA related works). Then, performance of CSMA/CA algorithms in several WBAN scenarios is extensively examined. Some of the results reported are among the firsts that can be found in the literature referring to networks based on the IEEE 802.15.6 standard. Finally, the behaviour of WBANs in the presence of interference from other wireless networks is analysed. This coexistence study accounts for detailed interference characterisation and specific models regarding the on-body channel and PHY layer. It represents a complete evaluation of a still quite uninvestigated but relevant issue in WBAN context.

In Chapter 3 an interference model for wireless access networks is presented. It is a mathematical model based on the integration of a stochastic geometry model for the interference power and Markov chain analysis for CSMA/CA. The main novelty lays in the consideration of the detailed operation of the CSMA/CA algorithm as described in the IEEE 802.15.4 standard, together with a stochastic description of the interference power and connectivity considerations, in order to evaluate success probability for nodes in the network.

Chapter 4 describes preliminary results of an experimental activity aiming at characterising human mobility and sociality, whose knowledge represents the necessary basis to develop B2B protocols. The experiments have been carried out distributing

wireless mobile devices to volunteer participants, in order to gather the contacts of each device with other mobile devices and with a fixed infrastructure. With respect to similar experiments described in the literature, this activity is focusing specifically on indoor scenarios and is characterised by higher temporal and spatial accuracy.

The research activities leading to many of the results described in the thesis have been carried out in the framework of the European Project WiserBAN, the Cost Actions 2100 (Pervasive Mobile and Ambient Wireless Communications) and IC1004 (Cooperative Radio Communications for Green Smart Environments). The experimental campaign described in Chapter 4 was realised at the Centre for Communication Systems Research (CCSR) of Surrey University, where six months were spent as a visiting PhD student.

Parts of the PhD activity described in the thesis brought to the following publications:

- Flavia Martelli, Roberto Verdone, Chiara Buratti. Link Adaptation in IEEE 802.15.4-Based Wireless Body Area Networks. *IEEE PIMRC2010 International Workshop on Body Area Networks*, Istanbul, September 2010;

- Flavia Martelli, Chiara Buratti, Roberto Verdone. On the performance of an IEEE 802.15.6 Wireless Body Area Network. *European Wireless Conference, EW 2011*, Vienna, April 2011 [also presented at the Joint Newcom++/Cost 2100 Workshop on Wireless Communications (JNCW 2011), Paris, March 2011];

- Flavia Martelli, Roberto Verdone, Chiara Buratti. Link Adaptation in Wireless Body Area Networks. *IEEE VTC 2011 Spring*, Budapest, May 2011 [also TD(10)12043 presented at the XII Management Committee Meeting of Cost 2100,

Bologna, November 2010];

- Chiara Buratti, Raffaele D'Errico, Mickael Maman, Flavia Martelli, Ramona Rosini, Roberto Verdone, Simon Huettinger. Design of a Body Area Network for Medical Applications: the WiserBAN Project. *ACM ISABEL 2011*, Barcelona, October 2011 [also TD(11)02020 presented at the II Management Committee Meeting of Cost IC1004, Lisbon, October 2011];

- Ramona Rosini, Flavia Martelli, Mickael Maman, Raffaele D'Errico, Chiara Buratti, Roberto Verdone. On-Body Area Networks: from Channel Measurements to MAC Layer Performance Evaluation. *European Wireless Conference, EW 2012*, Poznan, April 2012 [also TD(12)03060 of the III Management Committee Meeting of Cost IC1004, Barcelona, February 2012];

- Flavia Martelli, Roberto Verdone. Coexistence Issues for Wireless Body Area Networks at 2.45 GHz. *European Wireless Conference, EW 2012*, Poznan, April 2012 [also TD(12)03039 presented at the III Management Committee Meeting of Cost IC1004, Barcelona, February 2012];

- Flavia Martelli, Chiara Buratti, Roberto Verdone. Modeling Interference-Limited Wireless Access Networks with IEEE 802.15.4 – A Stochastic Geometry-Based Approach. *Submitted to IEEE Transactions on Vehicular Technology*;

- Riccardo Cavallari, Flavia Martelli, Ramona Rosini, Chiara Buratti, Roberto Verdone. A survey on Wireless Body Area Networks: Technologies and Design Challenges. *Submitted to IEEE Communications Surveys and Tutorials.*

Other Temporary Documents presented at Cost Action IC1004 Meetings follow:

- TD(12)03063 – Ramona Rosini, Flavia Martelli, Mickael Maman, Roberto Verdone, Raffaele D'Errico. Radio Channel Requirements for BAN Performance Evaluation. III Management Committee Meeting of Cost IC1004, Barcelona, February 2012;

- TD(12)04050 – Flavia Martelli, Chiara Buratti, Roberto Verdone. A Mathematical Model for Interference-limited Wireless Access Networks based on IEEE 802.15.4. IV Management Committee Meeting of Cost IC1004, Lyon, May 2012.

As for WiserBAN project, contributions to the following deliverables were given:

- D1.1 – Report about WiserBAN platform applications, edited by Jean-Francois Debroux, November 2010;

- D4.1 – BAN Upper Layers, Base Band and DSP Architecture Specification, edited by Laurent Ouvry, September 2011;

- D4.2 – Characterization and Validation of the first Base-Band version, edited by Laurent Ouvry, February 2012;

- D5.2 – Computer Simulation Results and Test of BAN Protocols over Benchmark Platform, edited by Chiara Buratti, April 2012.

Chapter 2

Medium Access Control Layer Performance for Wireless Body Area Networks

On-body communications are the focus of this chapter: the MAC layer performance of a wearable WBAN is evaluated through different perspectives. After a detailed description of relevant literature works (Section 2.1), the use of LA in WBANs is proposed and examined in Section 2.2. The two main reference standards for WBANs, IEEE 802.15.4 and IEEE 802.15.6, are analysed in Section 2.3, by means of extensive simulations in different realistic scenarios. Finally, Section 2.4 considers coexistence issues with other networks operating at 2.45 GHz, in a general framework that takes into account both time and frequency interference characterisation.

2.1 Related Works

Several works about WBAN MAC protocol solutions, proposals, and evaluations can be found in the literature of recent years.

Since there was no standard specifically devised for WBANs until IEEE 802.15.6

was released (February 2012), many contributions refer to the study of applicability of existing WSN protocols in WBAN scenarios, with a particular emphasis on IEEE 802.15.4 standard. Potential improvement and optimization of these existing protocols are also proposed. Reference [54], for example, evaluates via extensive simulations the suitability of IEEE 802.15.4 to the medical environment, underlining some scalability issues and problems due to interference caused by WLANs. Experiments with IEEE 802.15.4 compliant devices were carried out in [55], in order to test the connectivity of different on-body links. Results show how the position of the nodes can significantly impact the performance. In [56] and [57], modifications of IEEE 802.15.4 beacon-enabled mode are proposed, where BO and SO values are dynamically changed according to nodes requests. In the former, a different priority is given to requests based on a parameter computed taking into account the remaining energy level, buffer occupancy, and data time criticality for each node. In this way, energy efficiency is demonstrated to be improved. In the latter, instead, the network coordinator adjusts superframe timing parameters depending on nodes application characteristics (sample rate, data length), in order to improve the delivery ratio and reduce the energy consumption. The authors of [58] carried out an experimental comparison of Bluetooth and B-MAC protocol (which is similar to IEEE 802.15.4 one) in a wearable WBAN scenario composed of five nodes and a coordinator. They showed that Bluetooth can provide better success rates but at the expenses of a significantly higher power consumption. BAN Adaptive TDMA MAC (BATMAC) is proposed in [59]. It is a protocol based on an adaptation of IEEE 802.15.4 superframe structure, which automatically detects the shadowing effect on the channel in order to accordingly change the parameters of the superframe and to use relay nodes

when necessary. Latency outage probability is reduced at the expense of a reasonable increase in the power consumption for the nodes that act as relays.

Reference [60] gives a general overview of MAC protocols for WBANs, discussing also the possibility to use LPL or contention-scheduled mechanisms thought for WSNs, such as WiseMAC [61] and S-MAC [62]. The former is a preamble sampling based technique, while in the latter nodes sleep schedules are synchronised among neighbours and carrier sensing is performed before transmissions. Both approaches are not suitable to efficiently handle low-traffic or emergency events and do not represent an optimal solution to support both in-body and on-body communications simultaneously [8, 60]. A simulation comparison of S-MAC, WiseMAC, and IEEE 802.15.4 is reported in [63], where an improved mechanisms for beacon-enabled networks is also proposed. Beacons are not continually sent, but they are generated depending on the traffic of the different applications, in order to reduce the energy consumed for the reception of unnecessary beacon frames. Preamble sampling is considered also in [64], which presents a modified version of X-MAC [52]. The destination address is proposed to be encoded as the length of the preamble frame. In this way, it can be decoded without the need of demodulating the preamble, leading to a decrease in the energy consumption.

Many other WBAN-related contributions offer MAC proposals that are TDMA based. [65], for instance, describes a TDMA based strategy, focusing on a non dynamic network for vital signs monitoring. H-MAC [66] aims at improving energy efficiency by exploiting heartbeat rhythm information to perform time synchronisation. Following the rhythm, biosensors can achieve time synchronisation without having to turn on their radio to receive periodic timing information from the coordinator, so that the

energy cost for time synchronisation can be reduced and network lifetime can be prolonged. In [67] nodes can decide whether or not to transmit their data in the assigned slot, depending on their battery status and buffer occupancy, aiming at maximizing device lifetime. A wake-up strategy is introduced in [68] to deal with failed transmissions and alarms management. Reference [69] focuses on reducing devices' duty-cycle, using an out of band centralized and coordinated external wake-up mechanism. References [70] and [71] present dynamic features to adapt to time changing characteristics of WBANs: in particular, the former is traffic aware and consequentially varies the wake-up interval, while the latter proposes an adaptive scheme to allocate channel and time for coexisting networks.

The LA proposals of this thesis (Section 2.2) can be placed in the first research direction described above: the evaluation of IEEE 802.15.4 suitability in the WBAN context. Having realised that the standard as is cannot always achieve desirable performance, the introduction of LA is considered with the aim of improving PLR results, assuming different modulation schemes available at the PHY.

LA is a well-known technique that has been traditionally employed in cellular networks [72], according to which nodes change the modulation and coding scheme (and thus the bit rate) depending on the channel quality, in terms of shadowing, fading and interference. The possibility of selecting different bit rates in networks using contention-based protocols has been later investigated, with a particular focus on IEEE 802.11 networks. In [73] and [74], for example, rate adaptation mechanisms are proposed based on the measured Signal-to-Noise ratio (SNR) values or experienced loss rate, respectively. [75] introduces an adaptive rate control technique that dynamically changes success and failure thresholds based on which the rate change

decision is taken. The main purpose of the introduction of LA in all these works is to increase the throughput of the network. Only few papers are devoted to LA in IEEE 802.15.4 networks, for example [76], where a variable data rate scheme is proposed with the aim of reducing the average power consumption.

With respect to these works, in Section 2.2, a query-based WBAN scenario is considered, where the nodes have to send one fixed-size packet every time the coordinator requests it. In this case, the throughput is fixed by the application, and the LA is introduced to reduce packet losses. LA in itself is not a new idea, but its application in such a scenario, taking into account WBAN characteristics, is novel.

As for IEEE 802.15.6, a few studies can be currently found in the literature. [77] gives an overview of the different MAC mechanisms proposed in the standard, describing their pros and cons. In [78] a simple analysis of theoretical throughput and delay limits is carried out, considering an ideal channel with no transmission errors and the different IEEE 802.15.6 frequency bands and bit-rates. [79] extends the work in [78], comparing theoretical limits with simulation for networks with increasing number of nodes. An analytical model to examine the energy lifetime performance of periodic scheduled allocations is presented in [80]. Performance analysis based on a Markov chain model for CSMA/CA can be found in [81] and [82], which study networks in saturated and unsaturated conditions, respectively. All of these contributions so far account for simplified assumptions regarding WBANs.

IEEE 802.15.6 CSMA/CA performance is evaluated through simulations in Section 2.3. This evaluation is carried out in realistic scenarios, where WBAN specific applications are considered and the propagation around the human body is properly taken into account. Comparisons with IEEE 802.15.4 CSMA/CA and Slotted

ALOHA algorithms will also be reported.

Coexistence of WBAN with other systems operating at 2.45 GHz (e.g., IEEE 802.11 (Wi-Fi), Bluetooth, IEEE 802.15.4) is of primary importance to guarantee reliable use during daily life. However, this is a topic that has been only little investigated, yet. Some works about coexistence issues for other technologies working at 2.45 GHz can be found in the literature. Focusing on IEEE 802.15.4, experimental tests in a hospital room are described in [83]. The interference caused by an IEEE 802.11 network is shown to cause significant packet error rate degradation. Similar results are reported in [84] for experiments carried out in an apartment. Results show that IEEE 802.11 interference can be mitigated choosing an appropriate frequency channel. Tests of coexistence with a microwave oven are also performed, leading to the conclusion that its impact is negligible for distances longer than 2 meters. Similar experiments are described in [85], where tests with Bluetooth interfering devices are also illustrated. Authors of [86] validate experimentally the coexistence model between IEEE 802.15.4 and IEEE 802.11 of [87], which takes into account power and timing aspects, and they show that IEEE 802.11 interference impact on IEEE 802.15.4 networks is significant. Coexistence of Bluetooth and IEEE 802.11 networks has been addressed by several works. Impact of IEEE 802.11 interference on Bluetooth piconets is shown in [88] to cause packet errors and throughput degradation. Vice versa, the effect of Bluetooth transmissions on an IEEE 802.11 network is examined in [89].

The coexistence framework that is presented in Section 2.4, though describing a generally valid methodology to evaluate interference impact on a network, is referring specifically to WBANs and takes into account a complete system characterisation. A realistic channel model for on-body propagation is considered, together with a

frequency domain interference description, allowing to accurately model interference impact at PHY layer. Besides, a time domain interference characterisation leads to an appropriate simulation of MAC dynamics to evaluate network performance.

2.2 Link Adaptation in Wireless Body Area Networks

The use of LA in a wearable WBAN scenario is proposed in this section. The network is based on IEEE 802.15.4 standard, while different modulation schemes are assumed to be available at the PHY layer. Two different LA proposals are reported, with the aim of reducing packet losses. The underlying idea is that higher bit rates decrease the time the channel is occupied and then the collision probability due to the random channel access.

2.2.1 Reference Scenario

A WBAN composed of a set of wearable sensor devices, hereafter denoted as *nodes*, is considered, to monitor body parameters, like heart rate, body temperature, blood pressure, oxygen saturation, and movements. Up to ten nodes are deployed in different parts of the body as shown in Fig. 2.1. Small movements of the body are accounted for in the simulations. Results are, in fact, achieved by averaging over slightly different positions of the nodes in the body (without changing the considered parts of the body listed in Fig. 2.1).

A star topology and a query-based traffic are considered: the coordinator, which is placed in the center of the body, periodically sends a query to all nodes asking for

0.	Coordinator
1.	Hand
2.	Upper arm
3.	Ear
4.	Chest
5.	Thigh
6.	Rib
7.	Waist
8.	Shoulder
9.	Head
10.	Ankle
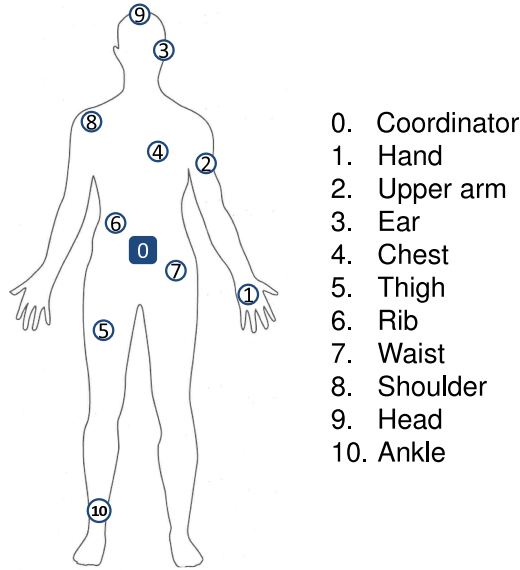
Figure 2.1: Reference WBAN for LA evaluation: position of the nodes on the body.

data and, upon reception of this query, the WBAN nodes transmit their packets to the coordinator through direct links. One packet per query is generated by nodes, with the assumption that all nodes have to transmit data having the same size. If a node is not able to transmit its packet before the next query, it has to discard it and the packet is considered as lost.

The channel loss, denoted as A, is modeled according to [90]:

$$A(d)[\text{dB}] = A_0 + 10\,n\,\log\left(\frac{d}{d_0}\right) + s, \qquad (2.2.1)$$

where d is the distance between transmitter and receiver, A_0 is the path loss in dB at a reference distance d_0 ($A_0 = 35.2$ dB for $d_0 = 0.1$ m), n is the path loss exponent ($n = 3.11$), and s is a random Gaussian variable, having zero mean and standard deviation $\sigma = 6.1$ dB.

For what concerns the packet capture model, a threshold model is accounted for.

A packet is correctly received when the two following conditions are both satisfied:

$$\begin{cases} P_{\mathrm{R}} > P_{\mathrm{R_{min}}} \\ \frac{C}{I} \geq \frac{C}{I}\big|_{\min} \end{cases} \tag{2.2.2}$$

where P_{R} is the received power given by: $P_{\mathrm{R}}[\mathrm{dBm}] = P_{\mathrm{tx}}[\mathrm{dBm}] - A[\mathrm{dB}]$, P_{tx} is the transmit power, A is given by Eq. (2.2.1), $P_{\mathrm{R_{min}}}$ is the receiver sensitivity, C is the power received from the useful transmitter, and I is the total power received from the interfering nodes. $\frac{C}{I}\big|_{\min}$ is the protection ratio, that is the minimum Signal-to-Interference ratio (SIR) ensuring the correct reception of a packet. The values of $P_{\mathrm{R_{min}}}$ and $\frac{C}{I}\big|_{\min}$ depend on the modulation and coding scheme used by the transmitter and are evaluated in the following section.

2.2.2 Physical Layer

The PHY is assumed to be compliant with IEEE 802.15.4 specification for the ISM band at 2.45 GHz, where the bandwidth allocated to each channel is $B = 5$ MHz and the bit rate $R_b = 250$ kbit/s. As described in Section 1.1.2, the modulation used is O-QPSK with half-sine pulse shaping, and DSSS as spreading technique, with a spreading factor $f = 8$.

Besides the IEEE 802.15.4 O-QPSK, DPSK with L modulation levels (L-DPSK), with $L = \{2, 4, 8, 16\}$, is considered, which is one of the modulation formats proposed for the IEEE 802.15.6 standard [91].

LA is assumed to be performed by varying the bit rate, once the bandwidth is fixed to a common value, that is the bandwidth of the IEEE 805.15.4. In the case of L-DPSK modulation, a SRRC filter is assumed to be used for equalization, with roll-off factor $\alpha = 0.2$, and a DSSS technique with spreading factor, f, equal to 8 (as

in the case of 802.15.4) is also applied. In such conditions, the bandwidth is given by:

$$B = \frac{R_b}{\log_2(L)} f(1 + \alpha). \tag{2.2.3}$$

By setting $B = 5$ MHz, the bit rates, R_b, achievable in the case of L-DPSK modulations can be derived (see Table 2.1).

The performance of O-QPSK with half-sine pulse shaping in terms of the bit error probability P_{eb} in an additive white gaussian noise (AWGN) channel can be expressed as:

$$P_{\mathrm{eb}} = \frac{1}{2} \operatorname{erfc} \sqrt{W}, \tag{2.2.4}$$

where W indicates the conventional SNR, given by: $W = \frac{P_{\mathrm{R}}}{2N_0 R_b}$, where P_{R} is the received power, N_0 is the bilateral power spectral density of the gaussian noise, and $\operatorname{erfc}(\cdot)$ is the complementary error function, defined as:

$$\operatorname{erfc}(x) = \frac{2}{\sqrt{\pi}} \int_x^\infty e^{-y^2} \, \mathrm{d}y. \tag{2.2.5}$$

The bit error probability for L-DPSK modulation in AWGN channel with SRRC equalization can be expressed as:

$$P_{\mathrm{eb}} = \begin{cases} \frac{1}{2} e^{-\frac{W}{b}} & \text{if } L = 2 \\ \frac{1}{\log_2(L)} erfc\left[\sqrt{\frac{W}{2b} \log_2(L)} \frac{\pi}{L}\right] & \text{if } L > 2 \end{cases} \tag{2.2.6}$$

b is the filter normalized equivalent noise bandwidth, that is set equal to 1.2.

A packet composed of N_{bit} bits is assumed to be successfully received if all its bits are correct, which happens with probability $P_{\mathrm{ep}} = (1 - P_{\mathrm{eb}})^{N_{\mathrm{bit}}}$. The receiver sensitivity is defined as the received power so that P_{ep} is equal to 0.99 [36].

Table 2.1 summarises the bit rates, the receiver sensitivities, and the protection ratios for the different modulation schemes. The values of $P_{\mathrm{R_{min}}}$ are obtained for

$N_{\text{bit}} = 960$ and $N_0 = 7.2 \cdot 10^{-19}$ W/Hz. The value $\frac{C}{I}|_{\min} = 1.3$ dB for O-QPSK has been derived experimentally [92]. The values of $\frac{C}{I}|_{\min}$ for L-DPSK are estimated from the one measured for O-QPSK, by adding the same amount that also shifts the P_{eb} curves over the SNR axis.

Table 2.1: Modulations parameters for LA evaluation.

Modulation	Bit rate [Mbit/s]	$P_{\mathbf{R_{\min}}}$ [dBm]	$\frac{C}{I}|_{\mathbf{\min}}$ [dB]
O-QPSK	0.25	-84.9	1.3
2-DPSK	0.5	-80.3	2.8
4-DPSK	1	-76.0	4.2
8-DPSK	1.5	-70.1	8.2
16-DPSK	2	-64.2	12.9

2.2.3 Medium Access Control Layer

The beacon-enabled mode of the IEEE 802.15.4 is considered [36], as described in Section 1.1.2. The beacon packet transmitted by the coordinator to manage the superframe coincide with the query of the scenario under investigation.

The acknowledge mechanism is taken into account: each node, after the transmission of a packet, waits for the ACK for an interval of time equal to 0.86 ms. In case the ACK is not received, the packet is retransmitted till the maximum number of retries is reached, or the superframe ends.

2.2.4 Proposed Link Adaptation Strategies and Results

First Proposal

The LA strategy proposed is based on the following considerations. When the SNR is low, meaning that the node is far from the coordinator or a deep shadowing occurs, the bit rate is decreased, so that a lower value of $P_{R_{\min}}$ is required and the probability to correctly receive the packet increases. When, instead, the SNR is high it can happen that packets are not successfully received because they collide with packets coming from other nodes. In this case, higher bit rates, which lead to packets transmitted in a shorter time, can be more suitable to reduce the probability that a collision happens.

Fig. 2.2 summarises the LA algorithm. It is assumed that at the beginning all nodes start with IEEE 802.15.4 O-QPSK modulation. As stated above, a beacon-enabled network is considered, therefore the nodes wait for the beacon (which corresponds to the query) coming from the coordinator, before sending their data. From the measure of the received beacon power each node estimates the SNR which characterises the channel between the coordinator and itself: if the estimated SNR is below the threshold Th_{SNR} the node decrements its bit rate. Otherwise, it estimates the SIR (i.e., the level of interference on the channel) through the evaluation of a failure probability, denoted as P_F, that is the probability that a packet sent is not received by the coordinator. This probability can be estimated as the ratio between the number of unacknowledged packets (i.e., packets for which the ACK is not received) and the number of packets which are sent on the channel (including retransmissions):

$$P_F = \frac{\#not\ received\ ACKs}{\#sent\ packets}. \tag{2.2.7}$$

P_F is evaluated counting the unacknowledged and sent packets over a window of 20

superframes. If P_F is above the threshold Th_{P_F}, the node is in a situation where many of its packets are lost and, since the channel quality is good (high SNR), these losses are due to interference. Therefore, in this case the bit rate is incremented, in order to reduce the packet transmission time and the probability of collision. If $P_F < \mathrm{Th}_{P_F}$ the node does not change the bit rate it is using.
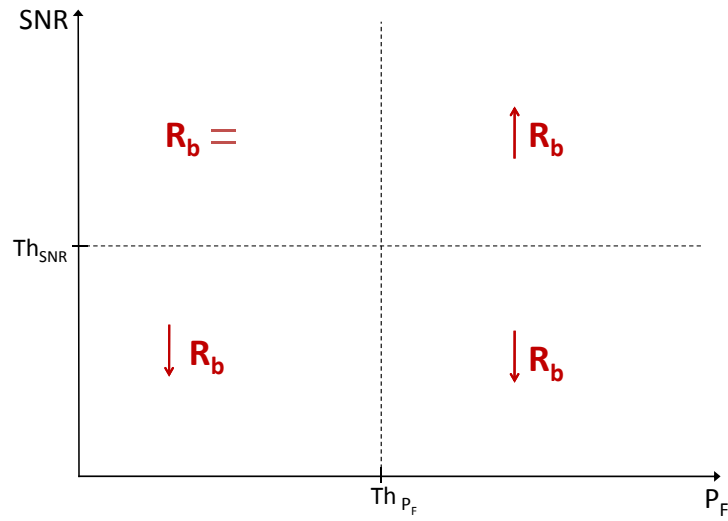
Figure 2.2: Scheme of the first proposed LA algorithm.

Numerical Results

A dedicated simulator has been written in C to numerically evaluate the performance of the proposed LA strategy. Results are achieved by simulating 25.000 superframes, meaning 25.000 transmissions from each node to the coordinator. The CSMA/CA parameters are set to the default values provided by the standard [36]: $\mathrm{NB}_{\mathrm{max}} = 4$, $\mathrm{BE}_{\mathrm{min}} = 3$, $\mathrm{BE}_{\mathrm{max}} = 5$, the maximum number of retransmissions equal to three. The superframe order is set equal to 3 (SO = 3).

Performance is evaluated in terms of average PLR, which represents the probability that a packet generated by a node is not received by the coordinator. This can happen because of four possible different causes:

a) the node cannot receive the beacon, meaning that it is not connected to the network;

b) the node cannot access the channel (the number of times the node tries to access the channel exceeds $\mathrm{NB_{max}} + 1$);

c) the node cannot transmit the packet correctly within the three retries (Eq.s (2.2.2) are not satisfied, i.e.: $P_\mathrm{R} \leq P_\mathrm{R_{min}}$ or $\frac{C}{I} < \frac{C}{I}|_{\min}$);

d) the node cannot succeed before the end of the superframe.

First, some simulations were run for N uniformly distributed nodes in a square scenario. In this scenario, the side of the square and the transmit power of the nodes are set so that no problems due to connectivity for any of the considered modulations occur, that is the received power at the coordinator is always higher than $P_\mathrm{R_{min}}$. The side of the square is equal to 7 m and the transmit power is set to 0 dBm. In this way it can be evaluated how the use of the different considered modulations affects the performance when packets are lost only because of interference. Fig.s 2.3 and 2.4 show the PLR as a function of the packet length in such a scenario, with $N = 50$ and $N = 10$ nodes, respectively. It can be noticed that, among the considered modulation schemes, there is not one single modulation which outperforms the others for every traffic load. In fact, for short packets, O-QPSK and 2-DPSK achieve a lower PLR than 4-DPSK and 8-DPSK, while for longer packets the situation is the opposite. The advantage of the shorter channel occupancy of packets transmitted at a higher
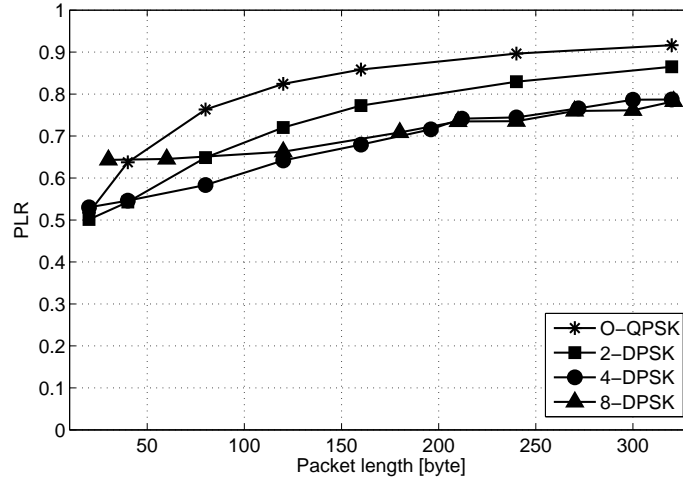
Figure 2.3: PLR as a function of the packet length for $N = 50$ nodes uniformly distributed in a square scenario, for different modulation schemes.
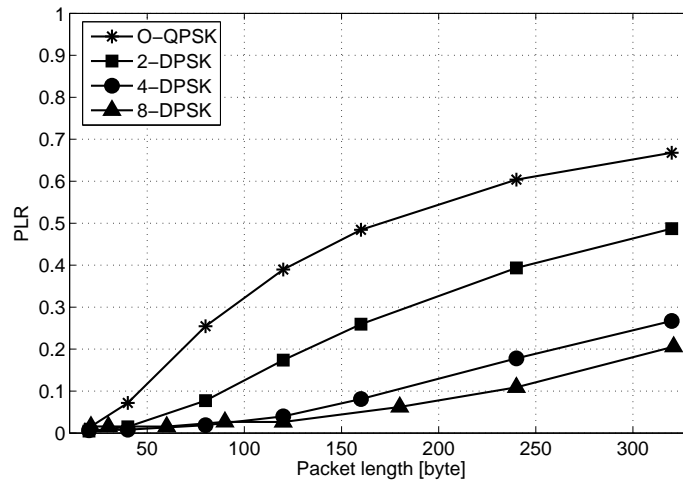
Figure 2.4: PLR as a function of the packet length for $N = 10$ nodes uniformly distributed in a square scenario, for different modulation schemes.

bit rate is increasingly relevant when the packet length increases, while for packets composed of a small number of bytes O-QPSK performs better. This is due to the higher $\frac{C}{I}|_{\min}$ requested by the modulations with a higher number of levels.

Fig.s 2.5 and 2.6 show the PLR as a function of the transmit power, P_{tx}, in the WBAN scenario described in Section 2.2.1, considering $N = 10$ and $N = 5$ nodes, respectively (that is, considering all the nodes listed in Fig. 2.1, or only the first five nodes of the list). N_{bit} is set to 960, corresponding to a packet length of 120 bytes, that is long enough to have significant differences in the time needed to transmit it with the different bit rates considered. Continuous curves show the performance
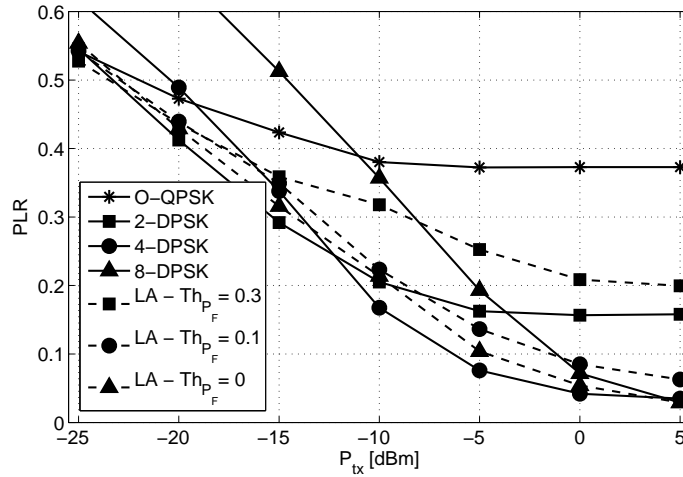
Figure 2.5: Comparison of the PLR for a WBAN with $N = 10$ nodes, for different modulation schemes and for the first proposed LA strategy.

achieved when all the nodes in the WBAN use the same modulation, while dotted curves represents the cases where the LA algorithm is applied. The LA curves are achieved by fixing $\text{Th}_{\text{SNR}} = 11$ dB and by varying Th_{P_F}. The use of LA with an optimum choice of thresholds allows to lower the PLR. As we can see, the optimum value of Th_{P_F} varies by changing P_{tx}: it assumes a large value when P_{tx} is low and it is
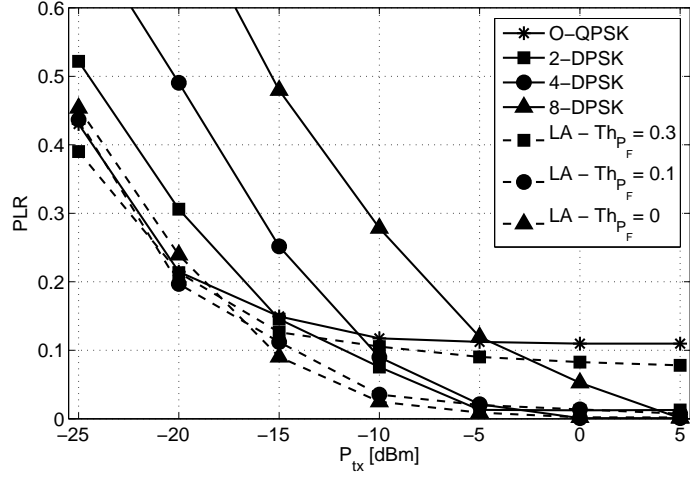
Figure 2.6: Comparison of the PLR for a WBAN with $N = 5$ nodes, for different modulation schemes and for the first proposed LA strategy.

low (equal to zero, meaning that the bit rate is simply increased when $\text{SNR} > \text{Th}_{\text{SNR}}$), when P_{tx} is high. This can be clearly seen in the case $N = 5$ (Fig. 2.6). This is due to the fact that when P_{tx} is low the network is limited by connectivity problems, whereas for large values of P_{tx} the main problem are interferences.

The use of a null threshold for P_F ($\text{Th}_{P_F} = 0$) suggested a change to the proposed LA strategy, leading to a second proposal, described in the following section.

Second Proposal

The second LA technique proposed is based on the observation of the channel quality in terms of SNR. Also in this case, it is assumed that the beacon is always sent with IEEE 802.15.4 O-QPSK modulation and that, at the beginning, all nodes start with O-QPSK.

The nodes wait for the beacon (which corresponds to the query) coming from the coordinator, before sending their data. From the measure of the power received, each

node estimates the SNR which characterises the channel between the coordinator and itself. According to this SNR value, the node chooses the modulation which yields the highest possible bit rate satisfying the condition on the receiver sensitivity (see first of Eq. (2.2.2)). Higher bit rates, in fact, lead to packets transmitted in a shorter time, and are more suitable to reduce the probability that a collision happens and that the packet is sent before the superframe ends.

A graphical representation of the algorithm is reported in Fig. 2.7. For every modulation two thresholds are defined: Th_i and Th_{i+1}, which correspond to the minimum SNR that must be guaranteed for the current modulation and to the one of the subsequent modulation with a higher bit rate (see Table 2.1), respectively. When the SNR is lower than Th_i the bit rate is decreased because it is not possible to satisfy first of Eq. (2.2.2) with the current modulation; when the SNR is higher than Th_{i+1} the node increases its bit rate since the channel is good enough to use a higher order modulation. Finally, when $Th_i < SNR < Th_{i+1}$ the bit rate is not changed, because the current bit rate is the highest possible that could be used in such channel conditions.
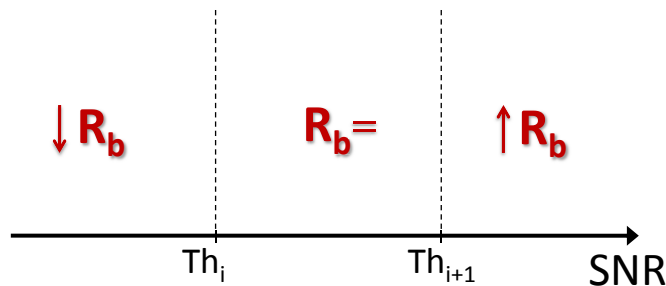
Figure 2.7: Scheme of the second proposed LA algorithm.

Numerical Results

The simulation settings are the same described in the previous section, if not otherwise

explicitly stated.

Fig.s 2.8 and 2.9 show the PLR as a function of the transmit power, P_{tx}, for SO = 0 and SO = 3, respectively.
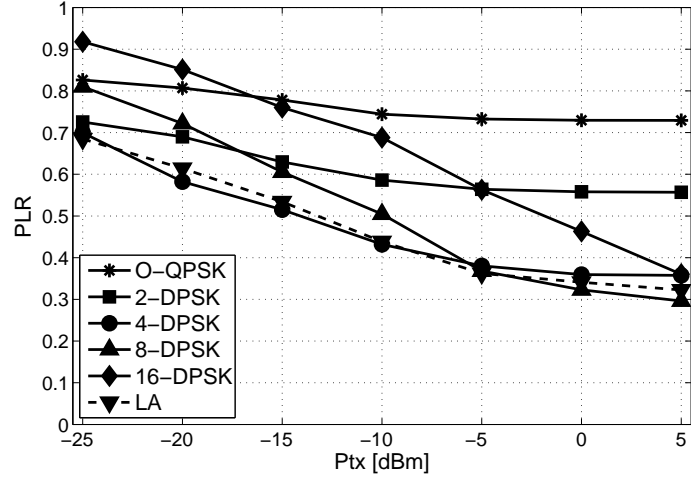
Figure 2.8: Comparison of the PLR for a WBAN with $N = 10$ nodes, for different modulation schemes and for the second proposed LA strategy, SO = 0.

Continuous curves show the performance achieved when all the nodes in the WBAN use the same modulation, while the dashed curve represents the results related to LA. As noticed above in the discussion of the results for the first LA proposal, among the considered modulation schemes, there is not a single modulation which outperforms the others for every value of P_{tx}. This is due to the fact that for low values of the transmit power the network is limited by connectivity, while for higher values it is limited by interference. Basically, the application of LA improves the performance; this is more evident with SO = 3.

In Fig.s 2.10 and 2.11 the different causes of packet loss are highlighted.

Only some modulations are shown, for conciseness; anyway, the trend of the cases which are not shown is similar to the ones plotted. When SO = 0 (Fig. 2.10), for
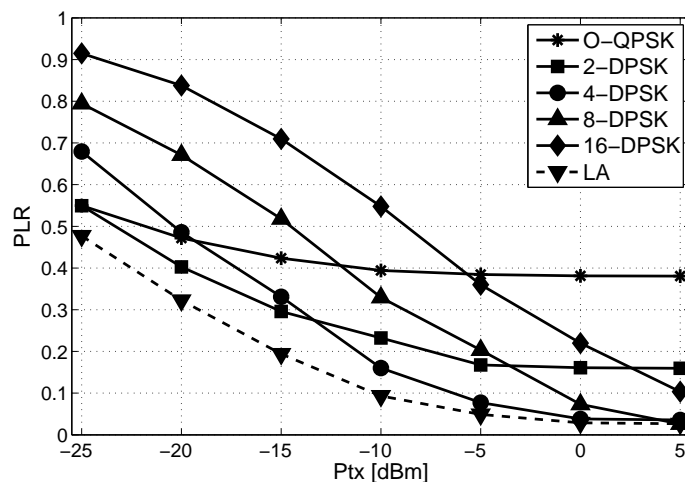
Figure 2.9: Comparison of the PLR for a WBAN with $N = 10$ nodes, for different modulation schemes and for the second proposed LA strategy, SO = 3.
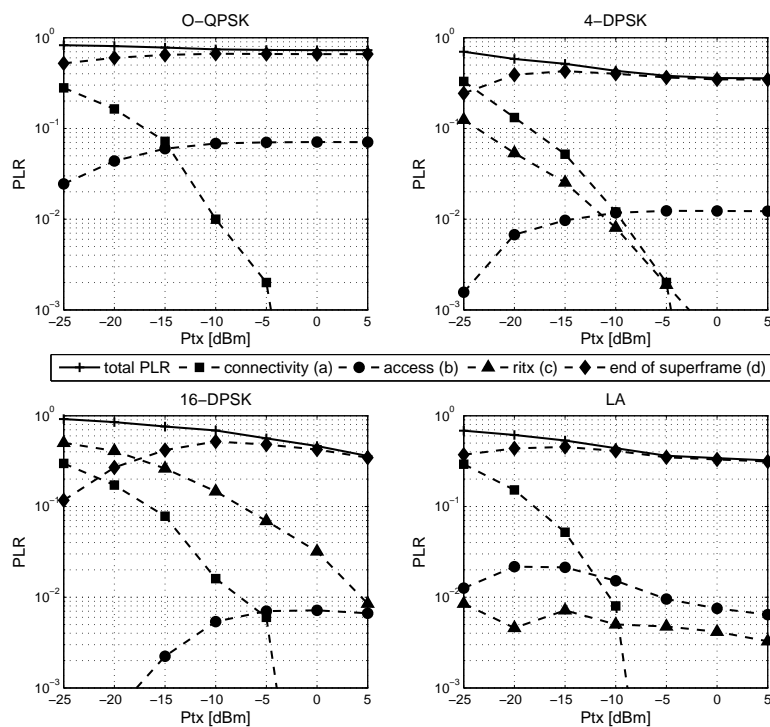
Figure 2.10: Causes of PLR for different modulation schemes and for the second LA strategy, SO = 0.

every modulation, the main cause of losses is the end of the superframe (cause (d)), that means that nodes do not have enough time to get access to the channel. When the superframe duration is longer (SO = 3, Fig. 2.11), losses are due to different causes for the different modulation schemes, as expected. When nodes use O-QPSK, almost all packets are lost because of cause (b): they cannot access the channel within $NB_{max}+1$ attempts, meaning that the channel is found busy with other transmissions. When nodes use 16-DPSK the retransmissions are the main reason for the losses. As already mentioned, in fact, the receiver sensitivity and the protection ratio for this modulation are higher, so packets are not correctly received.
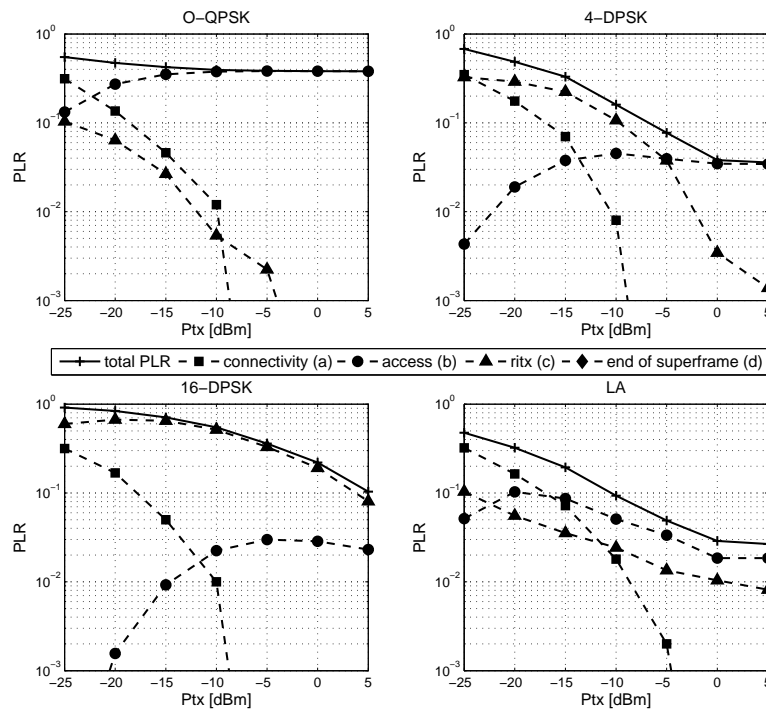
Figure 2.11: Causes of PLR for different modulation schemes and for the second LA strategy, SO = 3.

Finally, Fig. 2.12 shows the percentage of nodes which use the different modulation

schemes when LA is applied. The trend confirms previous considerations: schemes with more modulation levels (that need a higher receiver sensitivity) are used more often when P_{tx} is high.
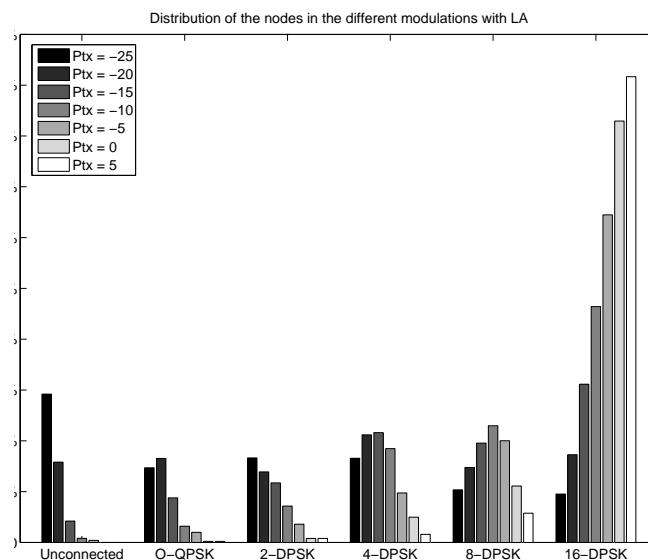
Figure 2.12: Percentages of the nodes using the different modulation schemes for different values of the transmit power when the second proposed LA strategy is applied.

2.2.5 Concluding Remarks

The reported results have shown how the use of LA in the considered WBAN scenario allows a performance improvement in terms of PLR. Packet losses reduction can be important for many applications. However, it has to be underlined that the possibility of applying such LA strategies usually comes at the expenses of a higher energy consumption (modulations characterised by higher bit rates usually require higher currents drained from the power supply) and a more complex hardware implementation of the devices. The impact of the former will be application dependent, a proper tradeoff between tolerable losses and low energy consumption has to be set

case by case. As for the latter, micro-electronics developments are allowing realisation of multi-modulation transceivers even on ultra-miniaturized chips (the Wiser-BAN project is a practical example in this direction), showing that the assumption of availability of different modulation schemes to choose from is feasible and reasonable.

2.3 Carrier Sense Multiple Access with Collision Avoidance Performance in Wireless Body Area Networks

CSMA/CA is one of the most common approaches for random access wireless networks. Indeed, several IEEE standards, among which 802.15.4 and 802.15.6, specify the use of a CSMA/CA algorithm for the contention-based accesses to the channel. In this section, its performance in WBANs is evaluated: first IEEE 802.15.6 standard is considered in a generic on-body scenario and it is compared to IEEE 802.15.4, then WiserBAN scenarios are examined, comparing the two different CSMA/CA algorithms of the mentioned standards and Slotted ALOHA, in realistic situations.

2.3.1 Comparison between IEEE 802.15.6 and IEEE 802.15.4 Standards in a Wearable Wireless Body Area Network Scenario

Reference Scenario

A WBAN composed of wearable sensor devices to monitor body parameters, like the one described in Section 2.2.1 for the evaluation of the LA, is considered. Ten

nodes deployed in different part of the human body (see Fig. 2.1) have to periodically report the measured data to a coordinator, according to a query-based traffic and a star topology.

Two different channel models for the 2.45 GHz band, taken from the IEEE 802.15.6 Channel Model (CM) document [93], are accounted for. They are indicated in the following as CM3 A and CM3 B. According to CM3 A, the path loss, denoted as L, is modeled as:

$$L(d)[\text{dB}] = a \cdot \log_{10}(d) + b + N, \tag{2.3.1}$$

where d is the distance between transmitter and receiver expressed in mm, N is a random Gaussian variable, having zero mean and standard deviation $\sigma_N = 3.8$, and a and b are two constants that depend on the environment under investigation. Considering the values referred to the hospital room case, we have $a = 6.6$ and $b = 36.1$ dB.

According to CM3 B, instead, L follows an exponential decay around the perimeter of the body and it is expressed as:

$$L(d)[\text{dB}] = -10 \cdot \log_{10}(P_0 \, e^{-m_0 \, d} + P_1) + N, \tag{2.3.2}$$

where $P_0 = -25.8$ dB, $m_0 = 2$ dB/cm, $P_1 = -71.3$ dB, and N is a random Gaussian variable, having zero mean and standard deviation $\sigma_N = 3.6$ dB.

The path loss as a function of the distance for these two channel models is shown in Fig. 2.13.

As far as the packet capture model is concerned, the same threshold model described in Section 2.2.1 is accounted for.
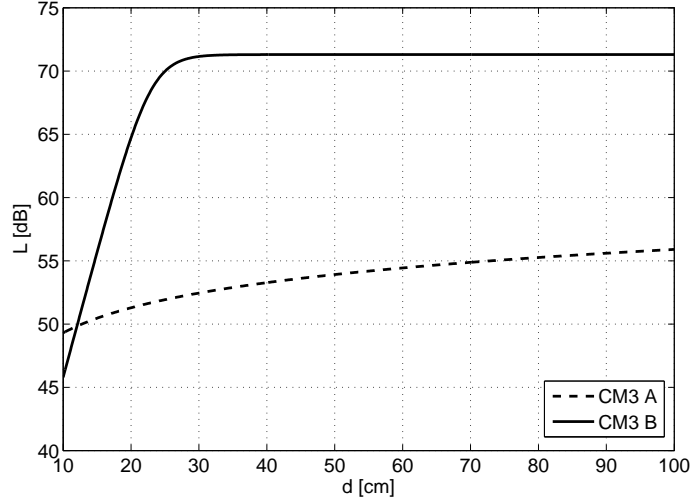
Figure 2.13: Comparison of the path loss for two different channel models from [93].

Physical and Medium Access Control Layers

As for IEEE 802.15.6, the narrowband PHY specified for the ISM 2.45 GHz band is considered, as described in Section 1.1.2. In the following of the section, the different combinations of modulations, coding, and spreading, which lead to the four possible information data rates for this PHY, will be referred to as Modulation and Coding Schemes (MCSs).

Table 2.2 reports the modulation scheme and information data rate for the different MCSs, together with the receiver sensitivity ($P_{\mathrm{R_{min}}}$) and protection ratio ($\frac{C}{I}|_{\mathrm{min}}$) values. The values of $P_{\mathrm{R_{min}}}$ are taken from the draft version of the standard [94], while the values of $\frac{C}{I}|_{\mathrm{min}}$ are estimated starting from the reference value $\frac{C}{I}|_{\mathrm{min}} = 3$ dB for MCS2 ($\pi/2$-DBPSK with no spreading) [95], by adding or subtracting the same amount that also shifts the receiver sensitivity values.

At the MAC layer, the beacon mode with superframes is considered, according to which a beacon is transmitted at the beginning of every beacon period (superframe).

Table 2.2: IEEE 802.15.6 Modulation and Coding Schemes

MCS	Modulation	Information Data Rate [kbit/s]	$P_{\mathbf{R}_{\mathbf{min}}}$ [dBm]	$\frac{C}{I}|_{\mathbf{min}}$ [dB]
0	$\pi/2$-DBPSK	121.4	- 95	- 2
1	$\pi/2$-DBPSK	242.9	- 93	0
2	$\pi/2$-DBPSK	485.7	- 90	3
3	$\pi/4$-DQPSK	971.4	- 86	7

In this way, the beacon will coincide with the query of the coordinator to the nodes of the WBAN under investigation. The superframe is assumed to be composed of a single RAP, during which nodes use CSMA/CA to access the channel, as described in Section 1.1.2. Immediate Acknowledgment (I-Ack) mechanism is considered, according to which the recipient sends back an ACK frame *pSIFS* after the end of a correctly received frame.

At the time this study was carried out, IEEE 802.15.6 was still in a draft form [94], therefore some values used for the parameters were different from what described in Section 1.1.2. Namely, $pCSMASlotLength = 125\,\mu$s and $pSIFS = 50\,\mu$s.

Numerical Results

Results reported hereafter are achieved through a simulator written in C, by simulating 25.000 superframes, meaning 25.000 transmissions from each node to the coordinator, where the shadowing samples on the links (random variable N in Eq.s (2.3.1) and (2.3.2)) are changed every 50 superframes.

The performance for the WBAN described above is evaluated, comparing the different IEEE 802.15.6 MCSs (see Table 2.2) and the performance achieved with

IEEE 802.15.4 standard in beacon enabled-mode [36]. The query of the considered application scenario coincides with the beacon, therefore every node has one packet to send in every superframe. The beacon period is set to 250 ms and nodes are supposed to have all the same user priority, equal to 6, which corresponds to medical data traffic, and which is characterised by $\mathrm{CW}_{\min} = 2$ and $\mathrm{CW}_{\max} = 8$ [41]. The maximum number of frame retransmissions is set equal to three. For IEEE 802.15.4, the MAC parameters are set to the default values provided by the standard and a superframe order of 4 (SO = 4) is considered, which corresponds to a superframe of 245.76 ms. Besides, the receiver sensitivity is equal to -85 dBm [36], and the protection ratio is 1.3 dB [92].

Performance is evaluated in terms of average PLR and average delay.

The PLR represents the probability that a packet generated by a node is not received by the coordinator. This can happen because of different possible causes:

- the node cannot receive the beacon, meaning that it is not connected to the network;

- the node cannot transmit the packet correctly within the three retries ($\frac{C}{I} < \frac{C}{I}|_{\min}$ for 4 subsequent times);

- the node cannot succeed before the end of the superframe.

For IEEE 802.15.4, there is another cause of loss: the channel is found busy for more than five subsequent times while trying to transmit the same packet [36].

Fig. 2.14 shows the PLR as a function of the MAC frame payload that is achieved with the path loss model CM3 A, Eq. (2.3.1). Different values of the transmit power have been simulated: $P_{\mathrm{tx}} = \{-20, -10, 0\}$ dBm; the results obtained were in all cases

equal to the ones reported in this figure. This is due to the fact that the values of
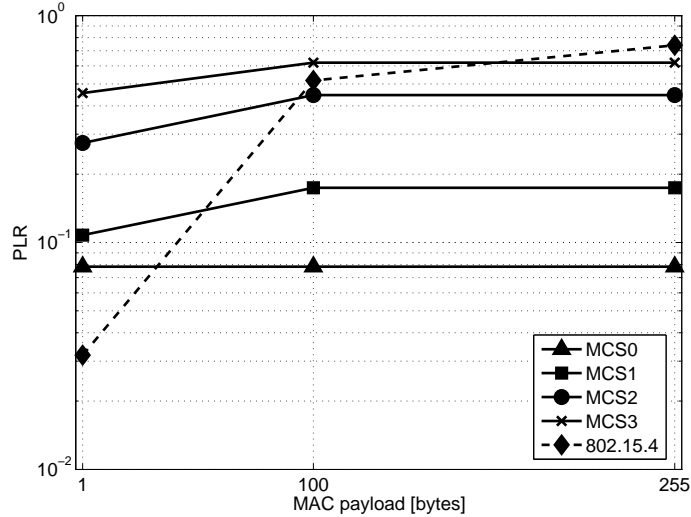
Figure 2.14: Comparison of the PLR for IEEE 802.15.6 MCSs and IEEE 802.15.4, channel model CM3 A, $P_{\text{tx}} = \{-20, -10, 0\}$ dBm.

the path loss for CM3 A are low enough ($L \approx 50$ dB, see Fig. 2.13) to guarantee that the received power is higher than the receiver sensitivity for all the simulated P_{tx}. For CM3 B, instead, the performance changes as P_{tx} varies. Fig.s 2.15 and 2.16 illustrate the PLR obtained with $P_{\text{tx}} = -20$ dBm and $P_{\text{tx}} = 0$ dBm, respectively. In this case, the value of the path loss ($L = 71.3$ dB for $d > 30$ cm, Fig. 2.13) is such that the condition on the receiver sensitivity is not always satisfied when the transmit power is low. From these figures, we can see that the use of different channel models has a great impact on the results. It is thus important to choose the most proper model for every specific scenario in order to have a realistic evaluation of the network performance.

A general consideration on the IEEE 802.15.6 PLR is that the MCSs with lower data rates perform better than the others. This is due to the higher protection ratios of the MCSs characterised by higher data rates, which lead to more losses in case of
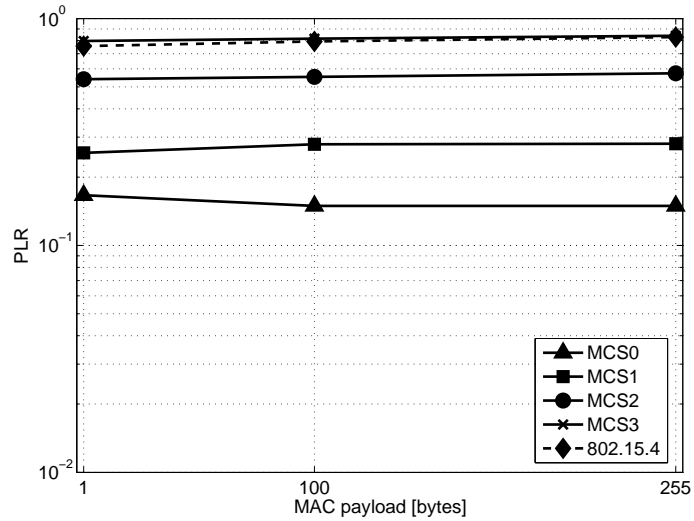
Figure 2.15: Comparison of the PLR for IEEE 802.15.6 MCSs and IEEE 802.15.4, channel model CM3 B, $P_{tx} = -20$ dBm.
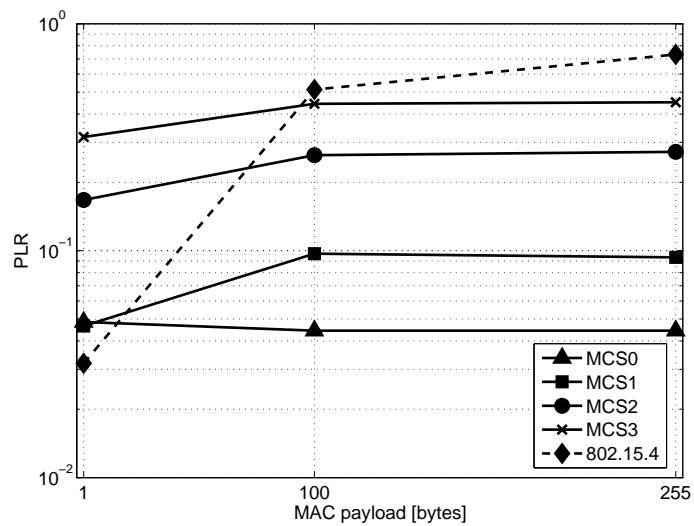
Figure 2.16: Comparison of the PLR for IEEE 802.15.6 MCSs and IEEE 802.15.4, channel model CM3 B, $P_{tx} = 0$ dBm.

collisions. The PLR obtained for CM3 B with $P_{tx} = -20$ dBm (Fig. 2.15) does not depend on the MAC payload. This happens because the main reason for loss in this case is the lack of connectivity: the beacon is received with $P_R < P_{R_{min}}$. As for IEEE 802.15.4, from Fig.s 2.14 and 2.16, we can notice that when the MAC payload is short the achieved performance is better than that of 802.15.6 MCSs, whereas when the payload is longer 802.15.4 PLR is very high. In fact, longer frames occupy the channel for a long time, leading to a higher probability to find the channel busy.

The delay is evaluated as the time elapsed between the reception of the beacon by the node and the correct reception of the node frame by the coordinator. Average delay results are shown in Fig.s 2.17, 2.18, and 2.19, as a function of the MAC payload, for CM3 A, CM3 B with $P_{tx} = -20$ dBm, and CM3 B with $P_{tx} = 0$ dBm, respectively.
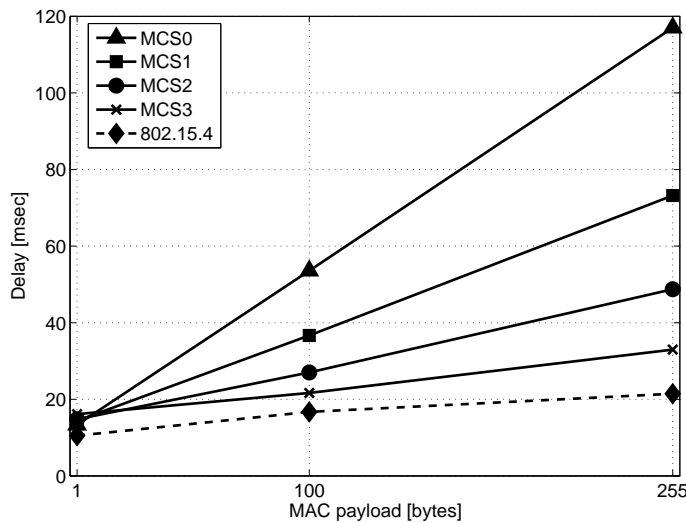
Figure 2.17: Comparison of the delay for IEEE 802.15.6 MCSs and IEEE 802.15.4, channel model CM3 A, $P_{tx} = \{-20, -10, 0\}$ dBm.

In all cases, the delay for MCSs with lower data rates is higher, as expected, since more time is needed to send the frame. Anyway the obtained values are always lower
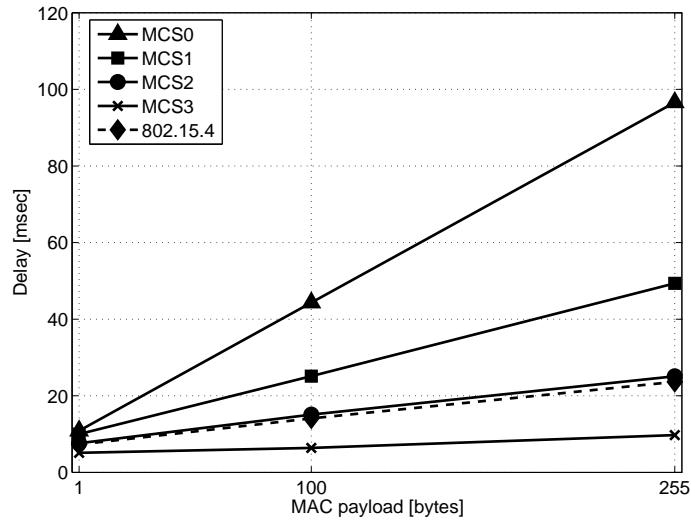
Figure 2.18: Comparison of the delay for IEEE 802.15.6 MCSs and IEEE 802.15.4, channel model CM3 B, $P_{\mathrm{tx}} = -20$ dBm.
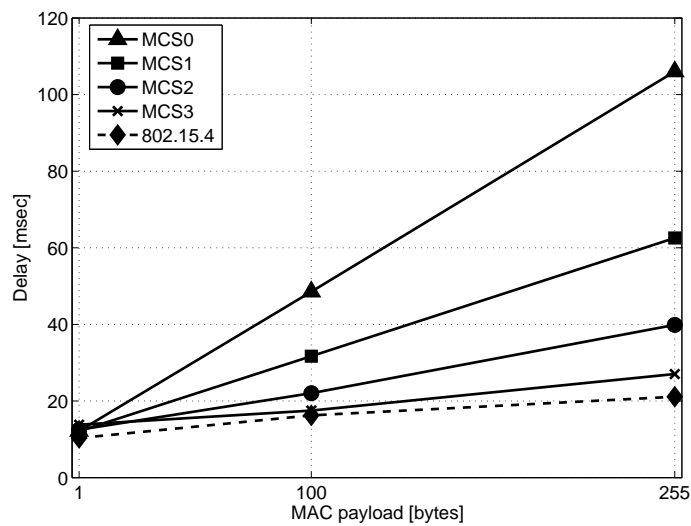
Figure 2.19: Comparison of the delay for IEEE 802.15.6 MCSs and IEEE 802.15.4, channel model CM3 B, $P_{\mathrm{tx}} = 0$ dBm.

than 125 ms, that is the maximum delay reference requirement for WBAN medical applications [16]. For IEEE 802.15.4, in Fig.s 2.17 and 2.19 the delay appears to be lower than that of 802.15.6. This is due to the different CSMA/CA strategy, which allows less nodes to transmit their data on the channel, because some nodes find the channel busy for more than 5 subsequent times, as stated above.

2.3.2 Performance in WiserBAN Scenario

Reference Scenario

In order to compare the performance of the random channel access solutions considered for the CAP according to WiserBAN protocol, extensive simulation campaigns have been performed. Some results will be shown both for CSMA/CA algorithms and Slotted ALOHA. The simulator for the formers was realised in this thesis work, while the latter was analyzed by one of the partners in WiserBAN project.

The reference network topology is a star one, composed of four nodes transmitting data to the RC, which acts as network coordinator. Each of the end-devices is placed in a specific on-body position related to the four WiserBAN use-cases (described in Section 1.1.3), as shown in Fig. 2.20. Nodes on the ears refer to the hearing-aids application or to the cochlear implant one, the node on the heart is related to the cardiac implant use-case, and the hip device accounts for the insulin pump application. As for the RC, it is considered to be placed in three different positions, each one corresponding to an investigated sub-scenario: sub-scenarios A and B are the cases when the RC is held in the left hand and in the right hand, respectively, while in sub-scenario C the RC is located on the thigh position. Both walking and standing situations are accounted for in the evaluation.
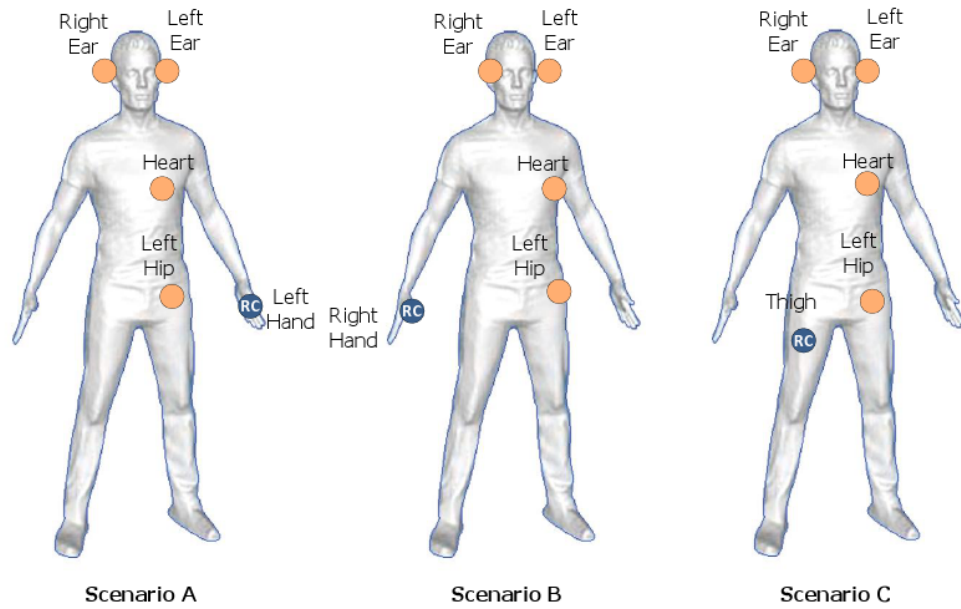
Figure 2.20: WiserBAN sub-scenarios and related nodes positions.
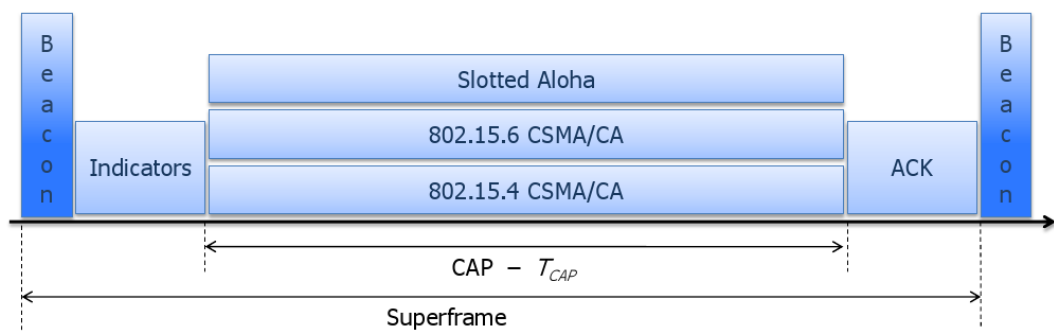
Figure 2.21: Reference WiserBAN superframe structure for the simulations.

A simplified traffic is taken into account, according to which at the beginning of every superframe each node has one packet to send to the coordinator, and packets have all the same length. Only the CAP portion of the superframe is considered to transmit data, as illustrated in Fig. 2.21.

Various simulation campaigns have been carried out in the framework of the project. In the remaining of this section, results for two of them will be reported: a preliminary study and the final more extensive campaign. The main difference between them regards how the propagation is modeled in the simulator. In the preliminary campaign, a joint mobility-channel model for the human body has been considered [96]. In this case, a semi-deterministic channel model is combined with a biomechanical representation of the body, in order to preserve spatial and temporal dependency based on geometrical analysis; the model was benchmarked with measurement data. An average walking speed of 3 m/s has been set in the simulations. As for the second campaign, instead, simulations have been performed using channel gain values derived from measurements realised by one of WiserBAN partners. In fact, a specific real-time measurements campaign was realised in order to characterise the propagation channel for on-body communications. These measurements were repeated using four different human subjects, two males and two females with different physical characteristics, with several scenarios and movements. For the simulation purposes, in particular, two sets of data were used: data acquired in anechoic chamber while the test subject stood still for the entire duration of the experiment, and data acquired in an indoor environment (office premises with general furniture) while the subject walked on a straight line for the duration of the acquisitions. In both

cases, measurements were repeated with two kinds of antenna characterised by a different polarisation: Top Loaded Monopole (TLM), normally polarised with respect to the body surface, and Planar Monopole (PM), tangentially polarised. A complete description of the measurements and their results can be found in [97] and in the project deliverable [98].

Another minor difference between the two simulation campaigns regards the exact nodes emplacement on the body. With respect to what is shown in Fig. 2.20, in the first campaign the node representing the insulin pump was placed on the right hip, instead on the left one, and in sub-scenario C the RC was located on the left thigh. These differences do not lead to meaningful changes in the results, due to the symmetry of the human body.

At the PHY, all the three modulation schemes defined in the framework of WiserBAN project (as detailed in Section 1.1.3) have been considered.

Packet Capture Model

This section illustrates how the packet capture phenomenon is modeled in the simulator. The model takes into account the fact that packets can overlap totally or partially. An example of a partial overlap between two packets is shown in Fig. 2.22.
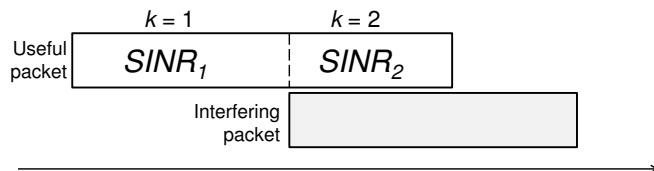
Figure 2.22: Example of packets partial overlap.

For a given packet of interest sent by a WBAN node, several Signal-to-Interference-and-Noise ratio (SINR) values can be computed depending on current variations of interference level. Therefore, for every packet portion k (see Fig. 2.22 for an example), we have:

$$\text{SINR}_k = \frac{P_R}{P_n + P_I},\qquad(2.3.3)$$

where P_R is the useful received power, P_n is the noise power, and P_I is the interfering power.

P_R can be expressed as:

$$P_R = P_T\, G_{\text{on}_u}\, \eta_C\, \eta_{ED},\qquad(2.3.4)$$

considering P_T as the power transmitted by WBAN nodes, G_{on_u} as the on-body channel gain for the useful link, η_C and η_{ED} as antenna factors that take into account the antenna efficiency at the coordinator and at the end-device when placed on the human body. These correction factors are used to consider the efficiency reduction due to the miniaturisation effect, according to the physical limitation of small antennas [99].

P_I is evaluated through:

$$P_I = \sum_m P_T\, G_{\text{on}_m} b_{k_m},\qquad(2.3.5)$$

where G_{on_m} is the on-body channel gain for the m-th link and b_{k_m} is a boolean variable indicating if the m-th interferer is present during the packet portion k (in the example of Fig. 2.22, $b_{1_1} = 0$ and $b_{2_1} = 1$).

For each computed SINR value, the Bit Error Rate (BER) or the Symbol Error Rate (SER) for each portion k is calculated in a different way for every PHY, in order

to derive the Packet Error Rate (PER) according to the following:

$$
\text{PER} =
\begin{cases}
1 - \prod_{k=1}^{N}(1 - \text{SER}_k)^{N_{s_k}} & \text{for PHY 1} \\[3mm]
1 - \prod_{k=1}^{N}(1 - \text{BER}_k)^{N_{b_k}} & \text{for PHY 2,3}
\end{cases}
$$

where N is the number of packet portions ($N = 2$ in the example of Fig. 2.22) and N_{b_k} (N_{s_k}) is the number of bits (symbols) in the portion k.

PHY 1

In this case the SER has to be computed:

$$
\text{SER}_k = \sum_{n=1}^{32} \binom{32}{n} \text{CER}_k^n \, (1 - \text{CER}_k)^{32-n} \cdot P_s(n), \tag{2.3.6}
$$

where $P_s(n)$ is the symbol error probability when n chips are not correctly received (values are taken from [100]) and CER is the Chip Error Rate. The expression of the Chip Error Rate (CER) as a function of the SINR is evaluated here through the formula $\text{CER}_k = \frac{1}{2}e^{-(\text{SINR}_k)^{0.66}}$. The latter has been obtained through the comparison between experimental derivations of [92] and the PER expression found in [100], and minimum least square fitting.

PHY 2

Without spreading, the expression given above (PHY 1) for the CER applies in this case to the BER, owing to the absence of any sort of bit aggregation to form multi-level symbols:

$$
\text{BER}_k = \frac{1}{2}e^{-(\text{SINR}_k)^{0.66}}. \tag{2.3.7}
$$

PHY 3

The following expression, empirically derived for Bluetooth Low Energy PHY [96], is

used:

$$\mathrm{BER}_k = \frac{1}{2} e^{-(\mathrm{SINR}_k)^{0.7}}. \tag{2.3.8}$$

Numerical Results

100 000 superframes have been simulated, meaning 100 000 packets to be transmitted by each node to the RC.

The packet reception decision is based on the PER value calculated as explained in the previous section: considering x as a uniformly distributed random variable in $[0, 1]$, drawn for each packet, if $x \geq$ PER the packet is correctly received, otherwise the packet is lost.

Relevant simulation parameters are shown in Table 2.3.

It can be noticed that the main difference in parameters between the two simulation campaigns lies in transmit power, receiver sensitivity, and antenna efficiency values. In the preliminary study, a reasonable general setting was considered, in order to evaluate the contention access schemes proposed for the CAP. For the second campaign, instead, updated and more precise values have been taking into account, according to hardware development in the project. The numerical values provided may negatively affect the connectivity between nodes and the RC, leading to a performance degradation.

Therefore, results from the preliminary campaign are useful to draw a comparison among the different proposed CAP solutions, but the numerical values obtained could be unrealistic for an actual deployed WBAN. On the other hand, the second campaign brings more realistic results, which have to be analyzed bearing in mind that in some cases losses are not due to the access protocols under consideration but to the lack of

Table 2.3: Simulation parameters for WiserBAN scenario

Parameter	Value		
	First campaign	**Second campaign**	
Transmit power, P_T	- 12 dBm	0 dBm	
Receiver sensitivity	- 87 dBm	PHY 1	- 96 dBm
		PHY 2	- 87 dBm
		PHY 3	- 90 dBm
Coordinator antenna efficiency, η_C	0 dB	- 3 dB	
End device antenna efficiency, η_{ED}	0 dB	- 15 dB	
Current consumption, transceiver on	10 mA		
Current consumption, stand-by	100 nA		
Supply voltage	1.2 V		
PHY header + preamble	121 bits	112 bits	
MAC header + FCS	9 bytes		
Maximum number of retransmissions	3		
CAP duration, T_{CAP}	37 ms		

connectivity.

If not explicitly otherwise stated, walking scenarios are considered.

Results will be reported for the following values of algorithms parameters: for 802.15.6 CSMA/CA, $CW_{\min} = 8$ and $CW_{\max} = 16$; for 802.15.4 CSMA/CA $BE_{\min} = 3$, $BE_{\max} = 5$, and $NB_{\max} = 4$; $CP_{\min} = 1/8$ and $CP_{\max} = 1/4$ for Slotted ALOHA. Outcomes from the preliminary simulations showed, in fact, that these were the values leading to the best performance for the scenarios under investigation.

Fig.s 2.23, 2.24, and 2.25 illustrate the PLR as a function of the MAC payload, from the preliminary simulation campaign, for the three considered PHYs. Results refer to CSMA/CA algorithms as defined in IEEE 802.15.4 (left) and in IEEE 802.15.6
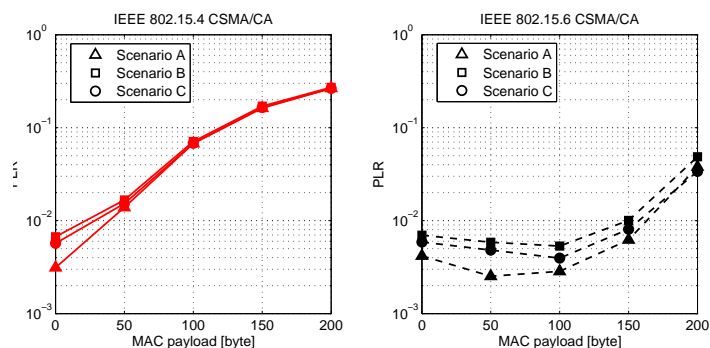
(right).

Figure 2.23: PLR for 802.15.4 CSMA/CA (left) and 802.15.6 CSMA/CA (right), obtained in the first WiserBAN simulation campaign, PHY 1.
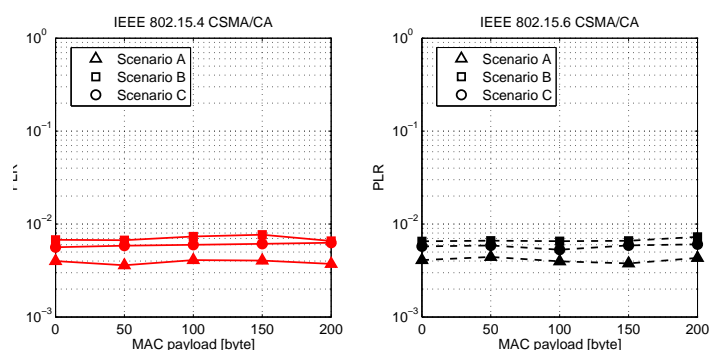
Figure 2.24: PLR for 802.15.4 CSMA/CA (left) and 802.15.6 CSMA/CA (right), obtained in the first WiserBAN simulation campaign, PHY 2.

Firstly, it can be noted that the PLR does not change significantly in the different sub-scenarios. Therefore, for the nodes emplacement under investigation, the RC position does not affect the performance. Then, IEEE 802.15.6 CSMA/CA outperforms 802.15.4 one in these cases. This fact is especially evident with PHY 1. This PHY is characterised by the lowest bit-rate among the ones considered, which leads to longer time needed to transmit a packet over the channel. In this case, 802.15.4 CSMA/CA mechanism, according to which a maximum number of backoff is allowed, leads to a
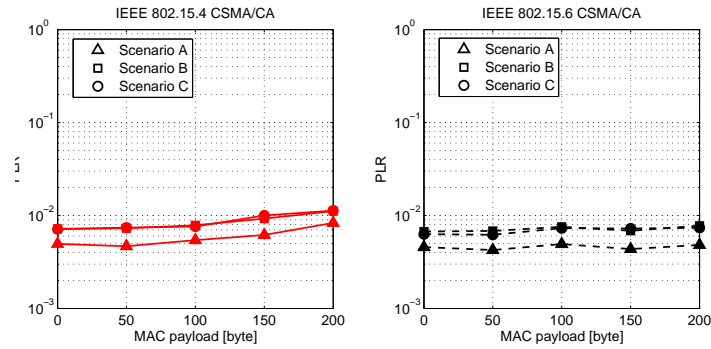
Figure 2.25: PLR for 802.15.4 CSMA/CA (left) and 802.15.6 CSMA/CA (right), obtained in the first WiserBAN simulation campaign, PHY 3.

higher amount of packets lost with respect to 802.15.6, because the channel is often found busy.

An example of average delay obtained in the preliminary simulations is shown in Fig. 2.26. The figure refers to PHY 3, but similar results have been obtained for the other PHYs. Also for this performance metric, the same two considerations drawn above for the PLR apply: RC position does not affect the outcomes and 802.15.6 CSMA/CA performs better than 802.15.4 algorithm.
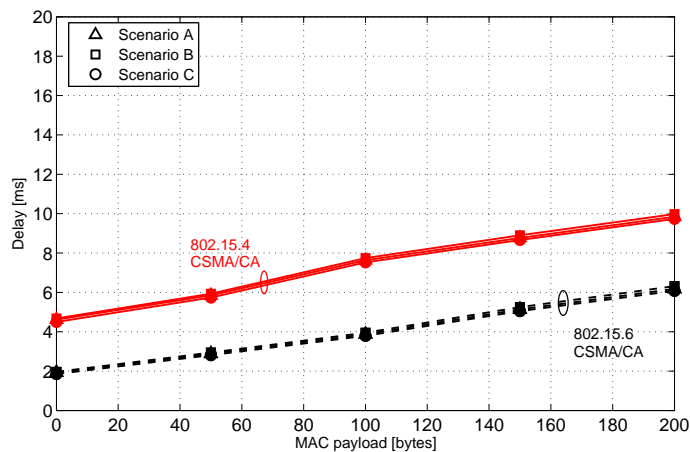
Figure 2.26: Delay for CSMA/CA algorithms, obtained in the first WiserBAN simulation campaign, PHY 3.

Results for the second simulation campaign are reported hereafter. Fig. 2.27 shows the PLR obtained with PHY 3 when TLM antennas are used. Again, the sub-scenario considered only slightly influences the values achieved.
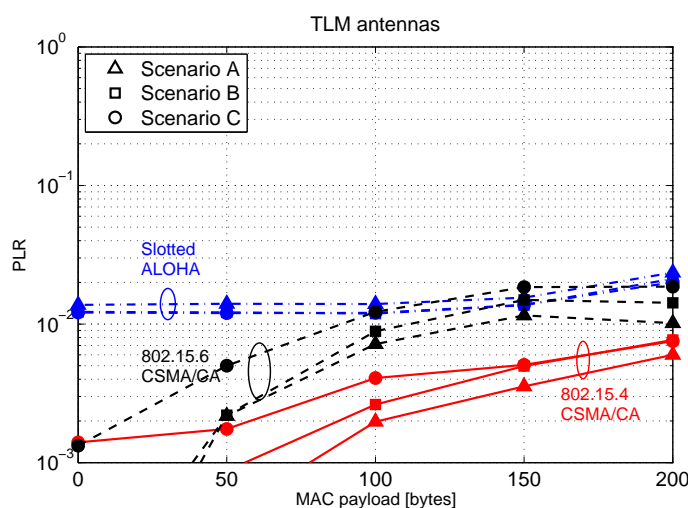
Figure 2.27: PLR for different channel access algorithms, obtained in the second WiserBAN simulation campaign, PHY 3, TLM antennas.

In this case, IEEE 802.15.4 CSMA/CA performs slightly better than 802.15.6 one. This could be explained considering that, with respect to the preliminary campaign, higher path losses among nodes are present (mainly due to the antennas efficiency values), leading to a less effective carrier sensing. This affects 802.15.6 CSMA/CA more since sensing is done for a longer time period. Slotted ALOHA, instead, is characterised in general by the worst PLR performance.

If a comparison with PLR obtained with PM antennas (presented in Fig. 2.28) is drawn, it can be noticed that PM antennas lead to worse PLR values. This confirms what was expected from the channel measurements; indeed, for their particular propagation and radiation characteristics, PM antennas present lower channel gain

values as compared to TLM, which results in a higher attenuation among nodes causing connectivity problems. TLM antennas present, in fact, a normal polarisation with respect to the body surface, which helps creeping waves propagation around the body [97].
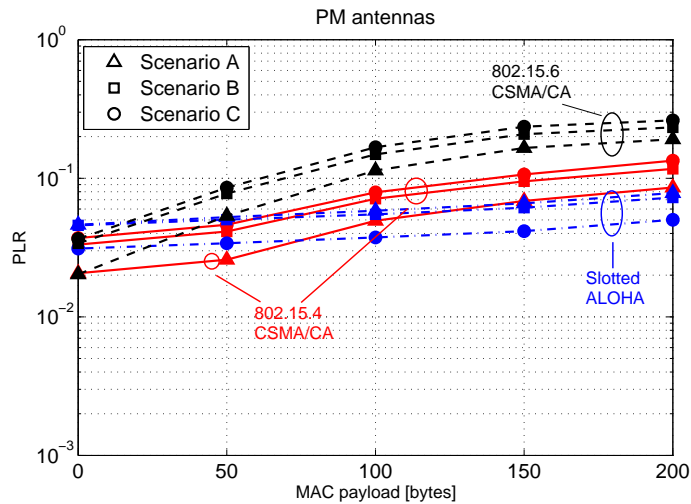
Figure 2.28: PLR for different channel access algorithms, obtained in the second WiserBAN simulation campaign, PHY 3, PM antennas.

This effect is confirmed in Fig. 2.29, where each curve represents a possible cause for packet loss, for CSMA/CA algorithms in sub-scenario A. It is possible to note that when the PM antennas are used (figures above), 2% of losses are due to connectivity problems; whereas, in the TLM case (figures below), packets are lost mainly because of collisions or maximum number of backoffs reached, and no problems related to high path loss values are present at all.

The PLR obtained for the other PHYs, using TLM antennas in sub-scenario A, is illustrated in Fig. 2.30, and the different causes are highlighted in Fig. 2.31.

As for PHY 1, the trends confirm what already stated for the preliminary results. PHY 2 PLR is comparable with the one achieved with PHY 3. Slotted ALOHA
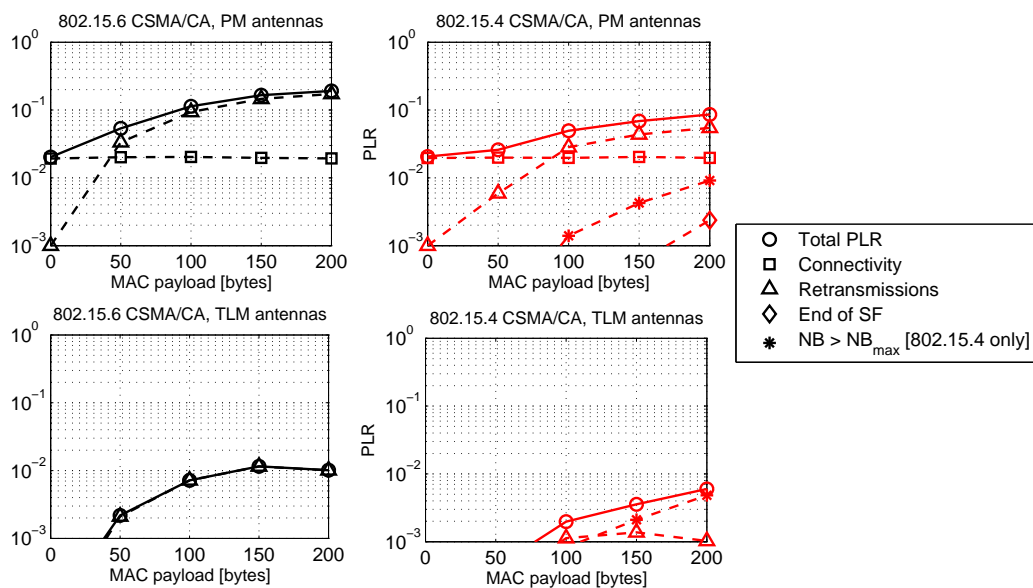
Figure 2.29: PLR causes, for 802.15.6 CSMA/CA (left) and 802.15.4 CSMA/CA
(right) algorithms, PM (above) and TLM (below) antennas, obtained in the second
WiserBAN simulation campaign, PHY 3, scenario A.
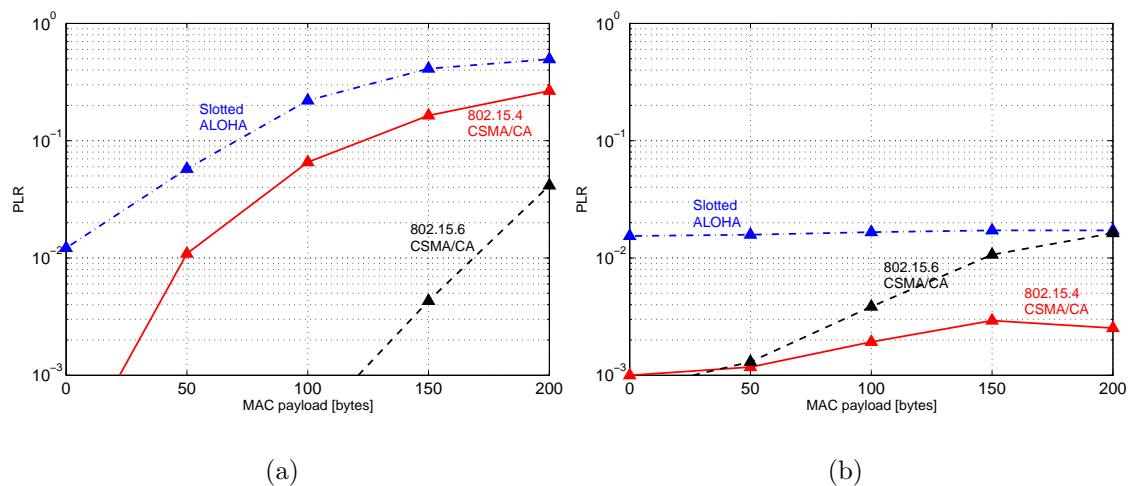
Figure 2.30: PLR for different channels access algorithm, obtained in the second
WiserBAN simulation campaign, with (a) PHY 1 and (b) PHY 2, TLM antennas,
scenario A.
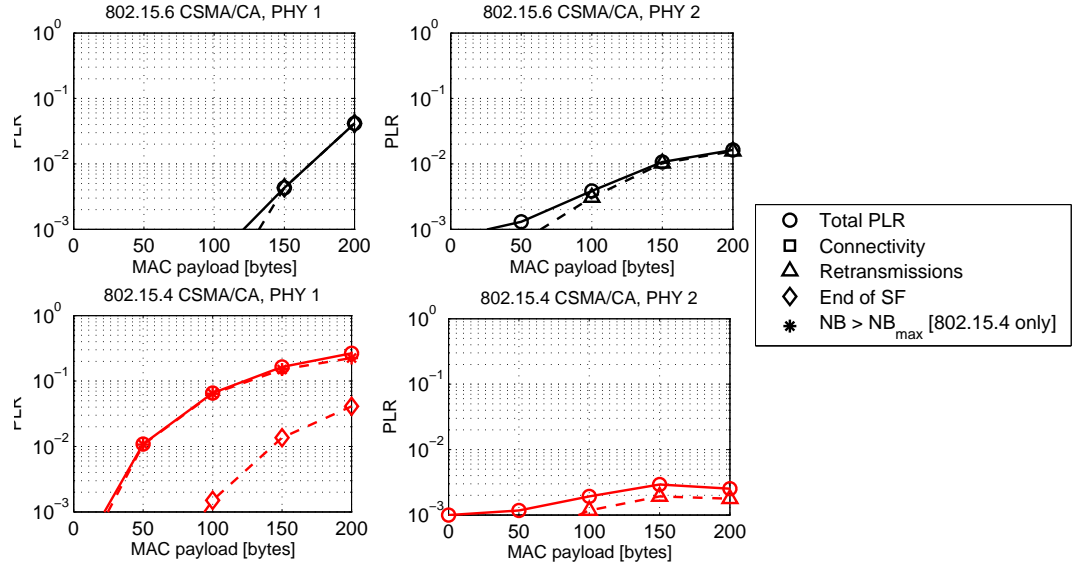
Figure 2.31: PLR causes, for 802.15.6 CSMA/CA (above) and 802.15.4 CSMA/CA (below) algorithms obtained in the second WiserBAN simulation campaign, with PHY 1 (left) and PHY 2 (right), TLM antennas, scenario A.

always shows the worst performance.

A comparison between performance obtained in walking and standing scenarios is reported in Fig. 2.32. In general, the performance attained is worst in the latter case. This is due to the fact that when the person is standing still, if there is not connectivity in one link (i.e., the received power is lower than the receiver sensitivity), this situation will never change during the duration of the simulations. On the contrary, when the subject walks, the obtained PLR is averaged among different relative positions of the nodes (corresponding to different channel gains), leading to an overall lower PLR.

Some simulations were performed considering an antenna efficiency reduction of -35 dB for the device located in the heart position, in order to take into account the in-body channel attenuation, from the heart to the body surface. This particular value was set considering a typical efficiency for implanted antennas [98]. The underlying
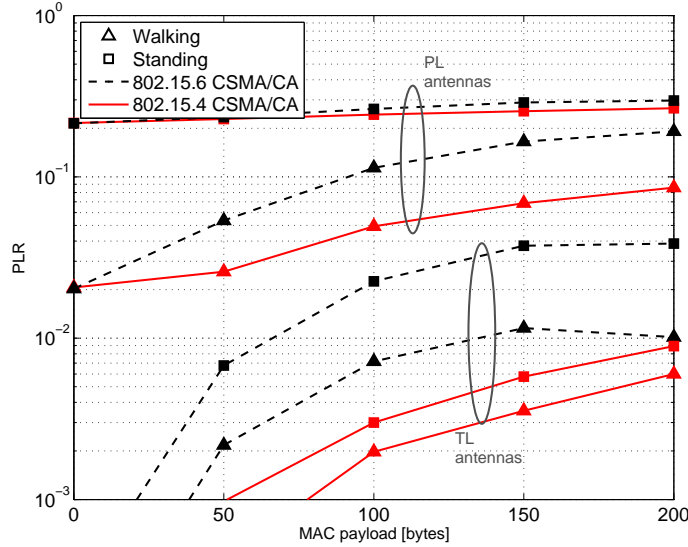
Figure 2.32: Comparison of the PLR in standing and walking cases for CSMA/CA algorithms, obtained in the second WiserBAN simulation campaign, PHY 3, scenario A.

assumption is that the implanted antenna radiation pattern is not modified with respect to the case when the node is placed on-body, and just an efficiency reduction is considered. Fig. 2.33 shows the values of PLR obtained using 802.15.4 CSMA/CA with TLM antennas in sub-scenario A, where each curve refers to a specific node position. The degradation of the performance is evident for the heart link when considering the efficiency reduction (dashed line with squares) if compared to the case where it was not taken into account (continuous line). In the former situation, in fact, the implanted device is not able to directly reach the coordinator in most of the cases.

In order to evaluate how the end-device antenna efficiency, η_{ED}, affects the system performance, an additional set of simulations was performed setting this parameter to different values, from -15 dB to -21 dB with a resolution of 2 dB, whereas the coordinator antenna efficiency, η_C , was set to -3 dB as before (Table 2.3). As
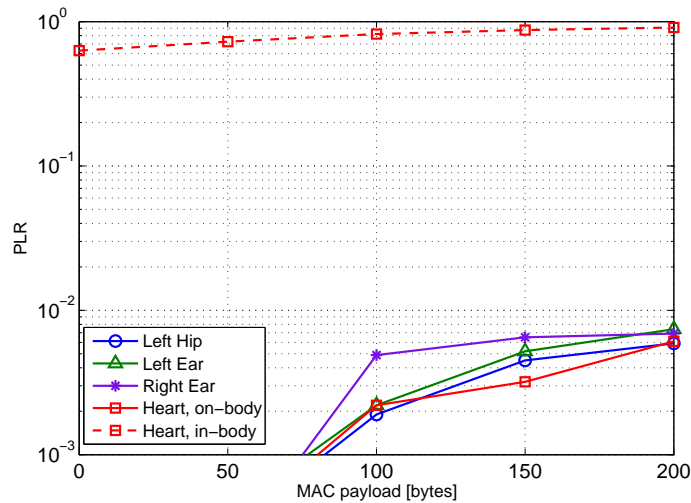
Figure 2.33: PLR per node for IEEE 802.15.4 CSMA/CA algorithm, obtained in the second WiserBAN simulation campaign, PHY 3, TLM antennas, scenario A.

expected, the PLR increases as the efficiency decreases, since the received power results to be lower, causing connectivity problems (see Fig. 2.34 for results obtained with 802.15.6 CSMA/CA). It is important to remark that antennas miniaturisation implies smaller efficiencies and hence Fig. 2.34 could be useful to define a proper trade-off between network performance and antenna size, considering that the size issue is of primary importance in WBAN context.

Delay results are reported in Fig.s 2.35 and 2.36. In the former, the different contention access schemes are compared, when PHY 3 is used. In the latter, 802.15.6 CSMA/CA values obtained for the different PHYs are plotted. IEEE 802.15.6 CSMA/CA, achieving the lowest delay values, is the best protocol solution from the delay viewpoint. For the specific case shown in Fig. 2.35 ALOHA delay is lower than 802.15.4 one for short payloads (i.e. < 140 bytes), whereas for longer payloads the situation is the opposite. As expected, when the PHY is varied, lower delay values are achieved when higher bit-rates are used (recalling that PHY 2 has
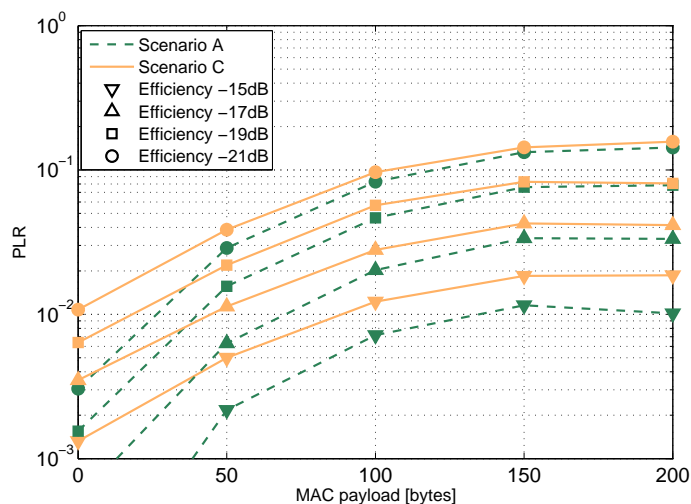
Figure 2.34: PLR for IEEE 802.15.6 CSMA/CA algorithm, obtained in the second WiserBAN simulation campaign, PHY 3, TLM antennas with varying efficiency.

the highest bit-rate, equal to 2 Mbit/s, while for PHY 3 the bit-rate is 1 Mbit/s, and PHY 1 is characterised by the lowest value, equal to 250 kbit/s).

The average energy consumed by the devices to complete their transmissions is presented in Fig. 2.37, for the different channel access schemes, when PHY 3 is used. From the energy consumption point of view, Slotted ALOHA is generally the best option, being the less consuming one among the three under investigation. This is due to the lack of backoff and sensing operations, with respect to CSMA/CA algorithms. Fig. 2.38 reports the comparison of consumptions for the different PHYs, with 802.15.6 CSMA/CA. Considerations parallel to the ones stated for the delay apply: when the bit-rate is higher, less energy is consumed, since the time needed to send a packet is lower, and thus the time spent with the transceiver on.
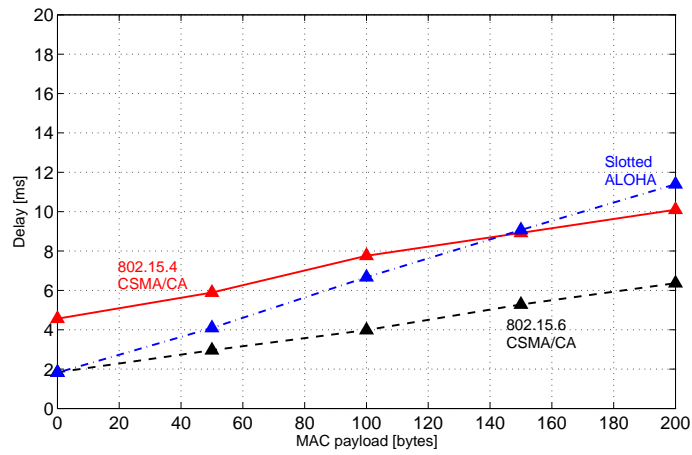
Figure 2.35: Delay for different contention access algorithms, obtained in the second WiserBAN simulation campaign, PHY 3, TLM antennas, scenario A.
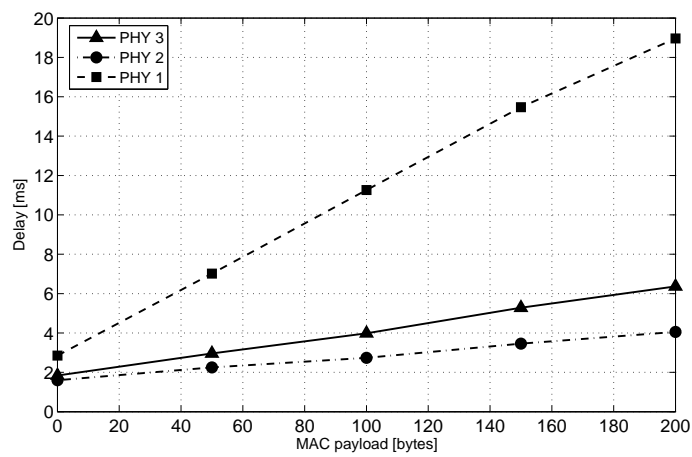
Figure 2.36: Delay for 802.15.6 CSMA/CA algorithm, obtained in the second simulation campaign with the different PHYs, TLM antennas, scenario A.
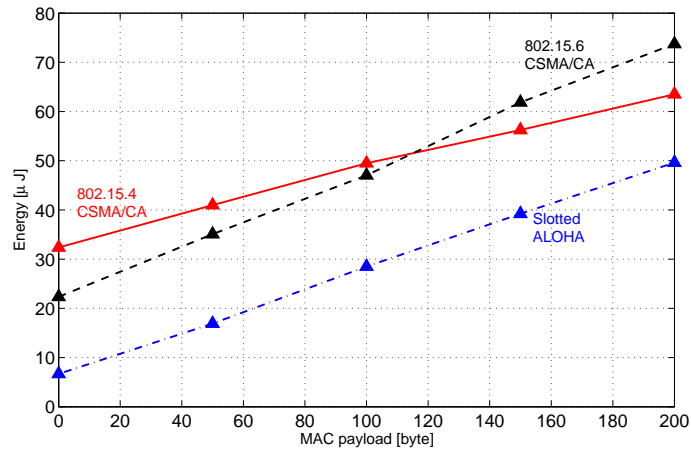
Figure 2.37: Average energy consumption for different contention access algorithms, obtained in the second WiserBAN simulation campaign, PHY 3, TLM antennas, scenario A.
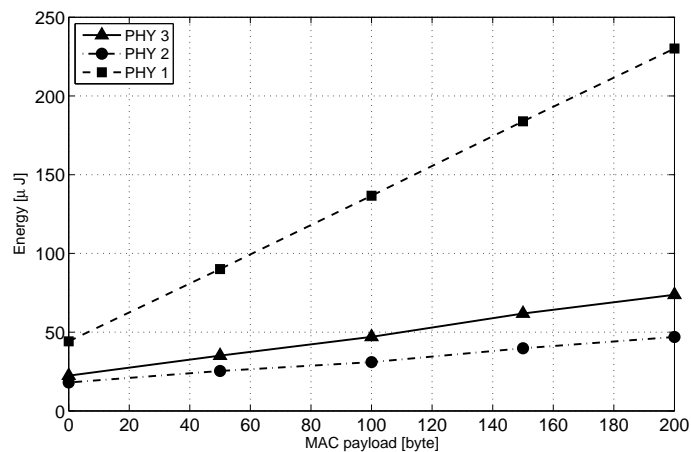
Figure 2.38: Average energy consumption for 802.15.6 CSMA/CA algorithm, obtained in the second WiserBAN simulation campaign with the different PHYs, TLM antennas, scenario A.

Validation of Simulation Results

In order to validate the simulation results, a set of experiments was performed in collaboration with other researchers of the working group. The Texas Instruments CC2530 platform was used. The chip contains an IEEE 802.15.4-compliant transceiver, working in the 2.45 GHz band [101]. The access to the channel is managed through the superframe shown in Fig. 2.21 and using the 802.15.4 CSMA/CA protocol in the CAP portion. As in the case of simulations, experiments were performed by locating five CC2530 devices (one coordinator and four end-devices) on a human subject, according to the simulated sub-scenario B (see Fig. 2.20). The coordinator, located on the right hand, periodically sends beacon packets and waits for replies from devices. As for the packet sizes, the beacon is composed of 20 bytes, whereas the data packets size is equal to 17 bytes (including PHY and MAC headers) plus the MAC payload (different payload lengths have been considered). For fair comparison with simulations, the transmit power was set equal to -22 dBm, instead of 0 dBm, to compensate the different antennas efficiency: the antennas used in the experiments have an efficiency of 4.1 dB at both the transmitter and the receiver.

Acquisitions were performed in an indoor environment while the human subject performed several continuous walking cycles.

Numerical results, in terms of PLR and average delays, were achieved by averaging over 10 000 packets transmitted by each end-device towards the coordinator.

Fig. 2.39 shows the PLR as a function of the MAC payload. The dashed line presents the values obtained from the experiments, while the continuous curve refers to the simulated results achieved considering PHY 1 and 802.15.4 CSMA/CA. This figure demonstrates a good agreement between simulation and experimental results;

97

the slight differences when comparing the two curves can be explained considering how differently the connectivity can affect the results. Indeed, the antennas used in the experiments and in the measurements campaign used for the simulations present different radiation characteristics, even if the polarisation is the same. Equivalent considerations can be done for the exact node emplacement and the environment considered in the two cases.

In Fig. 2.40 the comparison between simulated (continuous curve) and measured (dashed line) average delay, as a function of the packet payload, is presented. Also in this case, the curves follow the same trend, confirming the reliability of the numerical results obtained, except for a constant delay difference of approximately 5 ms. This has been proved to come from the inner data processing delays, which are not taken into account in the simulations.
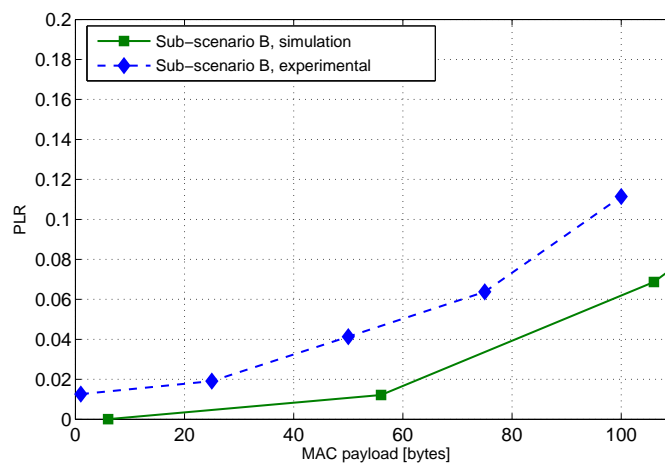
Figure 2.39: Comparison of simulated and experimental PLR results for 802.15.4 CSMA/CA, PHY 1, TLM antennas, scenario B.
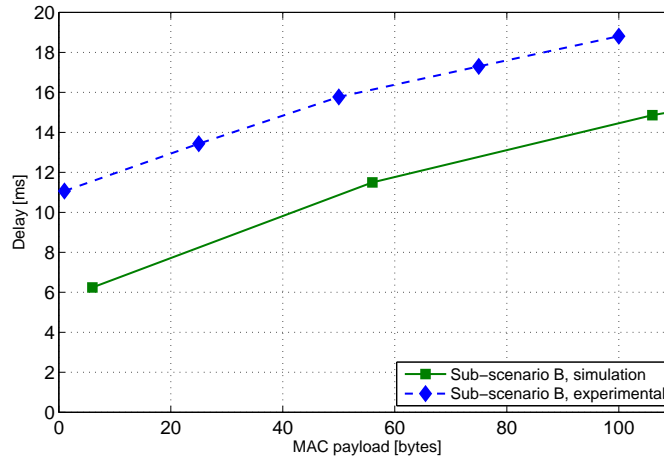
Figure 2.40: Comparison of simulated and experimental delay results for 802.15.4
CSMA/CA, PHY 1, TLM antennas, scenario B.

2.3.3 Concluding Remarks

Comparison of IEEE 802.15.6 and IEEE 802.15.4 standards for a wearable WBAN
and of different random channel access algorithms in WiserBAN scenarios has con-
firmed that a single optimum solution for diverse WBAN applications does not exist.
Depending on the performance metric of interest (PLR, delay, or energy consump-
tion), on the PHY layer used, on the movements of the subject, and on the antenna
polarisation, the "best" MAC algorithm may vary. Therefore flexible protocols al-
lowing a choice among different possibilities (as proposed in WiserBAN project) are
encouraged. The results obtained in this section can help in this choice, depending on
the application requirements. As a general consideration, CSMA/CA solutions are
preferred when PLR is of primary relevance, whereas Slotted ALOHA allows lower
energy consumption values.

The impact of proper channel characterisation on network performance at MAC
layer has also been demonstrated, together with the effect of antenna properties, such

as gain and polarisation, on the results.

2.4 Coexistence Issues

This section deals with coexistence issues that may arise for WBANs, since the 2.45 GHz band is already used by different wireless networks. In particular, IEEE 802.11 and IEEE 802.15.4 interference are considered. Firstly, the interfering systems are characterised both in the frequency and in the time domains. Then, the coexistence of a WBAN with these networks is assessed via simulations. The WiserBAN protocol stack is taken into account, therefore the performance is evaluated for three different modulation schemes at the PHY and two CSMA/CA algorithms at the MAC.

2.4.1 Reference Scenario

The reference WBAN scenario is a network composed of four nodes and a RC, as illustrated in Fig. 2.41.

The scenario defined for coexistence evaluation is shown in Fig. 2.42: in a room of 3m x 3.5m, a person wearing a WBAN is walking according to the trajectory represented by the arrow. In order to evaluate the coexistence with IEEE 802.11, a Wi-Fi access point (AP) and a notebook are located in the room (Fig. 2.42 left), while a Zigbee coordinator (ZC) and 4 Zigbee end-devices (ZEDs) are present (Fig. 2.42 right) to assess the performance achievable with IEEE 802.15.4 interference. The AP and the ZC are positioned at a height of 3 m, whereas the notebook and the ZEDs are at an average height of 0.8 m.

The same joint mobility-channel model for the human body, which was described
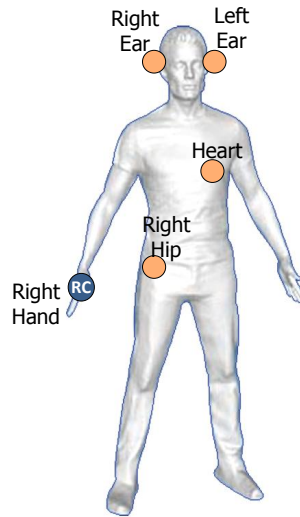
Figure 2.41: WBAN reference scenario for coexistence evaluation.
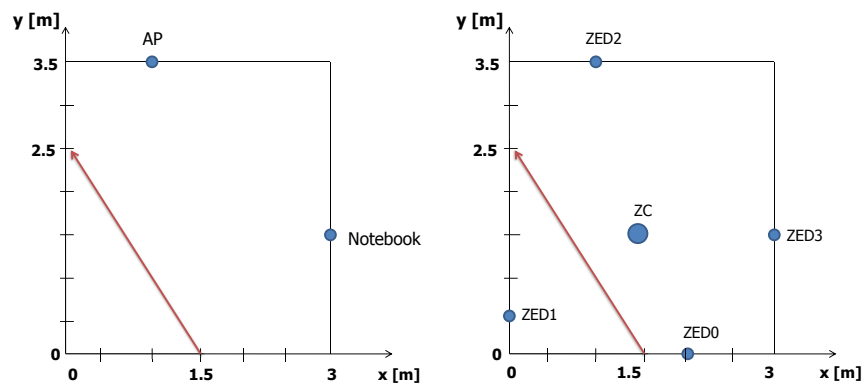
Figure 2.42: Reference scenario for WBAN coexistence evaluation with IEEE 802.11 (left) and with IEEE 802.15.4 (right).

in the previous section and used for the preliminary WiserBAN simulation campaign, is considered.

As for the channel model from the interfering devices to the WBAN nodes, the path loss, L, at a distance d, is evaluated in dB as:

$$L_{\mathrm{dB}}(d) = k_0 + k_1 ln(d), \tag{2.4.1}$$

where $k_0 = 40$ dB and $k_1 = 13.03$ (values obtained for the frequency of 2.45 GHz and a propagation exponent equal to 3).

2.4.2 Interference Characterisation

The sources of interference considered are IEEE 802.11 (Wi-Fi) and IEEE 802.15.4 (Zigbee). The interference has been characterised both in the frequency and in the time domain. The frequency characterisation, for the above mentioned interference sources, can be derived from the standards, while time characterisation has been performed through specific measurements. For the following studies it is considered that the WBAN can operate in 16 different frequency channels in the 2.45 GHz ISM band, which are characterised by:

- center frequencies: $f_c = 2405 + i \cdot 5$ [MHz], $i = \{0, \ldots, 15\}$;

- bandwidth: $B = 5$ MHz, when MSK modulation is used (PHY 1 and 2); $B = 2$ MHz, when GMSK modulation is used (PHY 3).

Frequency Characterisation

In order to have a frequency characterisation of the considered interference sources to be used as input for the simulator, the percentage of interfering power falling into

WBAN receiver band, denoted as $p_{int}^{(i,j)}$, has been computed. Indexes (i) and (j) refer to the channel used by the WBAN and by the interfering network, respectively. Due to the different bandwidth of WBAN and interfering channels, in fact, complete or partial channel overlapping may occur. A graphical example of channel overlapping with IEEE 802.11 is reported in Fig. 2.43, for WBAN MSK PHYs.
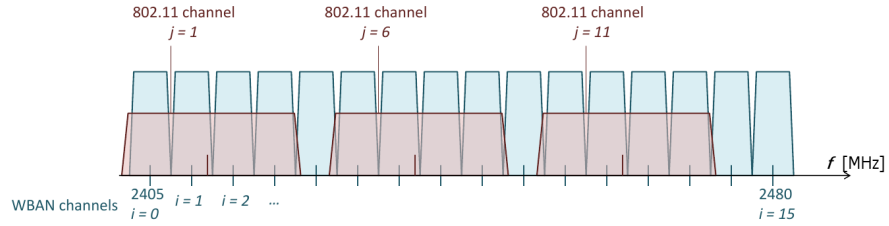
Figure 2.43: Example of overlapping between IEEE 802.11 and WBAN channels.

Indicating with $W(f)$ the power spectral density of the interfering signal and with $F_r(f)$ the receiver filter transfer function, we have:

$$p_{int}^{(i,j)} = \frac{1}{\int_{-\infty}^{+\infty} W^{(j)}(f)df} \cdot \int_{B^{(i)}} W^{(j)}(f)|F_r(f)|^2 df. \qquad (2.4.2)$$

In the following, an ideal receiver filter is assumed:

$$|F_r(f)| = \begin{cases} 1 & \text{if } f \in B^{(i)} \\ 0 & \text{otherwise} \end{cases} \qquad (2.4.3)$$

As for IEEE 802.11, the power spectral density is assumed to be compliant with the mask reported in Fig. 2.44 and the 13 frequency channels defined for operation in Europe at 2.45 GHz [46] are considered. The values of p_{int} obtained for WBAN channels $i = \{8, 9\}$ are shown in Table 2.4.

As for IEEE 802.15.4, the center frequencies defined in the standard for operation at 2.45 GHz are the same used for the WBAN network in this study, therefore all
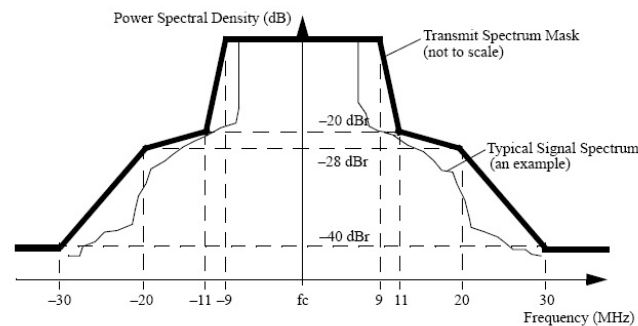
Figure 2.44: IEEE 802.11 transmit power spectrum mask [46].

the power transmitted by 802.15.4 devices falls into the WBAN receiver band when PHY 1 or 2 are considered, whereas only the 2/5 of the power will be source of interference when PHY 3 is used ($B = 2$ MHz), assuming that 802.15.4 signal is characterised by a 5 MHz bandwidth.

Time Characterisation

In order to characterise the traffic generated by an IEEE 802.11 network in the time domain, some experiments have been carried out. The traffic between an AP and a notebook, positioned at a distance of 2 m and in Line-of-Sight condition, has been measured using the network protocol analyzer Wireshark Version 1.6.2 [102]. Three different traffic flows have been evaluated:

- *no traffic*, in this modality only synchronisation packets are supposed to be exchanged;

- *web browsing*, that refers to simple navigation operations: alternating the opening of web pages with their reading;

- *heavy traffic*, meaning a more intense web navigation and the download of files

Table 2.4: Percentage of interference from IEEE 802.11 channels on WBAN channels

		PHY 1, 2		PHY 3	
		WBAN channel		WBAN channel	
		8	9	8	9
IEEE 802.11 channel	**1**	0.010	0.002	0.004	0.001
	2	0.028	0.010	0.011	0.004
	3	0.086	0.028	0.034	0.011
	4	0.508	0.086	0.081	0.034
	5	22.06	0.508	9.93	0.081
	6	24.82	22.06	9.93	9.93
	7	24.82	24.82	9.93	9.93
	8	24.52	24.82	9.93	9.93
	9	2.98	24.52	0.090	9.93
	10	0.109	2.98	0.044	0.090
	11	0.032	0.109	0.013	0.044
	12	0.014	0.032	0.005	0.013
	13	0.003	0.014	0.001	0.005

with dimensions up to 20 Mbytes.

All the above mentioned traffic modalities have been measured for a time interval of 5 minutes.

Similarly, an IEEE 802.15.4 (Zigbee) network of Freescale MC1322x devices has been set up. The devices implement the BeeStack protocol stack (Zigbee compliant, as it is defined by Freescale [103]). In order to measure the traffic exchanged between the devices, Daintree SNA software [104] has been used. Experiments were carried out for different numbers of ZEDs in the network, respectively 1, 2, and 4. The network was programmed to emulate a simple common monitoring application and

traffic exchanged could be described as follows:

- the ZC broadcasts a Time Synchronisation and Route Request (RREQ) packet every 60 s;

- each ZED replies to every received RREQ with a Route Response packet, broadcasts a Link Status frame every 15 s, and sends to the ZC a Report frame every 30 s.

Packet Capture Model

The same packet capture model described in the previous section is used. In this case, however, the interference power, P_I, in the computation of the SINR, see Eq. (2.3.3), takes into account both the power coming from other WBAN nodes, denoted as $P_{I_{\text{on}}}$, and the power coming from external interfering devices, indicated as $P_{I_{\text{off}}}$:

$$P_I = P_{I_{\text{on}}} + P_{I_{\text{off}}}. \tag{2.4.4}$$

$P_{I_{\text{on}}}$ is evaluated through Eq. (2.3.5), whereas $P_{I_{\text{off}}}$ is similarly computed as:

$$P_{I_{\text{off}}} = \sum_l P_l^{(j)} G_{\text{off}}^{(j)} \, p_{int}^{(i,j)} \, b_{k_l}, \tag{2.4.5}$$

where $P_l^{(j)}$ is the power transmitted by the l-th external interferer on channel (j), b_{k_l} is a boolean variable indicating if the l-th interferer is present during the packet portion k (see Fig. 2.22), and G_{off} is the off-body channel gain, given by $G_{\text{off}} = 1/L$, with L modeled according to Eq. (2.4.1).

2.4.3 Numerical Results

In order to evaluate the performance of the WBAN when interference is present, simulations (achieved through a C written simulator) have been performed. 100 000

superframes have been simulated, meaning 100 000 packets to be transmitted by each node to the RC.

Simulation parameters have been set as for the second WiserBAN campaign, reported in the previous section (see Table 2.3).

The interference characterisation described above has been integrated into the simulator through the proper consideration of p_{int} and b_k terms for the computation of the interfering power in Eq. (2.4.5). The captured traffic time patterns have been used to define b_k evolution in time.

For the results obtained in presence of IEEE 802.11 interference, we use the *heavy traffic* flow from the time characterisation measurements; *Case 1* and *Case 2* in the following figures refer to two different values of p_{int} (different WBAN-802.11 channels overlapping), that for PHY 1 and 2 are 0.028% and 24.82%, corresponding to an interfering power fraction equal to -15 dBm and +14 dBm, respectively (considering a total transmit power for 802.11 devices set to +20 dBm), while for PHY 3 they are equal to 0.011% and 9.93%, corresponding to an interfering power fraction equal to -20 dBm and +10 dBm.

As for performance achieved with IEEE 802.15.4 interference, instead, the interference transmit power is equal to 0 dBm and *Case 1* refers to an 802.15.4 network composed of only 2 nodes (ZC and Dev3), while *Case 2* indicates a networks with all the nodes shown in Fig. 2.42 (right).

Fig.s 2.45 and 2.46 show the PLR obtained when PHY 1 is used, as a function of MAC payload, for 802.15.4 CSMA/CA and 802.15.6 CSMA/CA, respectively.

It can be noticed that, as expected, the PLR is higher when interference sources are present, and this is more evident for IEEE 802.11 interference, since the traffic
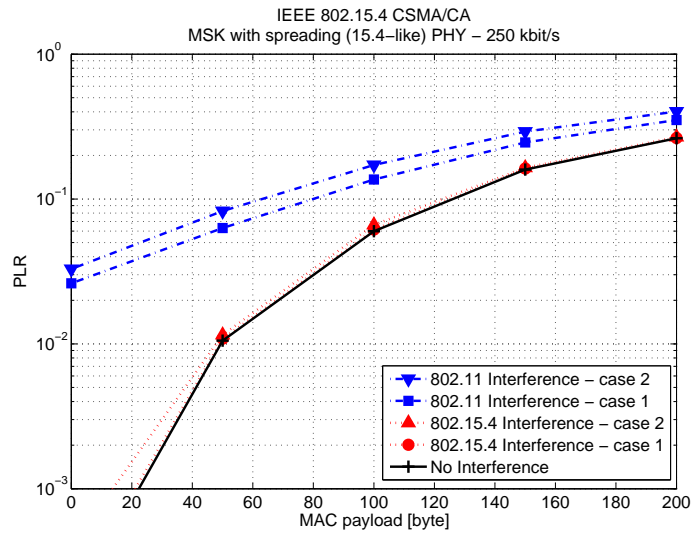
Figure 2.45: PLR for IEEE 802.15.4 CSMA/CA with interference, PHY 1.
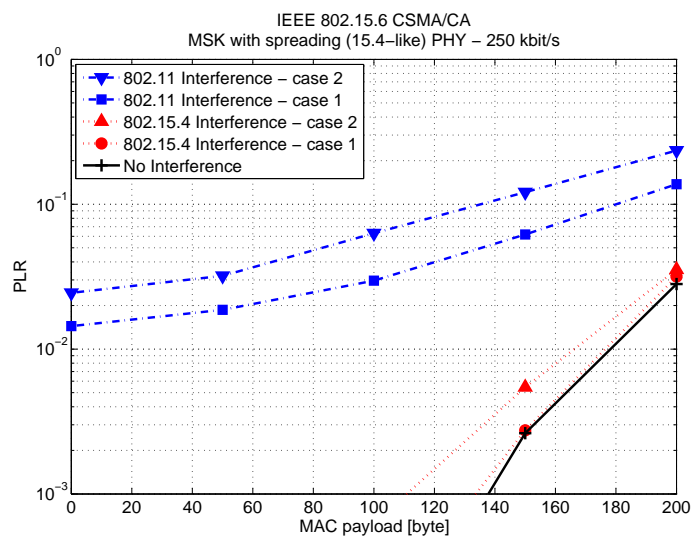
Figure 2.46: PLR for IEEE 802.15.6 CSMA/CA with interference, PHY 1.
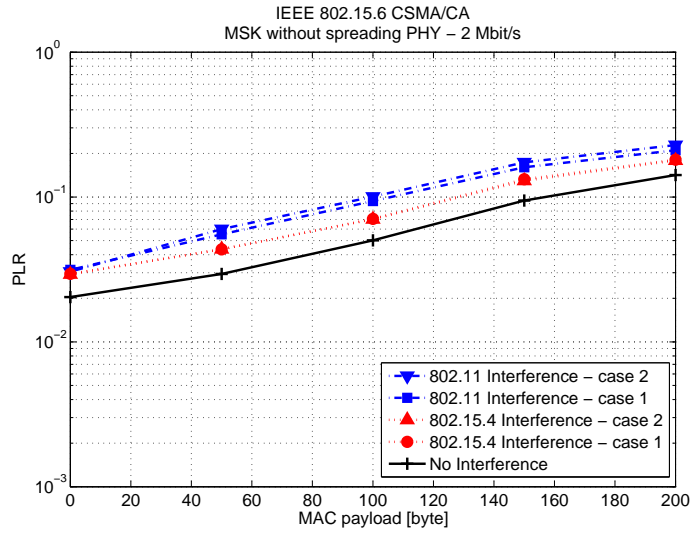
Figure 2.47: PLR for IEEE 802.15.6 CSMA/CA with interference, PHY 2.
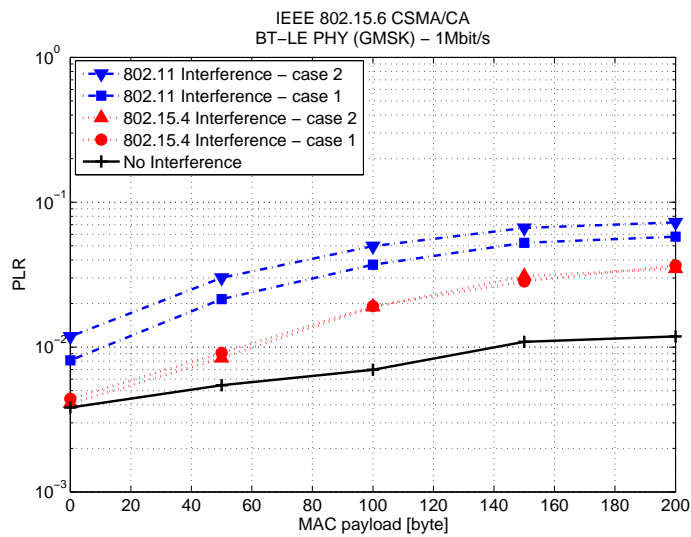
Figure 2.48: PLR for IEEE 802.15.6 CSMA/CA with interference, PHY 3.

generated is heavier than the one produced by an 802.15.4 network. Besides, even when the channels used by the WBAN and the 802.11 devices are only partially overlapping (*Case 1*), the degradation in the performance is significant, and this is also due to the heavy 802.11 traffic: the channel is very often found busy by WBAN devices, which are therefore not able to correctly transmit their data (main cause of losses for 802.15.4 CSMA/CA is the maximum number of backoff reached, while for 802.15.6 is the end of the superframe).

IEEE 802.15.6 CSMA/CA performs better than the 802.15.4 one when external interference is present, because nodes sense the channel for a longer period. Therefore, the PLR obtained with the other PHYs is shown only for 802.15.6, in Fig.s 2.47 and 2.48. For both PHY 2 and 3, the degradation of PLR performance in presence of interference is less evident, because many packets are lost due to connectivity problems (higher receiver sensitivity values).

Fig.s 2.49 and 2.50 show the average delay and energy as a function of MAC payload obtained with PHY 1, for both CSMA/CA algorithms.

Curves attained with 802.15.4 interference are not reported, because they overlap with the one obtained without interference. When IEEE 802.11 is present, both delay and energy consumption increase, but the degradation is not as significant as for the PLR.

2.4.4 Concluding Remarks

Coexistence evaluation results have shown that the presence of interfering sources degrades WBAN performance. In particular, it has been shown that the performance metric that is mainly affected by the interference is the PLR. The degradation is more
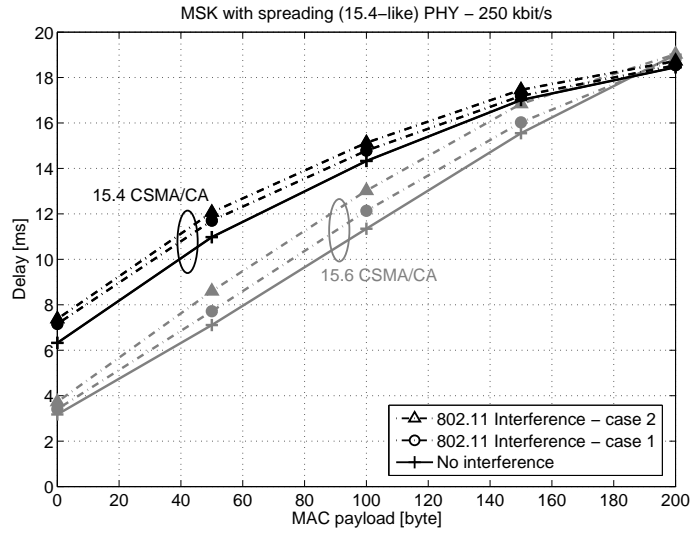
Figure 2.49: Average delay for IEEE 802.15.6 CSMA/CA with interference, PHY 1.
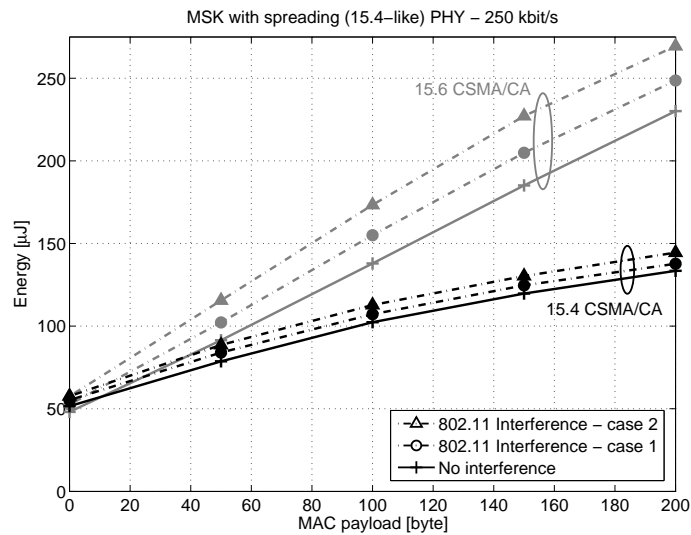
Figure 2.50: Average energy consumption per packet for IEEE 802.15.6 CSMA/CA with interference, PHY 1.

evident when the interfering sources generate more traffic compared to the WBAN under evaluation (802.11 interference with respect to 802.15.4 one in the reported studies). Therefore, in order to guarantee acceptable performance, an appropriate channel selection is of great importance, and, given the variability of the environment in which WBANs are supposed to operate, the selection procedure should also be periodically repeated.

The framework presented to evaluate WBAN coexistence with other wireless systems is fairly complete, since it takes into account specific models regarding the propagation channel and the PHY layer, and realistic interference characterisation. Nonetheless, it presents a limitation due to the fact that the possible impact of WBAN transmissions on the interfering system is ignored. This impact is anyway expected to be limited in case of IEEE 802.11 interference, because of the difference in the transmit power used.

Chapter 3

A Stochastic Geometry-Based Model for Interference-limited Wireless Access Networks

In this chapter a mathematical model to characterise the performance of interference-limited wireless networks based on IEEE 802.15.4 will be derived. It is developed through the integration of an interference power model from stochastic geometry and an IEEE 802.15.4 CSMA/CA model from Markov chains analysis. The considered framework is general and can be used for different possible applications where WSNs are involved. In particular, we can think of body-to-infrastructure (off-body) communications, in which devices carried around by humans exchange information with external fixed devices in the surroundings, such as in Smart Environments. The developed model focuses on cases where there is a single coordinator (infrastructure access point), towards which the devices randomly scattered around try to transmit their data when their are requested to do it (query-based traffic). The model jointly takes into account connectivity and MAC related issues.

3.1 Related Works

Stochastic geometry is a branch of applied probability that allows the study of random phenomena in different kinds of context [105, 106]. Its development was initially stimulated by applications in biology, astronomy, and material sciences; in the last decade it has also been extensively used in the analysis and design of wireless networks. In fact, it represents an useful tool for the study of the average behaviour over many spatial realisations of a network whose nodes are placed according to some probability distribution [106]. The basic objects studied in stochastic geometry are point processes, which can be visually depicted as a random collection of points in space. These points can thus represent nodes of the network and statistics of the received power, aggregate interference power, SNR, SINR, can be computed.

Several kinds of wireless networks have been studied applying stochastic techniques, from cellular systems [107], cognitive radios [108], ultra wideband communications [109], to ad hoc and sensor networks [110]. The latter category, in particular, being fully distributed and often characterised by random nodes locations, has received many relevant contributions.

Two main research areas can be identified as important basis for the following of this chapter: connectivity issues and interference characterisation. The former is related to the possibility for nodes of a network to communicate among each other. Several works can be found in the literature, both for single and multi-sink scenarios, considering infinite or finite regions. In [111], for example, the probability distribution of the distance between a pair of devices which can correctly communicate with one another is evaluated. The scenario considered is a plane where base stations and mobile phones are randomly deployed. Besides, the probability of the number

of audible base stations from a given mobile is obtained. These results were derived referring to cellular networks, but can straightforwardly apply also to ad hoc networks (evaluation of the number of nodes within range of a given node). In [112], a mathematical approach to evaluate the degree of connectivity of a multi-sink WSN is presented, taking into account both bounded and unbounded domains.

Interference can be one of the main factors affecting performance in wireless multi-user networks. A classical approach to model interference, which is suitable for situations with a large number of nodes and no dominant contribution, is to consider the sum of the interfering powers as a Gaussian random process. In the more recent literature, different frameworks were proposed for the cases in which the Gaussian approximation does not hold, as for example [113, 114]. In [114], in particular, a general framework is developed to characterise the aggregate network interference for nodes distributed according to a homogeneous spatial Poisson point process (PPP). All physical relevant parameters are taken into account: the spatial distribution of the interference, the transmission characteristics (e.g., modulation, power), the propagation characteristics of the medium. In case of infinite domain, the aggregated interference power is shown to follow an alpha-stable distribution. The proposed framework is then applied to the evaluation of interference in cognitive radio and wireless packet networks, and for the coexistence between ultra wideband and narrowband systems.

Homogeneous PPP is a useful model for location of nodes in a network when their position is not known a priori and it has been widely used in several of the studies based on stochastic geometry mentioned above. For a homogeneous PPP, the density of the nodes is constant throughout the considered domain. Nonetheless, if we look

at how the actual interfering nodes are spread, there could be several cases in which they are not homogeneously located, due for example to MAC mechanisms. In case of the Carrier Sense Multiple Access (CSMA) algorithm, a node may start transmitting only if it has sensed the channel to be free, meaning that no other node is already transmitting. This leads to a non uniform distribution of interferers in the space, which is not straightforward to model. In some works, CSMA-based MAC protocols are considered to create a guard zone around the receiver (e.g., [115]) or around the transmitter (as in [116]).

Jointly consideration of MAC and connectivity issues under an analytical approach can be found in few papers from the literature. Reference [117] presents a mathematical model to study multi-sink WSNs, evaluating the area throughput, i.e. the amount of samples per unit of time successfully transmitted to the sinks from a given area. Interference is taken into account implicitly in considering MAC layer packet collisions, but all interferers have the same impact on the receiver (the interference power statistics are not accounted for). In [118] performance of ALOHA and CSMA MAC algorithms is evaluated in terms of outage probability based on the SINR, but considering only the closest interferer node in the computation of the interfering power, providing a lower bound to the performance achievable.

The novelty of the work presented in this chapter lays in the precise consideration of CSMA algorithms in the framework of a mathematical approach based on stochastic geometry, with particular reference to the detailed operation of the CSMA/CA defined in IEEE 802.15.4 standard as a case study. Starting from the model presented in [119] for IEEE 802.15.4 networks working in non beacon-enabled mode, the probability that a given node in the network is interfered is derived. The latter is then integrated with

the stochastic description of the interference power as found in [114], together with connectivity considerations, in order to evaluate success probability for nodes in the network, that is the probability that a packet transmitted by a node is correctly received by the destination.

As described in Section 1.1.2, IEEE 802.15.4 is a standard developed for low data rate WPANs [36] that can be seen nowadays as the de-facto standard for WSNs. In the work presented in this chapter, query-based applications are considered: the network is managed by a coordinator that triggers the sensor nodes to send their sampled data. A star topology and the non beacon-enabled mode are taken into account: nodes send their data to the coordinator through direct links accessing the channel according to the unslotted CSMA/CA algorithm defined in the standard [36].

Different models have been proposed in the literature for the characterisation of the MAC of IEEE 802.15.4 networks (see for example [120–123]), but they typically apply to networks where nodes have always (saturated traffic conditions), or with a given probability, a packet to be transmitted. All the above mentioned models, in fact, assume that packets transmitted from different sources collide with constant and independent probabilities, regardless of the backoff stage. However, this assumption is not accurate for query-based applications, where the number of sensors accessing the channel varies over time. Moreover, some of these models (e.g., [120, 122]) do not show a good agreement with simulation results.

An analytical model for networks implementing query-based applications, where devices have only one packet per query to be transmitted, is presented in [119]. Such model has been validated through simulations [124] and experimental measurements [92]. The statistical distribution of the traffic generated by a network based on IEEE

802.15.4 is predicted by using a 2-D chain analysis. In this work neither connectivity issues nor hidden terminal node problem are considered. In Section 3.4, such model will be extended to properly characterise interference, taking into account also the hidden node problem.

3.2 Reference Scenario and Assumptions

Nodes are assumed to be distributed on a two-dimensional area according to a homogeneous PPP, with a spatial density equal to ρ [nodes $\cdot$ m^{-2}]. They have to communicate with a central coordinator (CC), which is conventionally located at the origin of the plane. A query-based application and a star topology are considered: the CC periodically triggers all nodes and those which correctly receive the query will try to access the channel and send their data to the CC through direct links.

The aim is to evaluate the performance achievable with CSMA/CA algorithm, considering the non beacon-enabled mode defined in IEEE 802.15.4 as a case study. In particular, the success probability for a generic node located at a distance r_0 from the CC (reference transmitter TX$_0$) to correctly transmit its data is mathematically derived. In the model, both connectivity and interference issues are taken into account:

- *connectivity* is considered since only the nodes that receive the query from the CC can attempt their data transmission;

- *interference* at the CC can happen because of the following causes: i) hidden node problem (i.e., two nodes cannot "hear" each other); ii) according to the query-based application considered, all nodes start the procedure to access the

channel simultaneously and this implies that two or more nodes may sense the channel at the same time, finding it free and transmitting simultaneously.

Fig. 3.1 shows the reference scenario, with the CC at the origin and the reference transmitter TX_0 at distance r_0. In the following of the analysis, a polar coordinate
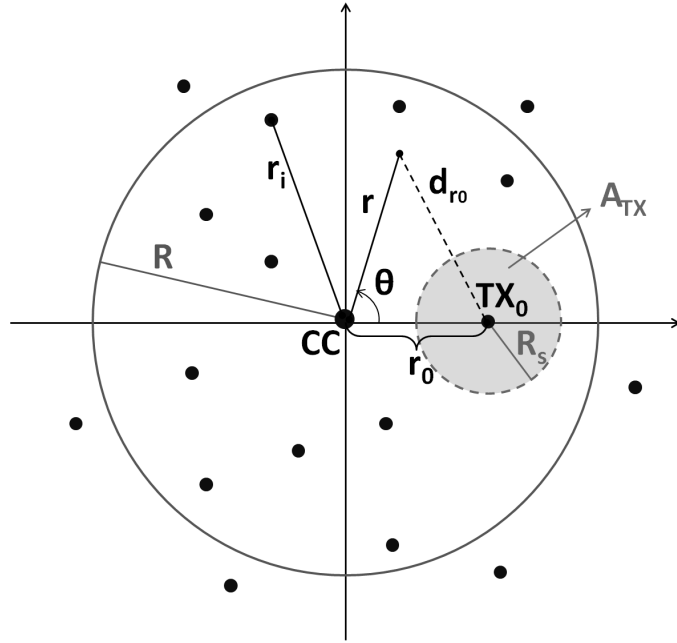
Figure 3.1: Reference scenario.

system will be used, according to which each point on the plane is determined by the distance r from the origin and the angle θ. For the sake of simplicity, TX_0 is considered to be located on the polar axis, i.e. $\theta_0 = 0$.

Channel propagation characteristics are taken into account modeling the received power, denoted as P_r, as a decreasing function of the transmitter-receiver distance d, that is:

$$P_r(d) = \frac{P_T}{d^\beta} Z, \tag{3.2.1}$$

where P_T is the power received at a reference distance of 1 meter from the transmitter

(all nodes are assumed to use the same transmit power), β is the power loss exponent, and Z is a random variable representing channel fluctuations, like shadowing and/or fading.

In the following, two different cases will be considered:

- *ideal channel*: $Z = 1$, which corresponds to a deterministic channel with no fluctuations;

- *lognormal channel*: Z follows a lognormal distribution with coefficient σ, $Z = e^{\sigma G}$, with $G \sim \mathcal{N}(0,1)$[1]; in this case probability density function (p.d.f.) of Z is

$$f_Z(z) = \frac{e^{-\left(\frac{\ln(z)}{\sqrt{2}\sigma}\right)^2}}{\sqrt{2\pi}\sigma z}. \qquad (3.2.2)$$

The receiver sensitivity is defined as the minimum power that has to be received by a node to consider it connected to another one and it is indicated as $P_{r_{\min}}$. The term sensing capability, $P_{s_{\min}}$, refers to the minimum power that has to be received by a node during the carrier sensing phase of the CSMA to hear another node that is transmitting and therefore to assess the channel as busy. In the case of ideal channel, $P_{r_{\min}}$ and $P_{s_{\min}}$ bring to the definition of the transmit and sensing range, respectively, once β and P_T are set. They are denoted as R and R_s, respectively (see Fig. 3.1): $P_{r_{\min}} = P_r(R)$ and $P_{s_{\min}} = P_r(R_s)$.

As for the capture model, a packet is assumed to be correctly received at the CC when $\frac{C}{I} \geq \alpha$, where C is the useful power received (equal to $P_r(r_0)$), I is the total power received from interferes, and α is the protection ratio (minimum Signal-to-Interference ratio that has to be received to guarantee a correct reception of the packet).

---

[1] $\mathcal{N}(a,b)$ indicates a Gaussian random variable with mean value a and standard deviation b.

3.3   Interference Model

Even starting from a homogeneous PPP, due to the query-based traffic and to the use of CSMA, the density ρ_{int} of the nodes that actually interfere with TX$_0$ will not be homogeneous. Specifically, it can be modeled as follows:

$$\rho_{\text{int}}(r, \theta) = q_{\text{int}}(r, \theta) \, p_{\text{con}}(r) \, \rho, \tag{3.3.1}$$

where q_{int} is the probability that a node will interfere with TX$_0$, conditioned on the fact that such node is connected to the CC, and $p_{\text{con}}(r)$ is the probability of being connected to the CC for a node situated at distance r from it. It holds that

$$p_{\text{con}}(r) = \mathbb{P}\{P_r(r) \geq P_{r_{\min}}\}, \tag{3.3.2}$$

since a node is connected to the CC if the power received from it is greater than the receiver sensitivity. $\mathbb{P}\{E\}$ denotes the probability of the event E.

The distance between the reference transmitter TX$_0$ and the location (r, θ) is indicated as d_{r_0} (see Fig. 3.1):

$$d_{r_0}(r, \theta) = \sqrt{r^2 + r_0^2 - 2rr_0 \cos(\theta)}. \tag{3.3.3}$$

The probability for TX$_0$ of hearing a node located at the position (r, θ) can hence be expressed as

$$p_{\text{sens}}(d_{r_0}(r, \theta)) = \mathbb{P}\{P_r(d_{r_0}(r, \theta)) \geq P_{s_{\min}}\}. \tag{3.3.4}$$

The introduction of q_{int} allows to account for MAC mechanisms in the model. In particular, to derive such probability for CSMA it is possible to distinguish between the contribution due to the nodes that can be heard by TX$_0$ and the one caused by those for which TX$_0$ is hidden. In the first case, interference is generated when a node

senses the channel at exactly the same time as TX_0, finding it free, and transmitting simultaneously to TX_0; whereas in the second case collisions are also due to the fact that a node cannot hear TX_0 and viceversa. Hereafter, the nodes that are within the sensing range of a given transmitter and that compete with it to access the channel will be denoted to as the *competitors* for that transmitter.

q_{int_1} and q_{int_2} will indicate the probability that a node will interfere, conditioned to the former or the latter condition, respectively.

Therefore, it is possible to account for different CSMA strategies properly defining q_{int_1} and q_{int_2}. In case of an ideal CSMA, q_{int_1} should be equal to zero, since all TX_0 competitors should be refrained from transmitting sensing TX_0 activity on the channel. Through q_{int_2}, the hidden node problem is taken into account.

In general it holds:

$$q_{int}(r, \theta) = \overline{q_{int_1}} \cdot p_{sens}(d_{r_0}(r, \theta)) + \overline{q_{int_2}} \cdot (1 - p_{sens}(d_{r_0}(r, \theta))), \qquad (3.3.5)$$

where

$$\overline{q_{int_1}} = \sum_{k=0}^{\infty} q_{int_1}(k) p_{n_{c_1}}(k), \qquad (3.3.6)$$

and

$$\overline{q_{int_2}} = \sum_{k=0}^{\infty} q_{int_2}(k) p_{n_{c_2}}(k). \qquad (3.3.7)$$

$p_{n_{c_1}}(k)$ is the probability that the number of competitors for TX_0 is equal to k, or, in an equivalent way, that k nodes are connected to the CC and can hear TX_0. In the case of ideal channel, these nodes are inside the circle of radius R_s depicted in Fig. 3.1. $p_{n_{c_2}}(k)$ is the probability that a generic connected node has k competitors. In the case of ideal channel, these nodes are inside a circle of radius R_s, centered in (r, θ) (not shown in Fig. 3.1). This means that, for the sake of simplicity, q_{int_2} is computed

by assuming that all nodes in the network (including TX_0) have the same number of competitors in the area, n_{c_2}. The derivation of $p_{n_{c_1}}(k)$ and $p_{n_{c_2}}(k)$ is described in the following subsection.

The probabilities q_{int_1} and q_{int_2} must be evaluated depending on the specific MAC scheme used. For the reference case of IEEE 802.15.4 CSMA/CA, they will be derived in Section 3.4.

3.3.1 Derivation of n_{c_1} and n_{c_2} Distributions

For a PPP with density $\rho(r, \theta)$, the probability of having n nodes inside the region $\mathcal{R}$ is given by [125]:

$$p_n(n) = \frac{(\iint_\mathcal{R} \rho(r,\theta) r \, \mathrm{d}r \, \mathrm{d}\theta)^n}{n!} \, e^{-\iint_\mathcal{R} \rho(r,\theta) r \, \mathrm{d}r \, \mathrm{d}\theta}. \tag{3.3.8}$$

The variable n_{c_1} represents the number of competitors for TX_0, whose density can be expressed as

$$\rho_{n_{c_1}}(r, \theta) = \rho \, p_{\text{con}}(r) \, p_{\text{sens}}(d_{r_0}(r, \theta)). \tag{3.3.9}$$

The probability $p_{n_{c_1}}(k) = \mathbb{P}\{n_{c_1} = k\}$ can hence be computed through Eq. (3.3.8), using $\rho_{n_{c_1}}$ density and integrating over the entire plane.

As for the variable n_{c_2}, it represents the number of competitors for a generic connected node. Considering a node located in (r_1, θ_1), the density of its competitors is equal to

$$\rho_{n_{c_2}|(r_1,\theta_1)}(r, \theta) = \rho \, p_{\text{con}}(r) \, p_{\text{sens}}(d_{(r_1,\theta_1)}(r, \theta)), \tag{3.3.10}$$

being $d_{(r_1,\theta_1)}(r, \theta)$ the distance between the considered node and the position (r, θ). With this density, the probability of having k competitors conditioned on being in the location (r_1, θ_1), i.e. $\mathbb{P}\{n_{c_2} = k|(r_1, \theta_1)\}$, can be computed from Eq. (3.3.8). From

this it follows that

$$p_{n_{c_2}}(k) = \int_0^{2\pi} \int_0^\infty \mathbb{P}\{n_{c_2} = k | (r_1, \theta_1)\} \cdot \mathbb{P}\{r_1\}\mathbb{P}\{\theta_1\}\, \mathrm{d}r_1\, \mathrm{d}\theta_1, \qquad (3.3.11)$$

where $\mathbb{P}\{r_1\}$ is the probability that a connected node is located at distance r_1, which can be found in [126], Eq. (10), whereas $\mathbb{P}\{\theta_1\} = 1/(2\pi)$ considering the circular symmetry of the scenario.

3.3.2 Ideal Channel

Assuming a channel without random fluctuations, the probability of being connected, Eq. (3.3.2), reduces to

$$p_{\mathrm{con}}(r) = \begin{cases} 1 & \text{if } r \leq R \\ 0 & \text{if } r > R \end{cases} \qquad (3.3.12)$$

Similarly,

$$p_{\mathrm{sens}}(d_{r_0}(r, \theta)) = \begin{cases} 1 & \text{if } (r, \theta) \in A_{\mathrm{TX}} \\ 0 & \text{otherwise} \end{cases} \qquad (3.3.13)$$

where A_{TX} is the sensing area, defined as the circular area centered at TX_0 and having radius R_s.

The total interference power at CC, I, can be expressed as [114]

$$I = \sum_{i=1}^\infty P_{I_i} = P_T \sum_{i=1}^\infty \frac{1}{r_i^\beta}, \qquad (3.3.14)$$

where P_{I_i} is the power received from i-th interfering node, located at distance r_i from the CC. The characteristic function of the aggregate interference, $\phi_I(\omega)$, is given by[2]

$$\phi_I(\omega) = \exp\left(-\int_0^{2\pi} \int_0^\infty \rho_{\mathrm{int}}(r, \theta)\big(1 - e^{j\frac{P_T\omega}{r^\beta}}\big)r\, \mathrm{d}r\, \mathrm{d}\theta\right). \qquad (3.3.15)$$

---

[2]This follows from Campbell's theorem for Poisson processes [125].

The success probability for TX_0, indicated as P_s, can be evaluated as follows:

$$P_s(r_0) = \mathbb{P}\left\{\frac{C}{I} \geq \alpha\right\} = \mathbb{P}\left\{I \leq \frac{P_T}{\alpha r_0^\beta}\right\} =$$

$$= F_I\left(\frac{P_T}{\alpha r_0^\beta}\right), \tag{3.3.16}$$

where $F_I(\cdot)$ is the Cumulative Distribution Function (CDF) of the interference power I.

As known from the probability theory [127], the CDF can be obtained from the p.d.f. of the interference, $f_I(\cdot)$, as

$$F_I(y) = \int_0^y f_I(x)\,\mathrm{d}x, \tag{3.3.17}$$

and the p.d.f. of I can be numerically evaluated from $\phi_I(\omega)$:

$$f_I(x) = \frac{1}{2\pi}\int_{-\infty}^{+\infty} \phi_I(\omega)e^{-j\omega x}\,\mathrm{d}\omega. \tag{3.3.18}$$

3.3.3 Lognormal Channel

When a lognormal channel is considered, the probability of being connected can be computed from Eq. (3.3.2) as

$$p_{\mathrm{con}}(r) = \mathbb{P}\left\{\frac{P_T}{r^\beta}Z \geq P_{r_{\min}}\right\} = \int_{\frac{P_{r_{\min}}r^\beta}{P_T}}^\infty f_Z(z)\,\mathrm{d}z = \frac{1}{2}\,\mathrm{erfc}\left(\frac{\ln\left(\frac{P_{r_{\min}}r^\beta}{P_T}\right)}{\sqrt{2}\sigma}\right), \tag{3.3.19}$$

where $\mathrm{erfc}(\cdot)$ is the complementary error function defined as

$$\mathrm{erfc}(x) = \frac{2}{\sqrt{\pi}}\int_x^\infty e^{-t^2}\,\mathrm{d}t. \tag{3.3.20}$$

Similarly, the sensing probability can be expressed from Eq. (3.3.4) as

$$p_{\mathrm{sens}}(d_{r_0}(r,\theta)) = \frac{1}{2}\,\mathrm{erfc}\left(\frac{\ln\left(\frac{P_{s_{\min}}(d_{r_0}(r,\theta))^\beta}{P_T}\right)}{\sqrt{2}\sigma}\right). \tag{3.3.21}$$

In this case, the total interference power I is equal to

$$I = \sum_{i=1}^{\infty} P_{I_i} = P_T \sum_{i=1}^{\infty} \frac{Z_i}{r_i^{\beta}} \tag{3.3.22}$$

and its characteristic function can be expressed as

$$\phi_I(\omega) = \exp\left(-\int_0^{\infty}\int_0^{2\pi}\int_0^{\infty} \rho_{\text{int}}(r,\theta)\left(1 - e^{j\frac{P_T\omega z}{r^{\beta}}}\right)f_Z(z)r\,\mathrm{d}r\,\mathrm{d}\theta\,\mathrm{d}z\right). \tag{3.3.23}$$

Finally, the success probability for TX_0 can be obtained as follows:

$$P_s(r_0) = \mathbb{P}\left\{\frac{C}{I} \geq \alpha\right\} = \int_0^{\infty}\left(\int_{ay}^{\infty} f_Z(z)\,\mathrm{d}z\right)f_I(y)\,\mathrm{d}y =$$
$$= \frac{1}{2}\int_0^{\infty} \text{erfc}\left(\frac{\ln(ay)}{\sqrt{2}\sigma}\right)f_I(y)\,\mathrm{d}y, \tag{3.3.24}$$

where $a = \frac{\alpha r_0^{\beta}}{P_T}$.

3.4 The IEEE 802.15.4 Model

In this section the probabilities q_{int_1} and q_{int_2}, introduced in the previous section, will be mathematically derived through extension of the mathematical model for IEEE 802.15.4 networks presented in [119]. For details on the protocol refer to Section 1.1.2 and to the standard [36]. Here we simply recall that each time a node finds the channel busy it moves to a new backoff stage, trying again to access the channel. Since there exist $\text{NB}_{\text{max}} + 1$ (where $\text{NB}_{\text{max}} = 4$) possible backoff stages, a maximum number of times a node can try to access the channel is imposed. According to this, there exists a maximum delay affecting packets transmission. The time resolution of the model in [119] is equal to backoff period, having a duration of 320 μs, denoted as *slot* in the following. Retransmissions are not allowed in this scenario.

It is assumed that nodes transmit packets of size L [byte], such that the corresponding packet duration is equal to D times the backoff period, being D an integer parameter.

By denoting as n_{c_1} the number of competitors of TX_0, the probability, q_{int_1}, that a node among the n_{c_1} interferes on the transmitter, given that TX_0 is transmitting, is computed as:

$$q_{\text{int}_1}(n_{c_1}) = \frac{p_{\text{coll}_1}(n_{c_1})}{p_{\text{acc}}(n_{c_1})}, \qquad (3.4.1)$$

where p_{coll_1} is the probability that TX_0 collides with a given node among its competitors, and p_{acc} is the probability that TX_0 has access to the channel, that is it succeeds in finding the channel free. The latter is given by:

$$p_{\text{acc}}(n_{c_1}) = \sum_{j=1}^{j_{\max}} p_{\text{acc}}^{(j)}(n_{c_1}) = \sum_{j=1}^{j_{\max}} \mathbb{P}\{C^{(j-1)}\} \cdot p_f^{(j-1)}(n_{c_1} + 1), \qquad (3.4.2)$$

where $p_{\text{acc}}^{(j)}$ is the probability that TX_0 accesses the channel is slot j, when it is competing with other n_{c_1} nodes, meaning that it will start the transmission in slot j, having sensed the channel finding it free in $j-1$. $\mathbb{P}\{C^{(j-1)}\}$ is the probability that a node senses the channel in slot $j-1$, given by Eq. (16) of [119], and $p_f^{(j-1)}(n_{c_1}+1)$ is the probability that the channel is free in $j-1$, when $n_{c_1}+1$ nodes are competing for the channel. The latter is given by Eq. (24) of [119] for the case $D=1$ (corresponding to a packet length $L=10$ bytes) and Eq. (25) of [119] for the case $D>1$ (packet length $L>10$ bytes), by setting the value of N_c defined in [119] as the number of nodes in the network and competing for the channel, equal to $n_{c_1}+1$. Finally, $j_{\max}$ is the last slot in which the transmission of a packet may start. The latter is obtained when the node extracts at every backoff stage the highest backoff time counter (denoted as W_k for the k-th backoff stage) and it always finds the channel busy. Therefore

$j_{\max} = \sum_{k=0}^{NB_{\max}} W_k = 120$, when $W_0 = 8$, $W_1 = 16$, and $W_k = 32$ for $k > 1$, according to the default parameters of the standard [36].

p_{coll_1} is the probability that TX_0 accesses the channel together with one of the competing nodes:

$$p_{\text{coll}_1}(n_{c_1}) = \sum_{j=1}^{j_{\max}} \mathbb{P}\{C^{(j-1)}\}^2 \cdot p_f^{(j-1)}(n_{c_1}), \tag{3.4.3}$$

where the fact that the competitors share the same channel of TX_0 is accounted for. In fact, p_{coll_1} is given by the probability that TX_0 and the generic interferer sense the channel together in slot $j-1$ (that is $\mathbb{P}\{C^{(j-1)}\}^2$), multiplied by the probability that the channel is found free in slot $j-1$. The latter is the probability that the remaining $n_{c_1} - 1$ competing nodes are not transmitting, and it is given by Eq. (24) of [119] for $D = 1$ ($L = 10$ bytes) and Eq. (25) of [119] for $D > 1$ ($L > 10$ bytes), by setting $N_c = n_{c_1}$.

By denoting as n_{c_2} the number of competitors for a generic node in the area, q_{int_2} is given by:

$$q_{\text{int}_2}(n_{c_2}) = \frac{p_{\text{coll}_2}(n_{c_2})}{p_{\text{acc}}(n_{c_2})}, \tag{3.4.4}$$

where p_{acc} is given by Eq. (3.4.2), whereas p_{coll_2} is given by:

$$p_{\text{coll}_2}(n_{c_2}) = \sum_{j=1}^{j_{\max}} p_{\text{acc}^{(j)}}(n_{c_2}) \cdot \sum_{i=i_a}^{i_b} p_{\text{acc}^{(i)}}(n_{c_2}), \tag{3.4.5}$$

with $i_a = \min\{0, j - (D-1)\}$ and $i_b = \min\{j + (D-1), j_{\max}\}$. The first term of Eq. (3.4.5) represents the probability that TX_0 accesses the channel (whatever the slot in which this happens is), while the second term is the probability that a node, hidden to TX_0, also accesses the channel, causing interference on TX_0. Eq. (3.4.5) accounts for the fact that, being TX_0 and the interferer hidden one to each other, also partial overlapping among packets may occur (this justifies the presence of the

second sum in the equation). Moreover, for the sake of simplicity in the analysis, in Eq. (3.4.5) it is assumed that: i) TX_0 and the interferer have the same number of competitors, n_{c_2}, meaning that border effects are neglected; ii) the channels seen by TX_0 and the interferer are uncorrelated, that is the fact that some nodes could be competitors of both and could inhibit TX_0 and the interferer simultaneously is not taken into account. The impact of the latter assumption decreases by decreasing R_s/R.

3.5 Numerical Results

In the results reported in this section, all nodes, including the CC, are supposed to use the same transmit power, equal to -12 dBm. $P_{r_{\min}}$ is set to -95 dBm and $\beta = 3$. These values lead to a connectivity range $R = 27$ m (assuming that the network operates at the 2.45 GHz ISM band). The protection ratio is fixed to $\alpha = 1.3$ dB. The node density is equal to $\rho = 0.02$ nodes$\cdot$m^{-2}. Different values of the sensing range, R_s, and of the packet length, L, are considered to see how these parameters affect the performance of the network.

Fig. 3.2 show $\overline{q_{\text{int}_1}}$ and $\overline{q_{\text{int}_2}}$ probabilities as a function of R_s/R (ratio between sensing and connectivity range), for different packet length values. The curves shown refer to $r_0 = 6$ m, but analogous trends were found for different values of the distance between the reference transmitter and the CC.

These trends can be better understood by looking first at the following figures. Probabilities q_{int_1} and q_{int_2} are reported in Fig.s 3.3 and 3.4, as a function of the number of competitors, n_{c_1} and n_{c_2}, respectively. q_{int_1} has also been validated by means of simulations. A dedicated simulation tool written in C was used [119],
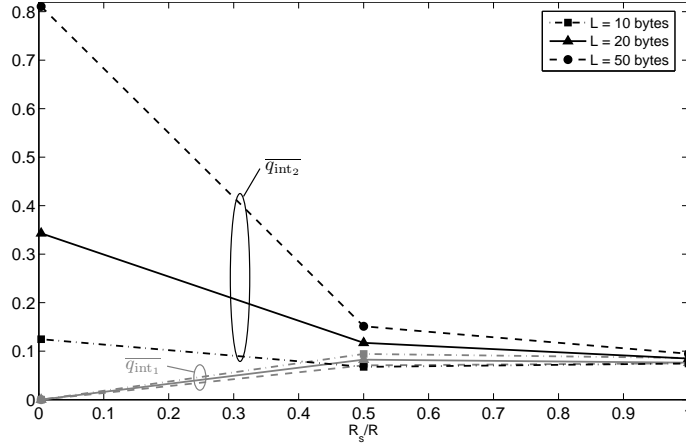
Figure 3.2: Probabilities $\overline{q_{\mathrm{int}_1}}$ and $\overline{q_{\mathrm{int}_2}}$ as a function of R_s/R, for $\rho = 0.02 \ \mathrm{nodes \cdot m^{-2}}$, $r_0 = 6$ m, different values of packet length, ideal channel.

where a query-based 802.15.4 network composed of a certain number of nodes in a star topology is simulated. $10\,000$ transmissions from the nodes to the coordinator were simulated, and the probability that a given node interferes with a reference transmitter was derived. A good agreement between q_{int_1} model and the simulations can be noted.

Fig. 3.5 shows the distribution probabilities for the number of competitors in case of ideal channel.

In Fig. 3.2 it can be noted that: i) as the sensing range increases, $\overline{q_{\mathrm{int}_1}}$ slightly increases, while $\overline{q_{\mathrm{int}_2}}$ decreases; ii) the former is not significantly affected by the packet size, while the latter is larger when L increases.

Remark i) can be explained considering that the number of competitors for the reference transmitter n_{c_1} increases when R_S gets larger (Fig. 3.5 (a)), while for $p_{n_{c_2}}$ the increase of the number of competitors with the sensing range is less significant. Therefore in this case the decrease in $\overline{q_{\mathrm{int}_2}}$ is due to the decrease of q_{int_2} as more competitors are present (see Fig. 3.4).
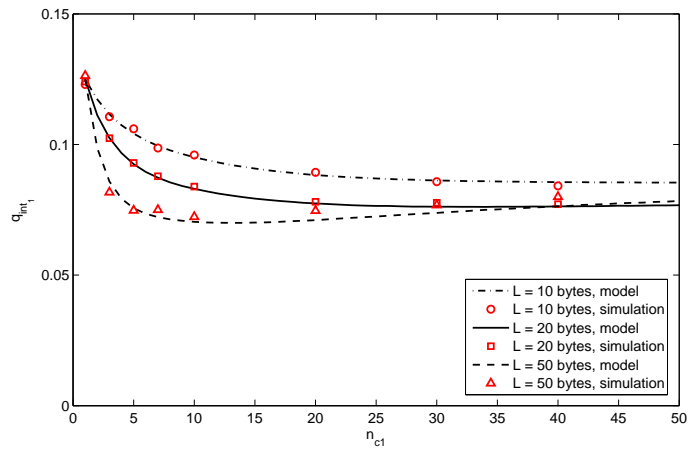
Figure 3.3: Probability q_{int_1} as a function of n_{c_1}, for different values of packet length, comparison of model and simulations.
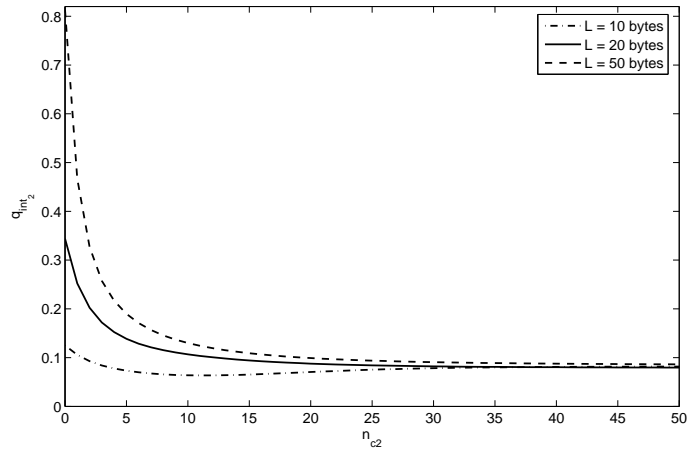
Figure 3.4: Probability q_{int_2} as a function of n_{c_2}, for different values of packet length.

131
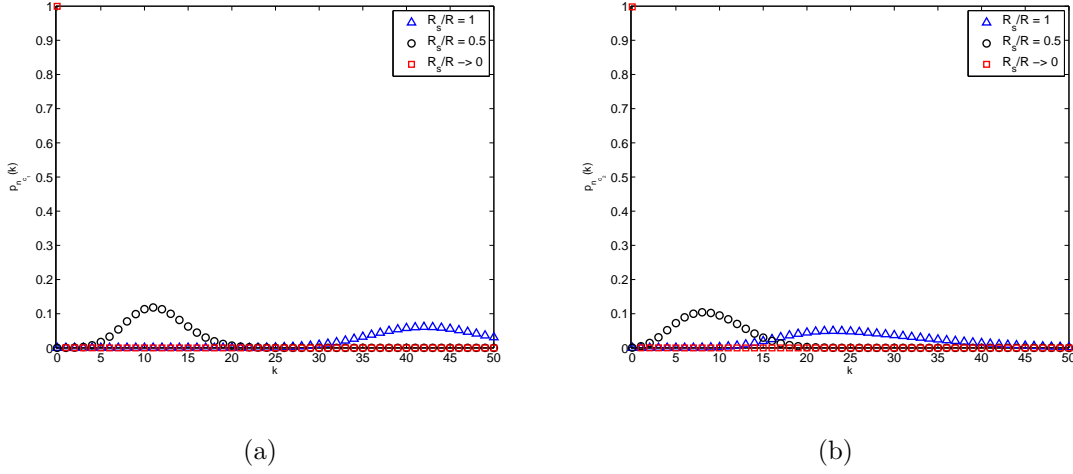
Figure 3.5: Probability distributions of the number of competitors for different values of R_s/R, $\rho = 0.02$ nodes$\cdot$m^{-2}, $r_0 = 3$ m, ideal channel: (a) $p_{n_{c_1}}(k)$, (b) $p_{n_{c_2}}(k)$

The effect of the packet size is more evident on q_{int_2} than on q_{int_1}, leading to ii). Specifically, q_{int_2} increases when L assumes larger values, since longer packets occupy the channel for a longer time, increasing the collision probability when nodes are hidden to each other.

The success probability is illustrated in Fig. 3.6 for the ideal channel case and in Fig. 3.7 for the lognormal channel, as a function of the distance of the reference transmitter from the CC.

Two values of sensing range ($R_S/R \to 0$ and $R_S = R$) and two different packet length values are reported. First, it can be seen that, obviously, when the reference transmitter goes further away from the CC, P_s decreases. Then, as expected, it can be noticed that increasing the sensing range leads to a performance improvement, since more nodes can be heard and the hidden node problem is reduced. When the sensing range is higher, the success probability is higher for longer packets, while the
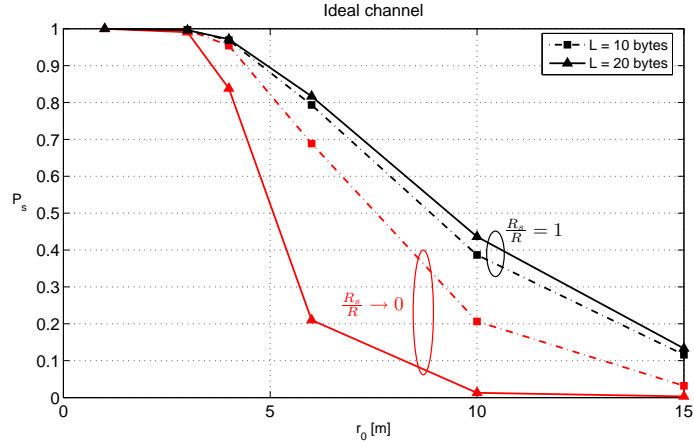
Figure 3.6: Success probability as a function of r_0, obtained for different values of the sensing range and packet length, ideal channel, $\rho = 0.02$ nodes $\cdot$ m^{-2}.
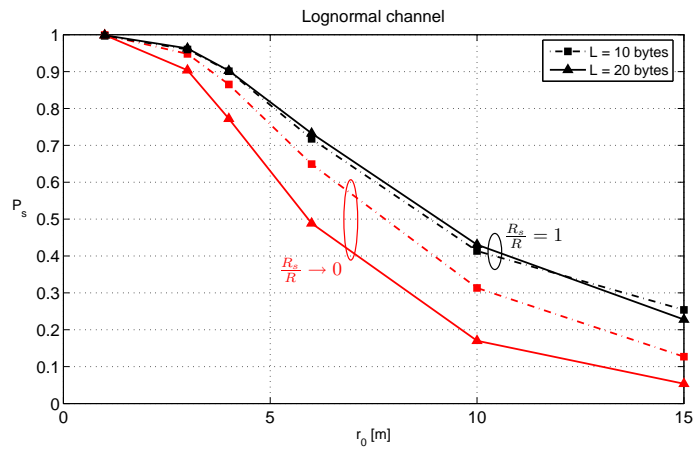
Figure 3.7: Success probability as a function of r_0, obtained for different values of the sensing range and packet length, lognormal channel with $\sigma = 6$ dB, $\rho = 0.02$ nodes $\cdot$ m^{-2}.

opposite holds for low sensing ranges. Indeed, when nodes cannot sense other nodes

transmissions, it is more convenient to use shorter packets, in order to reduce the time

needed to send a packet and hence the collision probability. In order to understand

the curves obtained for $R_S = R$, it has to be underlined that $L = 10$ bytes $(D = 1)$

represents a peculiar case for 802.15.4 CSMA/CA, where the packet duration is equal

to the backoff period. In this case the sensing is thus not effective, being nodes

synchronised by the query (i.e. they start CSMA/CA at the same time).

If we compare the success probability obtained with the ideal (Fig. 3.6) and the

lognormal (Fig. 3.7) channel, it can be noticed that for short distances from the

CC the success probability is higher in the former case, while when r_0 is larger, the

situation tends to invert. The difference between ideal and lognormal channel is more

evident for small values of R_S.

Finally, in Fig. 3.8 the success probability obtained for an intermediate value of

sensing range $(R_S = R/2)$ is shown, for different packet lengths, in case of ideal

channel.
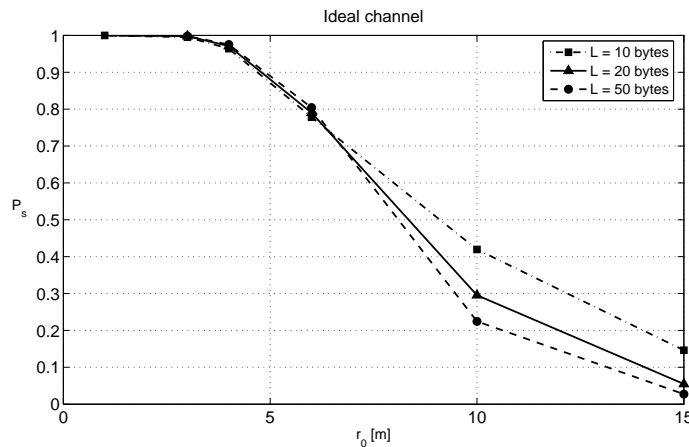
Figure 3.8: Success probability as a function of r_0, obtained for different values of the
packet length, ideal channel, $\rho = 0.02$ nodes$\cdot$m^{-2}, $R_S/R = 0.5$.

For nodes in proximity of the CC ($r_0 < 6 \div 7$ m), longer packets are more beneficial (even if the difference on P_S is almost negligible), while when r_0 increases the effect of the presence of more interferers closer to the CC becomes important, leading to more convenience in sending shorter packets.

3.6 Conclusions and Future Works

A mathematical model to characterise the performance of interference-limited wireless networks based on IEEE 802.15.4 standard was derived. Numerical results showed the impact of sensing range, packet length, and channel fluctuations on the success probability.

The model was developed integrating an interference power model from stochastic geometry with a model based on Markov chains analysis for 802.15.4 CSMA/CA. In particular, the impact of the MAC dynamics was accounted for through the consideration of the probability for one node to transmit simultaneously with the reference transmitter.

On one hand, the model is useful to optimize MAC performance depending on network parameters. On the other hand, the developed framework could be used as a tool to compare the performance of different MAC protocols, if the above mentioned interfering probability is properly taken into account for different channel access methods. This could be a first direction for future research: to extend the model for different access protocols relevant for the scenario under evaluation, such as Bluetooth Low Energy or IEEE 802.15.6. This would require an analytical description of the protocol to investigate, to extract the probability that a competitor node interferes with the reference one, as described in Section 3.4 for the case of IEEE 802.15.4

standard. Moreover, the consideration of different models for the channel random fluctuations would be interesting, possibly considering those specifically derived for off-body communications.

Further work could as well include a complete validation of the model, through simulations or experimental activities. Being a quite complex mathematical framework, approximation of integral formulas to be more easily processed by computers would also enhance its applicability.

Chapter 4

Human Mobility and Sociality Characterisation

This chapter presents preliminary results about experiments performed to gain an understanding on human mobility and sociality characteristics in an indoor scenario, since they represent a necessary knowledge to develop body-to-body (B2B) communications. After an introduction about possible applications of B2B communications with a special emphasis on opportunistic networking techniques, related experiments from the literature will be surveyed. Then, the set-up of the realised experiments will be described and the first results about temporal and social properties of human mobility will be presented.

4.1 Introduction and Related Works

B2B communications are a quite recent research topic that could represent an interesting and important component of future wireless systems and networks. Devices with wireless communication capabilities carried around by people everyday, such as the mobile phone as probably the most common one, could indeed be used to enhance

current existing networks on one side or to develop new applications and services on the other side. In both cases, applying the opportunistic paradigm could turn out as a fruitful direction.

Opportunism in wireless systems is a concept that has been spreading in the wireless research community in recent years. Generally speaking, it aims at jointly exploiting the resources of separate networks according to the needs of specific application tasks. These resources may include different device functionalities, such as: memory, processing, communication, sensing, and actuation.

Focusing on its application at the network layer, that is opportunistic networking, mobile nodes carried by people can be exploited to improve network connectivity and coverage. This is a concept coming from the DTN paradigm and that considers cases in which source and destination nodes might never be connected to the same network at the same time. A complete path between two nodes wishing to communicate may not exist; nonetheless, opportunistic networking techniques allow such nodes to exchange messages [11].

Just to cite some of the various applications that can be envisioned in this framework, human mobility can be opportunistically exploited in WSNs. Data sensed by nodes in a WSN are usually sent to one (or more) central device, denoted as sink, which collects the information and can either act as a gateway toward other networks (e.g. Internet), or properly process it to command actuators to perform specific tasks. If the sink cannot be directly reached by all sensor nodes, multi-hop is used to transmit data to it. In this context, the presence of people moving around in the area carrying mobile devices can help the delivery of the data coming from sensors distant from the sink. People can hence be seen as data mules or ferries to carry data from

sensor nodes to the sink [128]. Depending on the paths covered by the different subjects, in some cases it may be convenient to pass the data from one mule to another in order to reach the sink faster, then applying B2B communications.

In cellular networks, where there is an increasing demand for higher capacity in order to support high data rate applications, the networks users themselves may be exploited for this purpose. This could be achieved by creating B2B networks of interlinked wireless devices, carried, worn or integrated into clothing, allowing data to be routed from person to person before being forwarded to the recipient or the relevant infrastructure network if necessary [9].

Data dissemination and content distribution applications could also take advantage of opportunistic networking using people mobility. These refer to cases where the infrastructured network or some fixed nodes generate and/or distribute contents whose final users are specific groups of people. In an urban scenario for example local news could be circulated from some devices placed in public places and popular sites. In shopping malls, train stations, or airports, shops and restaurants may advertise their presence, exact location, and special offers to potential clients passing by. In offices and working places, reminders of meetings could be sent to appropriate participants. As in the above mentioned cases, devices carried by people moving in the area could be used to spread the messages to relevant destinations (i.e. interested users).

In order to efficiently develop the applications described above, a deep knowledge of human mobility and sociality characteristics is needed. Some studies related to human mobility features can be found in the literature of recent years. They were based on experimental activities summarised in Table 4.1.

Table 4.1: Experimental studies about human mobility

Traces		Environment	Duration	Devices number	Ref.
Wi-Fi	Dartmouth	University campus	11 weeks	~ 2000	[129]
	UCSD	University campus	11 weeks	275	[130]
GPS	KAIST	University campus	Some days	4	[131]
	NCSU	University campus		20	
	State fair	Fair		8	
	Disneyworld	Theme park		4	
	New York	City		8	
Cellular phones		Nation	6 months	~ 10 000	[132]
		City	2 months	~ 100 000	[133]
Bluetooth	Reality Mining	University campus	~ 9 months	100	[134]
	Intel	Research centre	3 days	8 (+ 1 fixed)	[135]
	Cambridge-Uni	University campus	5 days	12	
	INFOCOM05	Conference	3 days	41	[136]
	Cambridge-City	City	~ 2 months	36 (+ 18 fixed)	[137]
	INFOCOM06	Conference	4 days	78 (+ 20 fixed)	
	Singapore	University campus	4 months	9 (+ 3 fixed)	[138]
Bluetooth & Wi-Fi		University campus	3 weeks	28	[139]
On-purpose designed devices		University campus	19 days	44	[140]

Some works analyzed APs traces collected from Wi-Fi networks deployed on university campuses [129, 130]: the mobility of users is estimated from the AP they are connected to, and their proximity is inferred from the connection to the same AP (i.e., two users are considered to be in range of each other if they are connected to the same AP). The accuracy regarding both the position estimate and the social contacts is limited (the coverage area of a Wi-Fi AP can be of hundreds of meters).

Experiments performed with Global Positioning System (GPS) receivers are described in [131]. In these cases, traces are collected separately for the different participants, so mobility can be evaluated only at the individual level. Besides, traces refer only to outdoor settings.

The trajectories of mobile phone users tracked for a period of several months are examined in [132, 133], giving insights of spatial and temporal mobility characteristics on a macro-scale (nation or city wide).

Various experiments were conducted using Bluetooth enabled devices. In the Reality Mining project [134], 100 university students were given mobile phones with special software to collect information about their usage, including results from Bluetooth scanning performed every five minutes. No knowledge about behaviour in space can be inferred from such traces, but they are useful in providing information on social contacts. Researchers from the University of Cambridge used small Bluetooth transceivers to collect contact data in different settings, such as conferences [136], Cambridge campus [135] and city [137]. In this case, Bluetooth inquiry is performed every 2 minutes, but mainly inter-devices information is collected, since few fixed nodes are present, leading to a limited spatial accuracy. In [138] authors describe a smaller scale experiment conducted in a university campus using mobile phones.

An experiment performed with both Wi-Fi and Bluetooth is presented in [139]. The former is used to gather spatial data (locations visited in terms of seen APs), whereas the latter allows to collect social encounters information.

Finally, another experiment realised in a campus is reported in [140], where on-purpose designed devices were given to participants. Each device transmits a beacon packet every second, and for the rest of the time it listens to the channel and records data about beacon received from the other nodes.

The analysis of these works lead to the discovery of several properties and characteristics related to human mobility. Following and extending the taxonomy proposed in [141], they can be classified in three main categories:

- *Spatial properties* include all characteristics that pertain to the behavior of users in the physical space. The jump size, that is the travel distance of individuals (referred to also as flight length) has been found to follow a truncated Pareto distribution[1] [131] or a truncated power law[2] [132]. This means that we tend to move over short distances, taking long trips only occasionally, and underlines the difference between human and random motion. A truncated power law is

---

[1]For a truncated Pareto random variable X [142]:

$$\mathbb{P}\{X > x\} = \frac{\gamma^{\alpha}(x^{-\alpha} - \nu^{-\alpha})}{1 - (\gamma/\nu)^{\alpha}}, \qquad \text{for} \quad 0 < \gamma \leq x \leq \nu < \infty.$$

α is the shape (or tail) parameter.

[2]Indicating the jump size with Δr, its p.d.f. can be expressed as [132]

$$p(\Delta r) = (\Delta r + \Delta r_0)^{-\beta} \cdot e^{-\frac{\Delta r}{k}},$$

where Δr_0, the coefficient β, and the cutoff parameter k values depend on the experimental set considered.

also typical for the radius of gyration[3], which depicts the characteristic distance traveled by a user with respect to the "center of mass" of the trajectory [132], meaning that most people usually travel in close vicinity to their home location, while a few frequently make long journeys. In [143] a least action tendency is recognized: humans tend to make actions that require the least amount of effort, minimizing the total amount of traveled distance.

- *Temporal properties* refer to the time-varying features of human mobility. The visiting (or pause) time is the time spent in the same location and it has been modeled with a truncated Pareto distribution[1] [144]. The return time (or inter-visit duration) for the home location (location where the user spends most of its time) has been characterised by a power law with exponential decay [145]. The probability that a user returns after t hours to the position where he was first observed (return probability) has been shown to have peaks at 24, 48, ... hours [132], underlining the tendency of people to return regularly to locations they visited before.

- *Social properties* are related to the interactions between users. Number of contacts recorded are usually not uniformly distributed among nodes [136], nor evenly distributed for the different hours of the day or days of the week [146]. The contact time (or contact duration), that is the time interval during which two devices are in radio range of one another, has been thoroughly examined

---

[3]Similar to the jump size case, the p.d.f. for the radius of gyration r_g can be expressed as [132]:

$$p(r_g) = (r_g + r_g^0)^{-\beta_r} \cdot e^{-\frac{r_g}{k_r}},$$

where r_g^0, β_r, and k_r values depend on the experimental set.

and demonstrated to follow an approximate power law [135, 136, 140, 146]:

$$\mathbb{P}\{Y \geq t\} = \left(\frac{t_0}{t}\right)^{\alpha} \qquad \text{for} \quad t \geq t_0, \tag{4.1.1}$$

where Y is the random variable representing the contact time; the values of t_0 and of the coefficient $\alpha > 0$ depend on the data set under investigation. Similar findings apply to the any-contact time, which represents the time period that a node spends in contact with at least another node [136]. A power law trend has been recognized also for the inter-contact time (time elapsed between two successive contacts of a given pair of nodes) [137, 140], with different slopes characterising inter-contacts in various part of the day [135, 136], or for different devices pairs [145, 146]. Meeting times (duration of contacts with more than one node), inter-meeting times and meeting size have been evaluated in [146].

As far as opportunistic networking is concerned, on one hand knowledge about human mobility characteristics is useful to design proper forwarding and routing algorithms, on the other hand it can serve to develop realistic mobility models to use in the evaluation of the performance of the algorithms themselves. Several models have been proposed in the literature of recent years (e.g. [147–149]), trying to describe human movements according to the properties examined above. None of the existing models is able to comprise all the characteristics, and they usually focus on a city-scale spatial dimension, while global (world) and building views have been addressed only partially [141].

As for opportunistic routing algorithms, different proposals can be found in the literature. The main concept behind them is that routes are computed dynamically while the messages are being forwarded towards the destination, and contacts

among devices are opportunistically exploited (in a store-carry-and-forward mechanism). The first proposed approaches, such as Epidemic Routing [150] and Spray and Wait [151], are based on some sort of controlled flooding, which leads to a good delivery ratio at the expenses of high overhead and possibly network congestion. Other works, like Prophet [152] and 3R (fine gRained encounteR-based Routing) [153] algorithms, establish which the best forwarders are according to a delivery predictability (probability for a node to encounter a certain destination), the latter computed from the frequency of meetings between nodes. They allow to limit the overhead, but at the same time the delivery ratio is lower and the achieved delay higher. Moreover, the efficiency of this approach may strongly depend on the mobility characteristics of nodes. Social-based routing or forwarding represents an interesting quite recent approach, where metrics from social networks analysis are exploited, such as communities structure, nodes centrality, or similarity, as in Bubble Rap [154] and SimBetTS [155]. Authors in [156, 157] propose a routing scheme based on a sociability indicator, defined taking into account the frequency and type of encounters that nodes have.

In this chapter, preliminary results about experimental activities carried out to characterise human mobility and sociality in indoor environments are reported. With respect to the above mentioned works that had similar purposes, here the focus is specifically on an indoor scenario. Besides, the experiments involved a relevant number of both fixed and mobile (carried by people) devices, in order to evaluate mobility characteristics in all the three dimensions (spatial, temporal, social). In the following analysis, attention will be given to the study of social metrics, to assess if social-based opportunistic routing techniques could be usefully applied in scenarios of this kind.

4.2 Experiments

4.2.1 Set-up

The experimental activity described in this chapter was carried out at the Centre for Communication Systems Research (CCSR) of Surrey University. The research center is located in a three floors building (with few rooms at the ground floor, half of the first floor, the entire second floor).

The basic principle guiding the experiments is the use of short range communication signals to gain understanding of proximity among devices carried by humans and those deployed in the environment, similarly to other works described in the previous section. Two different wireless technologies were exploited: Bluetooth (using Android-based mobile phones) and IEEE 802.15.4 (implemented in TelosB Motes). In the former case, periodic Bluetooth scanning was performed to discover nearby Bluetooth-enabled devices, and for the remaining time the phones were left in discoverable mode, while in the latter one, each device periodically sent beacon messages every 3 seconds and listened to possible incoming messages for the rest of the time. In both cases, the following information was recorded (for every scanned Bluetooth device and for each IEEE 802.15.4 beacon received): MAC address, timestamp, Received Signal Strength Indicator (RSSI).

Thirty-one volunteer participants were involved, from CCSR administrative staff, PhD students, researchers, and professors. Both a mobile phone and an 802.15.4 Mote were given to each of them to carry around during daily activities. These distributed devices will be referred to as *mobile devices* in the remainder of the chapter.

Besides, the experiments leveraged on the SmartCampus infrastructure of CCSR,

which is a testbed deployed inside CCSR building to act as an inter-disciplinary exper-
imental environment for future smart spaces and which consists of several embedded
computing devices distributed across all offices and public places (such as meeting
rooms). Each of these devices offers different short range communication capabilities
(e.g., 802.15.4 or Bluetooth). Forty-six of these devices were considered (all of them
with Bluetooth interface, sixteen also with IEEE 802.15.4). As these devices are static
and permanently installed in the premises they will be referred to as *fixed devices*.

Fig.s 4.1, 4.2, and 4.3 show the maps of the three CCSR floors, with indication of
the location of involved devices. As for the mobile devices, the positions reported in
the maps refer to where the desks of the participants were situated.

Figure 4.1: Map of CCSR ground floor.

The experiments lasted for one month, data were collected every day from 8 am
to 8 pm.

Figure 4.2: Map of CCSR first floor.
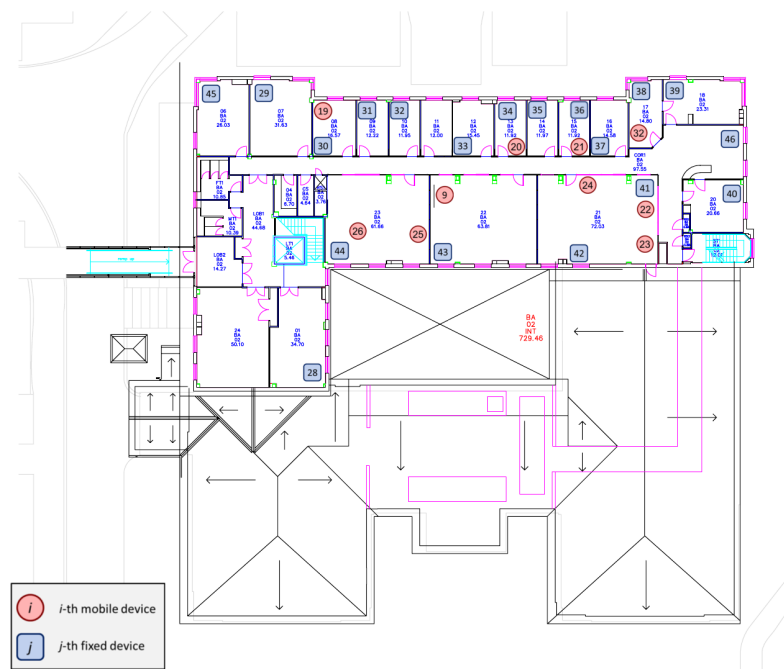
Figure 4.3: Map of CCSR second floor.

4.2.2 Results

In this section preliminary results about analysis of IEEE 802.15.4 traces are reported. The basic information that can be directly extracted from the log files regards the time instants at which different devices are met by every participant. A graphical representation of such information is given in Fig. 4.4, considering device 26 as an example.

(a)   (b)
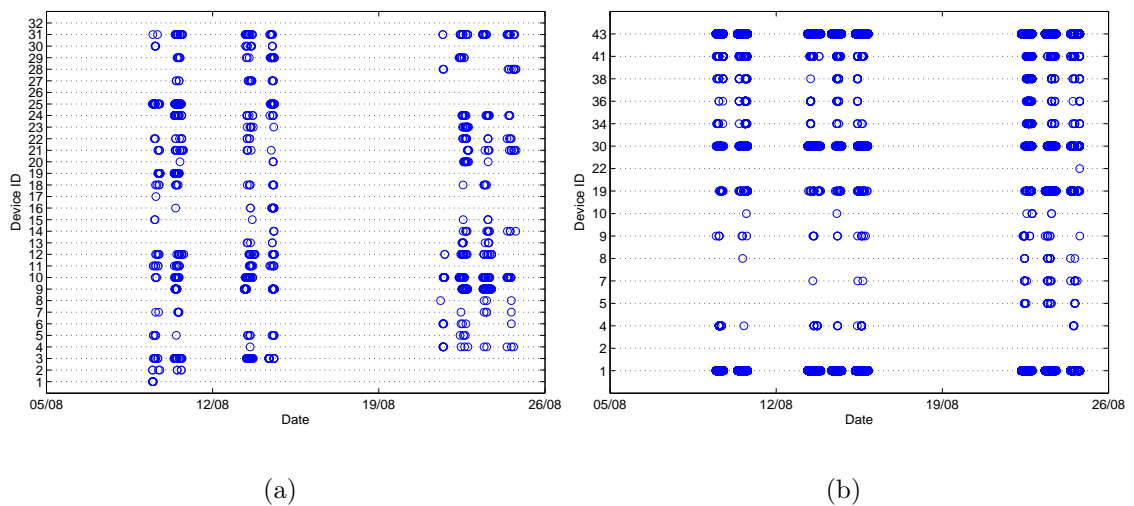
Figure 4.4: Devices met by device 26 during the experiment: (a) mobile devices, (b) fixed devices.

In the following analysis, the assumption is that if a device receives a beacon packet from another device at time instant t_0, then the two are in contact (i.e. in range of each other) from $t_0 - 1.5$ [s] to $t_0 + 1.5$ [s], since beacons are sent every 3 seconds. This applies for both mobile-mobile and mobile-fixed device pairs. Furthermore, only data logs from 8 days were considered, during which most devices were active (in the other days, only information from few devices could be gathered, due to expiration of the batteries or to absences of the participants). Since data during the experiments were

gathered only from 8 am to 8 pm, all metrics and properties are analysed considering the different days separately, that is the maximum measurable duration is equal to 12 hours.

Temporal Properties

Fig. 4.5 shows the distributions of visiting time and return time. The former is the time spent by a device in a certain location, while the latter represents the inter-visit duration (i.e., the time elapsed between two consecutive visits of a device to the same location). A location is identified by a fixed infrastructure device; more specifically, a mobile device is considered to be in a certain location at a certain time instant according to the fixed device from which it receives the beacon with highest RSSI in that instant.
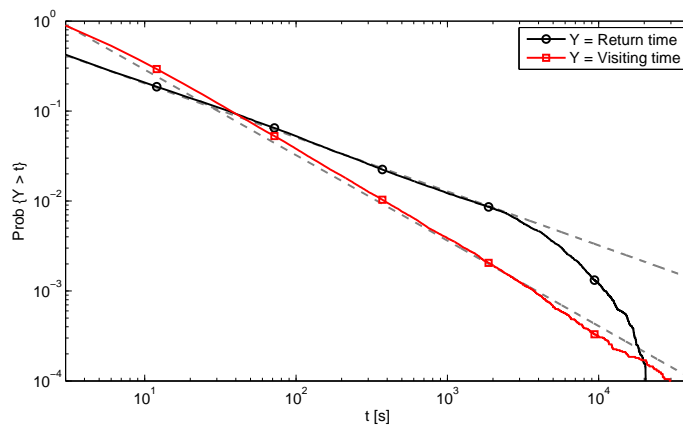
Figure 4.5: Visiting and return time distributions.

Both visiting and return time appear to follow heavy tail distributions, that can be approximate with power laws (as in Eq. (4.1.1)), with (t_0, α) equal to $(0.7, 0.95)$ and $(2.7, 0.6)$, respectively. These results are in line with related studies that were mentioned in Section 4.1.

Social Properties

Contact and Inter-contact Times

Contact and inter-contact times are the two metrics among social properties of human mobility that have been more extensively examined in the literature, since they are strictly connected to the feasibility of opportunistic networking techniques and the performance achievable by them. Contact times are related to the amount of data exchangeable between nodes, and thus to the capacity of this kind of networks, while inter-contact times affect the delay in the reception of packets by destinations.

Due to the inner nature of human mobility, contacts characteristics vary when considering different device pairs. This can be seen for example from Fig. 4.6, where the cumulative contact duration versus the number of contacts is reported for various experiment days. Each point in the figure refers to a different device pair.
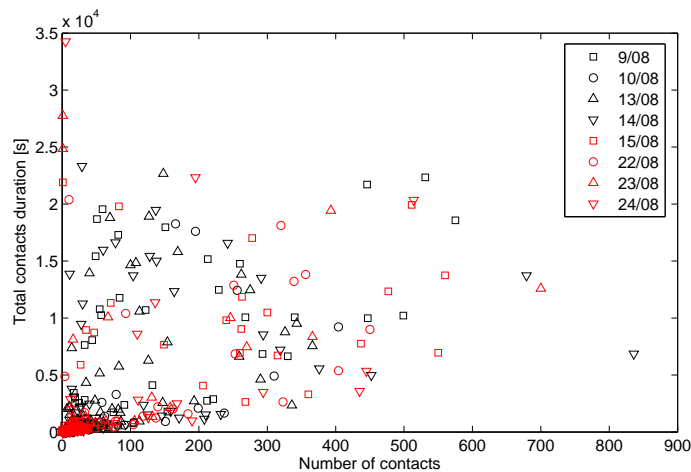
Figure 4.6: Contacts number versus contact duration for all mobile devices pairs, different experiment days.

The examined behaviour is similar from day to day. It can be seen that most of the pairs are characterised by a small number of contacts and short contact duration.

151

Some of the pairs present a high number of contacts with short duration, or small number of contacts with long duration, while very few have high number of contact and long contact duration.

Contact times distribution is shown in Fig. 4.7. Its power law trend can be noticed ($t_0 = 7.4$, $\alpha = 1.15$). This distribution refers to aggregated contact times for different device pairs. Because of the heterogeneity in people behaviour described above, the contact distribution of specific device pairs is different, as illustrated in Fig. 4.8.

In Fig. 4.7 the any-contact time distribution is also reported. The any-contact time is the duration of time spent in contact with at least another device. An approximated power law trend is visible ($t_0 = 5.25$, $\alpha = 1.3$).
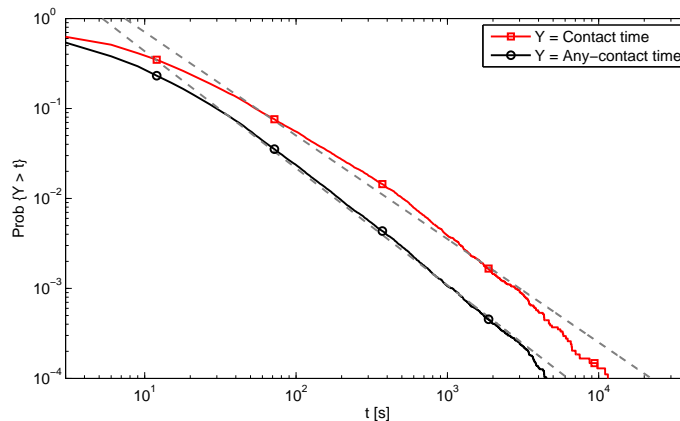
Figure 4.7: Contact and any-contact time distributions.

Fig. 4.9 reports inter-contact and inter-any-contact times distributions. Similar considerations as the ones drawn for the contact times hold; in this case (t_0, α) equal to $(1.8, 0.62)$ and $(0.85, 0.65)$, respectively.

All the described results about contact and inter-contact times are in line with the other studies about parallel experiments that can be found in the literature, demonstrating that inner characteristics about human mobility patterns remain the
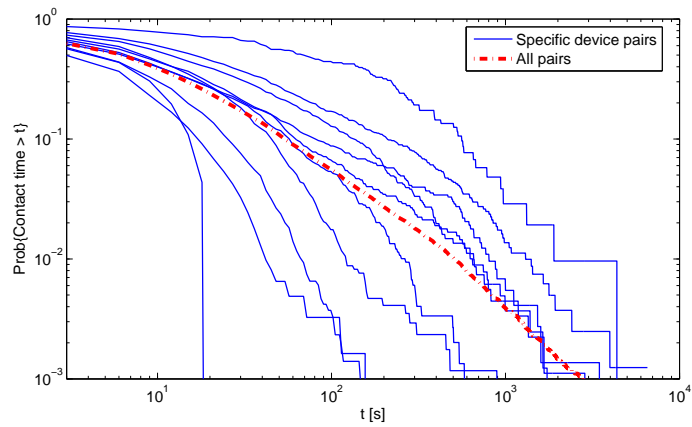
Figure 4.8: Contact time distribution for specific device pairs.
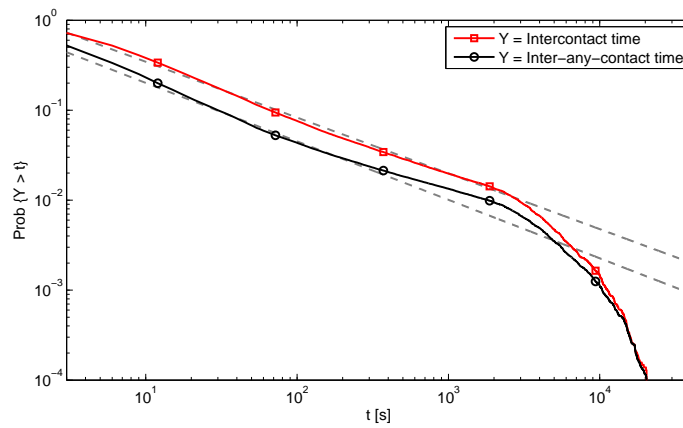
Figure 4.9: Inter-contact and inter-any-contact time distributions.

same in different environments and scenarios.

Social Network Analysis

A recent approach in opportunistic routing algorithms is the exploitation of social network analysis metrics to identify best possible forwarders [158], as proposed in [154, 155]. Social network analysis is based on the examination of social graphs, which are abstract graphs mapping people into vertices and their social ties into edges. Social graphs can be estimated from the contact graphs obtained by experimental activities; anyway, how to detect peoples relationships and create the relative social graph from the recorded contact graph may affect estimation accuracy and the efficiency of social-based approaches [158].

Fig. 4.10 shows the contact graphs of mobile devices considering different durations for aggregating contacts. A link between two nodes is considered if the devices had at least one contact in the period under investigation. Besides, nodes dimension in the figure is proportional to their degree (i.e. the total number of edges they have). As expected, considering longer periods leads to a more connected graph (as in Fig. 4.10(a) where more days of the experiment are aggregated). Moreover, being the network under evaluation a dynamic network evolving in time, the contact graph varies when different days are considered.

Among different metrics of centrality, which can quantify the importance of a node in a graph, in the remaining of the section the focus will be on the degree centrality. In fact, the degree (counting how many edges a node has, that is how many other devices have been encountered) represents the simplest measure of how much social a device is in the network. Besides, the degree can be easily computed by each device individually without need of knowledge of all network topology, allowing

| (a) | (b) | (c) |
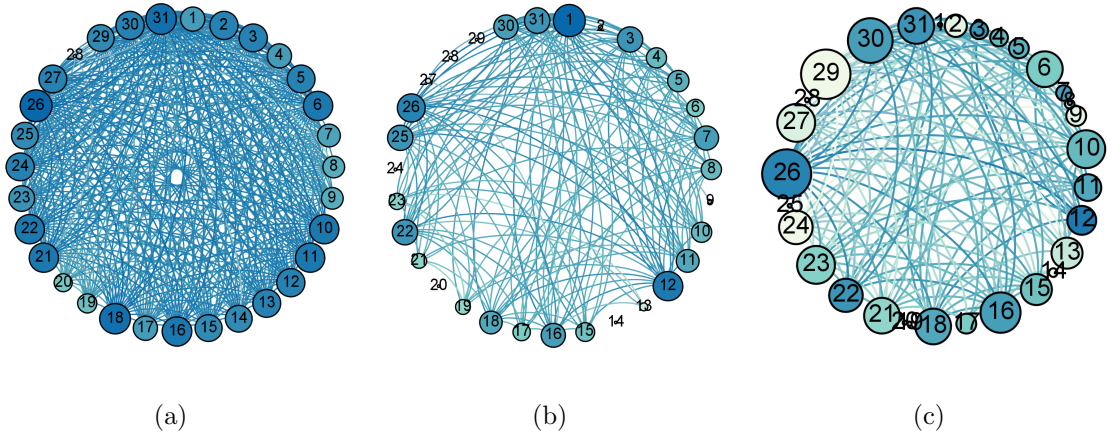
Figure 4.10: Contact graphs obtained for different days of the experiment: (a) all experiment duration (8 useful days), (b) 09/08, (c) 13/08.

straightforward use for opportunistic forwarding.

In particular, it will be shown how the degree varies with respect to the different devices, to different days or moments of the day, and to various durations of the time window considered for constructing the graph (denoted as Δ_t).

Considering a network of N nodes, the degree for node n_i $(i = 1, \ldots, N)$ can be formally defined as [159]:

$$D(n_i) = \frac{d(n_i)}{N-1}, \tag{4.2.1}$$

being $d(n_i)$ the number of neighbours for n_i. According to this definition, $0 \leq D \leq 1$: $D = 0$ corresponds to an isolated node, whereas $D = 1$ represents the most possible social node, which has an edge with all the other network nodes.

A graphical visualization of the degree evolving in time is given in Fig. 4.11, where the degree values computed every 60 s in several experiment days for two devices are shown. These values are evaluated on a time window of length $\Delta_t = 1$ h.

The variation of degree when considering different days in the experiment can
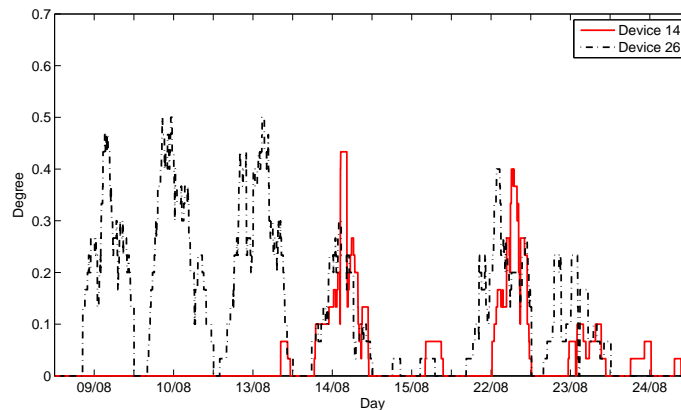
Figure 4.11: Variation of the degree during several experiment days for two devices, $\Delta_t = 1$ h.

be noted from Fig. 4.12, where the percentage of nodes characterised by different degree values is shown, for some experiment days, considering $\Delta_t = 12$ h (the contact graph is formed taking into account all devices contacts happening in one day). The percentage distribution is different for each day, even if the range of degree values obtained turns out to be the same (from 0 to 0.7).
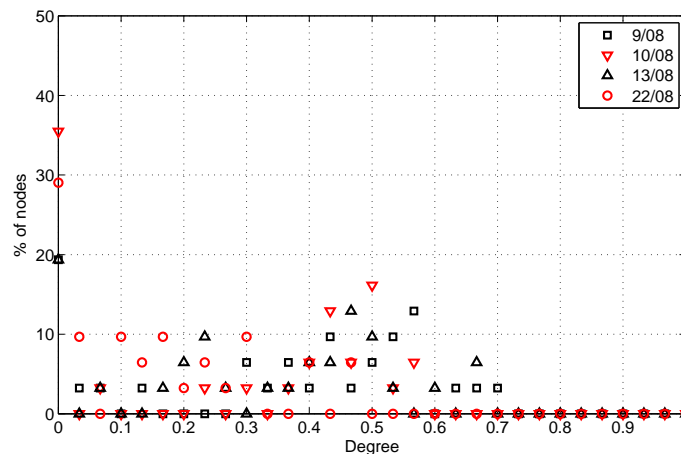
Figure 4.12: Degree distribution for different experiment days, $\Delta_t = 12$ h.

The heterogeneity in people sociality can be appreciated from Fig. 4.13, which

reports degree values for different nodes in a specific experiment day. Degree values have been computed every 60 s on time windows of an hour ($\Delta_t = 1$ h); the figure shows the average degree obtained, with the corresponding variation interval (minimum and maximum values experienced). Similar results were obtained for the other days or other Δ_t. As expected, there are some devices that are more social than others, meeting more devices. This poses the necessary basis for consideration of application of social-based opportunistic routing, since these nodes could be used as suitable forwarders, since they are supposed to meet others with higher probability.
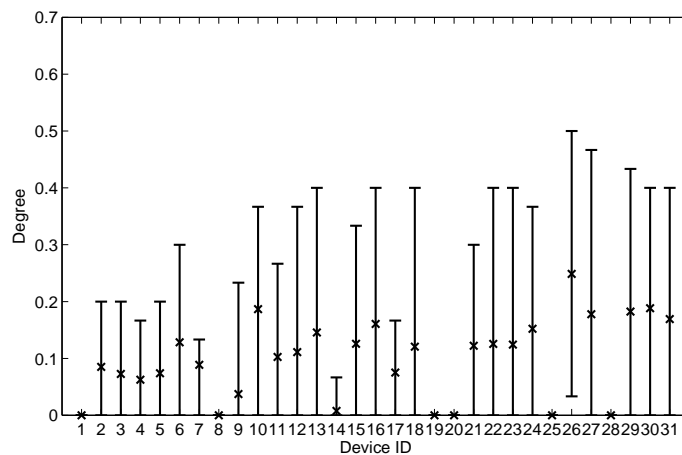
Figure 4.13: Degree values for the different devices in a specific day (13/08), $\Delta_t = 1$ h: average value and variation interval (minimum and maximum values).

The impact of the choice of Δ_t on the degree is illustrated in Fig. 4.14. Degree values obtained when varying Δ_t from 3 s to 12 h are shown for two devices taken as example. As for Fig. 4.13, these values have been computed in a specific day every 60 s, and the figure reports the average and the variation interval. Device 26 can be considered a quite social device, since during the day it meets up to 70% of the other nodes, whereas device 14 appears to be less social, encountering only less than 10% of other devices.
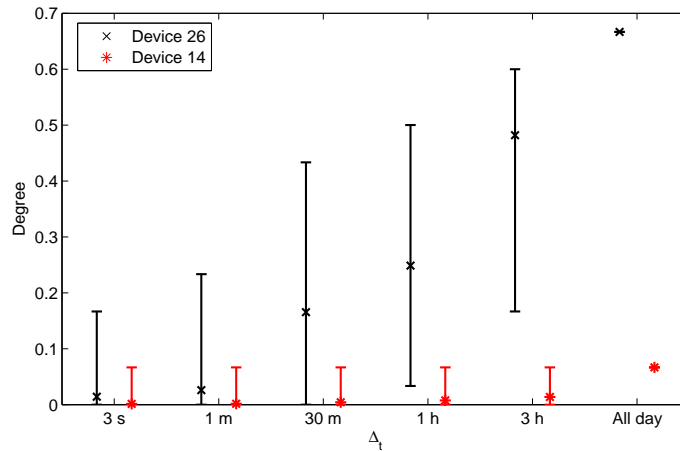
Figure 4.14: Degree values for two devices as a function of Δ_t, in a specific day (13/08): average value and variation interval (minimum and maximum values).

Not surprisingly, the degree assumes larger values as Δ_t increases, since a longer period is considered in constructing the graph and it is more likely for a node to meet more devices. This increase is much more evident for the more social device than for the other one. The most suitable Δ_t value to use in the evaluation of social metrics to apply in opportunistic routing surely depends on the application requirements (acceptable delays and delivery ratios) and needs further study to be determined, but it clearly appears from this figure how a proper tradeoff has to be found to obtain significant degree values. On one hand, small Δ_t values lead to similar degrees for different nodes and cannot deeply capture differences in devices behaviour; on the other hand, very large Δ_t values taking into account past history could be not good indicators of current sociality of a device.

For some applications or scenarios where opportunistic networking techniques could be exploited, the presence of fixed infrastructure should also be taken into account and possibly leveraged, as for example in WSNs with mules or in data content dissemination, as described in Section 4.1. Therefore it is important to assess not

only sociality of devices with respect to the other mobile network devices, but also mobility characteristics with regards to the fixed nodes present in the environment.

Parallel to the degree definition in Eq. (4.2.1), for each mobile device n_i a degree evaluated with respect to the fixed devices can be considered as follows:

$$D_F = \frac{f(n_i)}{N_F}, \tag{4.2.2}$$

where $f(n_i)$ is the number of fixed devices met by node n_i, and N_F is the total number of fixed devices.

Fig. 4.15 illustrates D_F for individual devices in a specific day (D_F values have been computed every 60 s on a time window $\Delta_t = 1$ h, the average and the variation interval are plotted). Its variation both in terms of average and maximum values among the different nodes can be noted: some devices could be more suitable than others to use as forwarders towards fixed destinations.
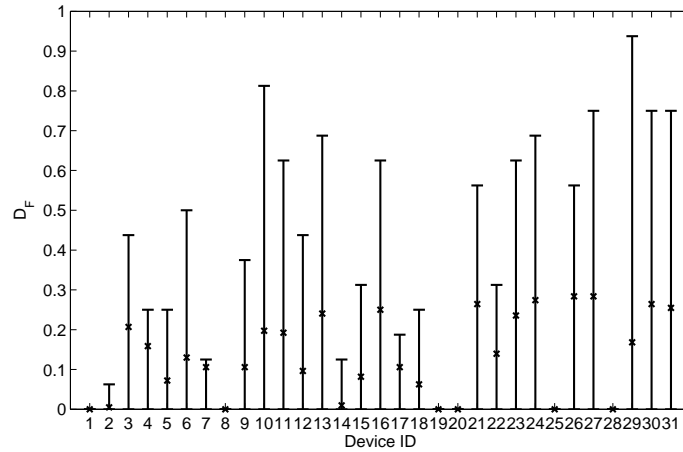
Figure 4.15: D_F values for the different devices in a specific day (13/08), $\Delta_t = 1$ h: average value and variation interval (minimum and maximum values).

Considerations about variability in time and dependence on Δ_t similar to the ones detailed for the degree apply also to D_F, as Fig. 4.16 shows.
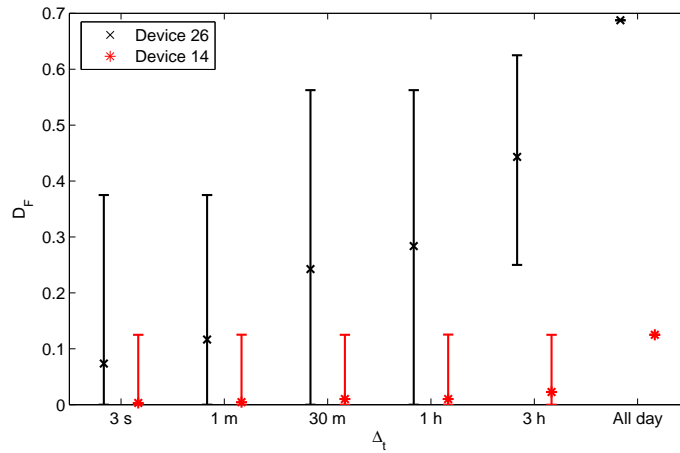
Figure 4.16: D_F values for two devices as a function of Δ_t, in a specific day (13/08): average value and variation interval (minimum and maximum values).

4.3 Conclusions and Further Work

Preliminary results about experimental activities to characterise human mobility and sociality in indoor scenarios have been reported in this chapter. With respect to works with similar purposes that can be found in the literature, the scope of the realised experiments and related analysis is only on indoor scenarios, as offices of a university department.

The initial analysis presented regarding temporal properties and social properties in terms of contact and inter-contact times revealed trends of human mobility that are similar to those found for other scenarios in past experiments. This means that some characteristics of mobility are intrinsic to human nature. Therefore human mobility models that have been developed for other environments could be easily adapted also to indoor scenarios, with proper settings of the model parameters.

A first possible direction for future works regards a detailed analysis about spatial properties of human mobility from the performed experiments, to assess if analogy to

other scenarios could be found also in this regard.

In order to evaluate the suitability of the opportunistic networking paradigm to the scenario under investigation, and in particular of social-based approaches, the degree of devices has been extensively examined. Degree variability in time and with regard to the different nodes has been shown, together with considerations on the impact of the length of the time window used for creating the social graph. Moreover, devices heterogeneity has been explored not only in terms of number of other mobile nodes met, but also taking into account the fixed infrastructure nodes.

Social-based opportunistic routing appears to be a promising technique to apply in such scenarios, with adequate methods to compute the social metric to base the forwarding decision on. This aspect needs further investigations. One one side, it could be interesting to account for weighted graphs in the definition of nodes centrality. A weight may be assigned to each edge depending for example on the contact duration, in order to consider both number of contacts and their duration in the delineation of the importance of devices for forwarding. On the other side, mixed metrics based on both device sociality with other devices and mobility with respect to fixed network nodes could be designed for applications and scenarios where both people and infrastructure are involved.

Conclusions

In this thesis, several aspects of wireless systems for body-centric communications have been explored. It has been shown how the presence of the human body with its peculiar and distinctive characteristics, such as its impact on the propagation medium, the subject's mobility and social patterns, should be taken into account for a proper design and development of this kind of networks.

In particular, a relevant part of the work has been devoted to on-body communications, evaluating the performance of Wireless Body Area Network (WBAN) under different perspectives. First, the application of Link Adaptation (LA) has been proposed in a wearable WBAN scenario to improve performance reducing packet losses. Two strategies have been introduced and evaluated, showing how the possibility of choosing among different bit-rates at the physical layer, depending on the interference experienced, allows an enhancement in network performance, since the packet loss rate is decreased. Then, the channel access methods of two reference WBAN standards (IEEE 802.15.4 and IEEE 802.15.6) have been thoroughly examined. Results have been obtained accounting for several realistic scenarios, with different on-body nodes

positions, a proper characterisation of the propagation channel, and appropriate consideration of physical layer and packet capture mechanisms. They demonstrated how a single protocol solution is not suitable in this context, since WBAN applications can be quite diverse. Depending on the most stringent and important requirements (in terms of packet losses, delays, or energy consumption), the optimum channel access method may vary. As a general statement, Carrier Sense Multiple Access with Collision Avoidance (CSMA/CA) algorithms have proved to be preferable when reducing packet losses is desirable, while Slotted ALOHA mechanism is more suitable when low energy consumption is a primary concern. Results reported may help in guiding in the choice of the right solution. Finally, coexistence issues of WBANs with other wireless networks operating at the same frequency band have been studied. A general framework has been developed, to take into account realistic WBAN features (propagation, packet capture) on one side, and precise frequency and timing characterisation of interfering sources on the other side. The study pointed out the impact of interference on WBAN performance, which can be significant in some cases.

The work presented leaves some open issues that can be interesting to investigate. As for LA in WBAN, the heuristic approach followed has been useful to prove the utility of its introduction to enhance network performance, but a more analytical characterisation would help to find an optimal solution and setting of the decision thresholds. A documentation of energy consumption would as well be useful to better assess the possible packet losses/consumed energy performance tradeoff. CSMA/CA evaluation has been carried out for query based applications, which are significant in WBAN context, for example in case of vital signs monitoring. The analysis can be completed with the consideration of different traffic patterns generated by nodes, to

account also for non periodic cases.

Furthermore, off-body and body-to-body communications have been partially addressed. A mathematical model to characterise the performance of interference-limited wireless access networks has been developed. It integrates an interference power model from stochastic geometry and an IEEE 802.15.4 CSMA/CA model from Markov chain analysis and it allows the evaluation of packet success probability for nodes in a query-based network. Results have shown the impact of sensing range, packet length, and channel fluctuations on it. The framework is general and could be used for several applications; it can be applied for example to communications between devices carried around by humans and fixed infrastructure devices (off-body communications). In this case, an interesting open research direction is related with the consideration of different models to characterise random channel fluctuations, taking into account in particular those developed for off-body links. Further work can also be performed to account for other channel access methods (instead of IEEE 802.15.4 CSMA/CA) to integrate in the developed framework, and possibly to compare the different performance achievable.

As far as body-to-body (B2B) communications are concerned, an experimental activity aimed at evaluating human mobility and sociality properties has been presented. Understanding how people move and interact with each other is in fact a basic groundwork to develop networks involving communications of this type. The realised experiment focused on an indoor scenario; devices were distributed to people working in a university department, and the contacts of these devices among them and with fixed infrastructure nodes deployed in the building were recorded. Analysis

of the collected traces has shown that basic temporal properties of human movements in the examined scenario are similar to the outcome of previous experiments from the literature, which were carried out in diverse environments. Social properties have then been investigated, mainly in terms of degree of the devices in the network. These preliminary results have indicated that social-based opportunistic networking techniques could be promisingly applied in this context. The main open issue in this context regards the complete study of opportunistic routing protocols based on the collected traces. This requires first of all the definition of which metric to consider in the selection of the best forwarders. Starting from node centrality as proposed by some related works, an optimal metric could be found taking into account weighted social graphs. A proper evaluation of the time window used to construct the social graph is also needed. Consideration of nodes sociality characteristics related both to other mobile nodes and to the fixed infrastructure would then be interesting for some application contexts. Finally, a proper evaluation of the opportunistic routing paradigm would have to account for accurate modeling of the propagation channel, PHY and MAC features. In this respect, the work presented in the first chapters of the thesis would be helpful to point out how to consider the various important aspects in the analysis.

List of Acronyms

6LowPAN IPv6 over Low power WPAN

ACK acknowledgment

AP access point

AWGN additive white gaussian noise

B2B body-to-body

BAN Body Area Network

BC backoff counter

BCH Bose, Ray-Chaudhuri, Hocquenghem code

BER Bit Error Rate

BI beacon interval

BO beacon order

BPSK Binary Phase Shift Keying

List of Acronyms

BR Basic Rate

CAP Contention Access Period

CC central coordinator

CCSR Centre for Communication Systems Research

CDF Cumulative Distribution Function

CER Chip Error Rate

CFP Contention Free Period

CP Contention Probability

CSS Chirp Spread Spectrum

CSMA Carrier Sense Multiple Access

CSMA/CA Carrier Sense Multiple Access with Collision Avoidance

CW Contention Window

DBPSK Differential Binary Phase Shift Keying

DPSK Differential Phase Shift Keying

DQPSK Differential Quadrature Phase Shift Keying

DSME Deterministic and Synchronous Multi-channel Extension

DSSS Direct Sequence Spread Spectrum

DTN Delay Tolerant Network

EAP Exclusive Access Phase

ECG Electrocardiogram

EDR Enhanced Data Rate

EEG Electroencephalogram

EMG Electromyogram

FCS frame check sequence

GFSK Gaussian Frequency Shift Keying

GMSK Gaussian Minimum Shift Keying

GPS Global Positioning System

GTS Guaranteed Time Slot

HBC Human Body Communications

I-Ack Immediate Acknowledgment

IEEE Institute of Electrical and Electronics Engineers

IETF Internet Engineering Task Force

IP Integrating Project

IR-UWB Impulse Radio-Ultra Wideband

ISM Industrial, Scientific, and Medical

ISO International Organization for Standardization

L-**DPSK** DPSK with *L* modulation levels

LA Link Adaptation

LE Low Energy

LL Link Layer

LLDN Low Latency Deterministic Networks

LPL Low Power Listening

MAC Medium Access Control

MAP Managed Access Phase

MCS Modulation and Coding Scheme

MFR MAC Footer

MHR MAC Header

MICS Medical Implant Communication System

MPDU MAC Payload Data Unit

MSDU MAC Service Data Unit

MSK Minimum Shift Keying

O-QPSK Offset Quadrature Phase Shift Keying

OSI Open System Interconnection

PC Personal Computer

PDA Personal Digital Assistant

p.d.f. probability density function

PHR Physical Header

PHY Physical layer

PER Packet Error Rate

PLCP Physical Layer Convergence Protocol

PLR Packet Loss Rate

PM Planar Monopole

POS Personal Operating Space

PPDU Physical layer Protocol Data Unit

PPP Poisson point process

PSDU Physical Service Data Unit

QoS Quality of Service

RAP Random Access Phase

RC Remote Control

RF Radio Frequency

RFID Radio Frequency Identification

RREQ Route Request

RSSI Received Signal Strength Indicator

SD superframe duration

SER Symbol Error Rate

SHR Synchronization Header

SIR Signal-to-Interference ratio

SINR Signal-to-Interference-and-Noise ratio

SNR Signal-to-Noise ratio

SO superframe order

SRRC square root raised cosine

TDMA Time Division Multiple Access

TG Task Group

TLM Top Loaded Monopole

TSCH Timeslotted Channel Hopping

UWB Ultra Wideband

WBAN Wireless Body Area Network

WBASN Wireless Body Area Sensor Network

WBSN Wireless Body Sensor Network

WG Working Group

Wi-Fi Wireless Fidelity

WLAN Wireless Local Area Network

WMTS Wireless Medical Telemetry System

WPAN Wireless Personal Area Network

WSN Wireless Sensor Network

ZC Zigbee coordinator

ZED Zigbee end-device

List of Figures

List of Tables

Bibliography

[1] T.M. Siep, I.C. Gifford, R.C. Braley, and R.F. Heile. Paving the way for personal area network standards: an overview of the IEEE P802.15 Working Group for Wireless Personal Area Networks. *IEEE Personal Communications*, 7(1):37–43, Feb. 2000.

[2] M. Patel and J. Wang. Applications, challenges, and prospective in emerging body area networking technologies. *Wireless Communications, IEEE*, 17(1):80–88, Feb. 2010.

[3] H. Cao, V. Leung, C. Chow, and H. Chan. Enabling technologies for Wireless Body Area Networks: A survey and outlook. *Communications Magazine, IEEE*, 47(12):84–93, Dec. 2009.

[4] P.S. Hall and Y. Hao. *Antennas and Propagation for Body-Centric Wireless Communications, Second Edition.* Artech House antennas and propagation library. Artech House, 2012.

[5] IEEE 802.15 WPAN Task Group 6. Website: http://www.ieee802.org/15/pub/TG6.html.

[6] L. Liu, P. De Doncker, and C. Oestges. Fading correlation measurement and modeling on the front side of a human body. In *Antennas and Propagation, 2009. EuCAP 2009. 3rd European Conference on*, pages 969–973, March 2009.

[7] R. D'Errico and L. Ouvry. A Statistical Model for On-Body Dynamic Channels. *International Journal of Wireless Information Networks*, 17:92–104, 2010.

[8] S. Ullah, H. Higgins, B. Braem, B. Latré, C. Blondia, I. Moerman, S. Saleem, Z. Rahman, and K. Kwak. A comprehensive survey of wireless body area networks. *Journal of Medical Systems*, 36:1065–1094, 2012.

[9] S.L. Cotton and W.G. Scanlon. Using smart people to form future mobile wireless networks. *Microwave Journal*, Dec. 2011.

[10] R. Rosini, R. D'Errico, and R. Verdone. Body-to-Body communications: A measurement-based channel model at 2.45 GHz. In *Personal Indoor and Mobile Radio Communications (PIMRC), 2012 IEEE 23rd International Symposium on*, pages 1763–1768, Sept. 2012.

[11] L. Pelusi, A. Passarella, and M. Conti. Opportunistic networking: data forwarding in disconnected mobile ad hoc networks. *Communications Magazine, IEEE*, 44(11):134–141, Nov. 2006.

[12] R. Kohno, K. Hamaguchi, Huan-Bang Li, and K. Takizawa. R&D and standardization of body area network (BAN) for medical healthcare. In *Ultra-Wideband, 2008. ICUWB 2008. IEEE International Conference on*, volume 3, pages 5–8, Sept. 2008.

[13] H.-B. Li, K. Takizawa, B. Zhen, and R. Kohno. Body Area Network and Its Standardization at IEEE 802.15.MBAN. In *Mobile and Wireless Communications Summit, 2007. 16th IST*, July 2007.

[14] B. Latré, B. Braem, I. Moerman, C. Blondia, and P. Demeester. A survey on wireless body area networks. *Wireless Networks*, 17(1):1–18, Jan. 2011.

[15] A. Boulis, D. Smith, D. Miniutti, L. Libman, and Y. Tselishchev. Challenges in body area networks for healthcare: the MAC. *Communications Magazine, IEEE*, 50(5):100–106, May 2012.

[16] B. Zhen, M. Patel, S. Lee, E. Won, and A. Astrin. TG6 Technical Requirements Document (TRD). Available at: https://mentor.ieee.org/802.15/documents, Nov. 2008.

[17] M. Chen, S. Gonzalez, A. Vasilakos, H. Cao, and V.C. Leung. Body area networks: A survey. *Mobile Networks and Applications*, 16(2):171–193, Apr. 2011.

[18] M. Ghovanloo. An overview of the recent wideband transcutaneous wireless communication techniques. In *Engineering in Medicine and Biology Society, EMBC, 2011 Annual International Conference of the IEEE*, pages 5864–5867, Sept. 2011.

[19] S. Mai, C. Zhang, M. Dong, and Z. Wang. A Cochlear System with Implant DSP. In *Acoustics, Speech and Signal Processing, 2006. ICASSP 2006 Proceedings. 2006 IEEE International Conference on*, volume 5, May 2006.

[20] D.B. Shire, S.K. Kelly, J. Chen, P. Doyle, M.D. Gingerich, S.F. Cogan, W.A. Drohan, O. Mendoza, L. Theogarajan, J.L. Wyatt, and J.F. Rizzo. Development and Implantation of a Minimally Invasive Wireless Subretinal Neurostimulator. *Biomedical Engineering, IEEE Transactions on*, 56(10):2502–2511, Oct. 2009.

[21] S. Ullah, P. Khan, N. Ullah, S. Saleem, H. Higgins, and K. Sup Kwak. A review of wireless body area networks for medical applications. *Int'l J. of Communications, Network and System Sciences*, 2(8):797–803, 2009.

[22] A. Pantelopoulos and N.G. Bourbakis. A survey on wearable sensor-based systems for health monitoring and prognosis. *Systems, Man, and Cybernetics, Part C: Applications and Reviews, IEEE Transactions on*, 40(1):1–12, Jan. 2010.

[23] S. Drude. Requirements and application scenarios for body area networks. In *Mobile and Wireless Communications Summit, 2007. 16th IST*, pages 1–5, July 2007.

[24] F. Dijkstra. Requirements for BAN and BAN standardization from the point of view of gaming. In *BodyNets 2012, 7th International Conference on Body Area Networks*, Sep. 2012.

[25] V. Jones. From BAN to AmI-BAN: micro and nano technologies in future Body Area Networks. In *Proceedings of Symposium on Integrated Micro Nano Systems: Convergence of Bio and Nanotechnologies*, June 2006.

[26] NATO Network Enabled Capability. Website: http://www.act.nato.int/mainpages/nnec, Nov. 2012.

[27] M. Montanari and S. Schillaci. Ban in defence applications. In *BodyNets 2012, 7th International Conference on Body Area Networks*, Sep. 2012.

[28] F. Petre, F. Bouwens, S. Gillijns, F. Masse, M. Engels, B. Gyselinckx, K. Vanstechelman, and C. Thomas. Wireless vibration monitoring on human machine operator. In *Communications and Vehicular Technology in the Benelux (SCVT), 2010 17th IEEE Symposium on*, pages 1–6, Nov. 2010.

[29] C.-H. Lin, K. Saito, M. Takahashi, and K. Ito. A Compact Planar Inverted-F Antenna for 2.45 GHz On-Body Communications. *Antennas and Propagation, IEEE Transactions on*, 60(9):4422–4426, Sept. 2012.

[30] J. Espina, H. Baldus, T. Falck, O. Garcia, and K. Klabunde. *Towards Easy-to-Use, Safe, and Secure Wireless Medical Body Sensor Networks*, pages 159–179. Hershey: IGI Global, 2009.

[31] D. Singelée, B. Latré, B. Braem, M. Peeters, M. Soete, P. Cleyn, B. Preneel, I. Moerman, and C. Blondia. A Secure Cross-Layer Protocol for Multi-hop Wireless Body Area Networks. In *Proceedings of the 7th international conference on Ad-hoc, Mobile and Wireless Networks*, ADHOC-NOW '08, pages 94–107. Springer-Verlag, 2008.

[32] M. Guennoun, M. Zandi, and K. El-Khatib. On the use of biometrics to secure wireless biosensor networks. In *Information and Communication Technologies: From Theory to Applications, 2008. ICTTA 2008. 3rd International Conference on*, pages 1–5, Apr. 2008.

[33] D.C. Hoang, Y.K. Tan, H.B. Chng, and S.K. Panda. Thermal energy harvesting from human warmth for wireless body area network in medical healthcare system. In *Power Electronics and Drive Systems, 2009. PEDS 2009. International Conference on*, pages 1277–1282, Nov. 2009.

[34] T. von Buren, P.D. Mitcheson, T.C. Green, E.M. Yeatman, A.S. Holmes, and G. Troster. Optimization of inertial micropower generators for human walking motion. *Sensors Journal, IEEE*, 6(1):28–38, Feb. 2006.

[35] M.A. Hanson, H.C. Powell, A.T. Barth, K. Ringgenberg, B.H. Calhoun, J.H. Aylor, and J. Lach. Body Area Sensor Networks: Challenges and Opportunities. *Computer*, 42(1):58–65, Jan. 2009.

[36] IEEE Standard for Information Technology - Telecommunications and Information Exchange Between Systems - Local and Metropolitan Area Networks - Specific Requirements Part 15.4: Wireless Medium Access Control (MAC)

and Physical Layer (PHY) Specifications for Low-Rate Wireless Personal Area Networks (WPANs). *IEEE Std 802.15.4-2006 (Revision of IEEE Std 802.15.4-2003)*, pages 1–305, 2006.

[37] IEEE 802.15 WPAN Task Group 4. Website: http://www.ieee802.org/15/pub/TG4.html.

[38] Zigbee Alliance. Website: http://www.zigbee.org.

[39] N. Benvenuto and G. Cherubini. *Modulation Techniques for Wireless Systems*, pages 1189–1248. John Wiley & Sons, Ltd, 2003.

[40] IEEE Standard for Local and metropolitan area networks–Part 15.4: Low-Rate Wireless Personal Area Networks (LR-WPANs) Amendment 1: MAC sublayer. *IEEE Std 802.15.4e-2012*, pages 1–225, Apr. 2012.

[41] IEEE Standard for Local and metropolitan area networks - Part 15.6: Wireless Body Area Networks. *IEEE Std 802.15.6-2012*, pages 1–271, Feb. 2012.

[42] A. Reichman. Standardization of body area networks. In *Microwaves, Communications, Antennas and Electronics Systems, 2009. COMCAS 2009. IEEE International Conference on*, pages 1–4, Nov. 2009.

[43] Specification of the Bluetooth System version 4.0. *Bluetooth SIG*, June 2010.

[44] Bluetooth products. Website: http://www.bluetooth.com/Pages/Bluetooth-Smart-Devices.aspx, Oct. 2012.

[45] S. Tozlu. Feasibility of Wi-Fi enabled sensors for Internet of Things. In *Wireless Communications and Mobile Computing Conference (IWCMC), 2011 7th International*, pages 291–296, July 2011.

[46] IEEE 802.11 Std. *IEEE Local and metropolitan area networks - Specific requirements Part 11: Wireless LAN Medium Access Control (MAC) and Physical Layer (PHY) specifications.* IEEE, 2011.

[47] Wi-Fi Alliance. Website: http://www.wi-fi.org/.

[48] S. Folea and M. Ghercioiu. Ultra-low power wi-fi tag for wireless sensing. In *Automation, Quality and Testing, Robotics, 2008. AQTR 2008. IEEE International Conference on*, volume 3, pages 247–252, May 2008.

[49] ANT message protocol and usage. Available at: http://www.thisisant.com.

[50] WiserBAN - Smart miniature low-power wireless microsystem for Body Area Networks. Website: http://wiserban.eu/.

[51] A. El-Hoiydi and J.-D. Decotignie. Low power downlink MAC protocols for infrastructure wireless sensor networks. *Mobile Networks and Applications*, 10(5):675–690, Oct. 2005.

[52] M. Buettner, G.V. Yee, E. Anderson, and R. Han. X-MAC: a short preamble MAC protocol for duty-cycled wireless sensor networks. In *Proceedings of the 4th international conference on Embedded networked sensor systems*, SenSys '06, pages 307–320. ACM, 2006.

[53] L. Ouvry et al. BAN Upper Layers, Base Band and DSP Architecture Specification. WiserBAN Deliverable D4.1, Sep. 2011.

[54] N. Golmie, D. Cypher, and O. Rebala. Performance analysis of low rate wireless technologies for medical applications. *Computer Communications*, 28(10):1266–1275, June 2005.

[55] R.C. Shah and M. Yarvis. Characteristics of on-body 802.15.4 networks. In *Wireless Mesh Networks, 2006. WiMesh 2006. 2nd IEEE Workshop on*, pages 138 –139, Sept. 2006.

[56] H. Li and J. Tan. An ultra-low-power medium access control protocol for body sensor network. In *Engineering in Medicine and Biology Society, 2005. IEEE-EMBS 2005. 27th Annual International Conference of the*, pages 2451–2454, 2005.

[57] D.Yun, S.-E. Yoo, D. Kim, and D. Kim. OD-MAC: An on-demand MAC protocol for body sensor networks based on IEEE 802.15.4. In *Embedded and Real-Time Computing Systems and Applications, 2008. RTCSA '08. 14th IEEE International Conference on*, pages 413–420, Aug. 2008.

[58] R.C. Shah, L. Nachman, and C.-Y. Wan. On the performance of Bluetooth and IEEE 802.15.4 radios in a body area network. In *Proceedings of the ICST 3rd international conference on Body area networks*, BodyNets '08, pages 25:1–25:9. ICST (Institute for Computer Sciences, Social-Informatics and Telecommunications Engineering), 2008.

[59] M. Maman and L. Ouvry. BATMAC: An adaptive TDMA MAC for body area networks performed with a space-time dependent channel model. In *Proc. of IEEE ISMICT 2011*, pages 1–5, March 2011.

[60] S. Ullah, B. Shen, S. M. Riazul Islam, P. Khan, S. Saleem, and K. S. Kwak. A Study of Medium Access Control Protocols for Wireless Body Area Networks. *ArXiv e-prints*, Apr. 2010.

[61] A. El-Hoiydi and J.-D. Decotignie. WiseMAC: An Ultra Low Power MAC Protocol for Multi-hop Wireless Sensor Networks. In *Algorithmic Aspects of Wireless Sensor Networks*, volume 3121 of *Lecture Notes in Computer Science*, pages 18–31. Springer Berlin Heidelberg, 2004.

[62] W. Ye, J. Heidemann, and D. Estrin. Medium Access Control With Coordinated Adaptive Sleeping for Wireless Sensor Networks. *IEEE/ACM Transactions on Networking*, 12(3):493–506, June 2004.

[63] S. Ullah and L. Kwak. Performance Study of Low-power MAC Protocols for Wireless Body Area Networks. In *Body Area Networks - Enabling Technologies for Wearable and Implanable Body Sensors, 2010. IEEE PIMRC 2010 International Workshop on*, pages 111–115, Sept. 2010.

[64] M. Patel and D. Wang. Energy Efficient Methods of Encoding Destination Address to Address Overhearing Problem in BAN. In *Body Area Networks - Enabling Technologies for Wearable and Implanable Body Sensors, 2010. IEEE PIMRC 2010 International Workshop on*, Sept. 2010.

[65] S.J. Marinkovic, E.M. Popovici, C. Spagnol, S. Faul, and W.P. Marnane. Energy-Efficient Low Duty Cycle MAC Protocol for Wireless Body Area Networks. *Information Technology in Biomedicine, IEEE Transactions on*, 13(6):915–925, Nov. 2009.

[66] H. Li and J. Tan. Heartbeat-driven medium-access control for body sensor networks. *Information Technology in Biomedicine, IEEE Transactions on*, 14(1):44–51, Jan. 2010.

[67] H. Su and X. Zhang. Battery-dynamics driven TDMA MAC protocols for wireless body-area monitoring networks in healthcare applications. *Selected Areas in Communications, IEEE Journal on*, 27(4):424–434, May 2009.

[68] O. Omeni, A. Wong, A.J. Burdett, and C. Toumazou. Energy Efficient Medium Access Protocol for Wireless Medical Body Area Sensor Networks. *Biomedical Circuits and Systems, IEEE Transactions on*, 2(4):251–259, Dec. 2008.

[69] M. Al Ameen, N. Ullah, M.S. Chowdhury, SM R. Islam, and K. Kwak. A power efficient MAC protocol for wireless body area networks. *EURASIP Journal*, 2012(1):33, 2012.

[70] M.M. Alam, O. Berder, D. Menard, and O. Sentieys. TAD-MAC: Traffic-Aware Dynamic MAC Protocol for Wireless Body Area Sensor Networks. *Emerging and Selected Topics in Circuits and Systems, IEEE Journal on*, 2(1):109–119, March 2012.

[71] N. Thepvilojanapong, S. Motegi, A. Idoue, and H. Horiuchi. Adaptive channel and time allocation for body area networks. *Communications, IET*, 5(12):1637–1649, Dec. 2011.

[72] T. Halonen, J. Romero, and J. Melero. *GSM, GPRS and EDGE Performance*. John Wiley & Sons, Ltd., Oct. 2003.

[73] J. Zhang, K. Tan, J. Zhao, H. Wu, and Y. Zhang. A practical SNR-guided rate adaptation. In *INFOCOM 2008. The 27th Conference on Computer Communications. IEEE*, pages 2083–2091, Apr. 2008.

[74] S.H.Y. Wong, H. Yang, S. Lu, and V. Bharghavan. Robust rate adaptation for 802.11 wireless networks. In *ACM Mobicom*, pages 146–157, Sept. 2006.

[75] Q. Xia, X. Jin, and M. Hamdi. Cross layer design for the IEEE 802.11 WLANs: Joint rate control and packet scheduling. *Wireless Communications, IEEE Transactions on*, 6(7):2732–2740, July 2007.

[76] S. Lanzisera, A.M. Mehta, and K.S.J. Pister. Reducing average power in wireless sensor networks through data rate adaptation. In *Communications, 2009. ICC '09. IEEE International Conference on*, pages 1–6, June 2009.

[77] N. Bradai, S. Belhaj, L. Chaari, and L. Kamoun. Study of medium access mechanisms under IEEE 802.15.6 standard. In *Wireless and Mobile Networking Conference (WMNC), 2011 4th Joint IFIP*, pages 1–6, Oct. 2011.

[78] S. Ullah and K.S. Kwak. Throughput and delay limits of IEEE 802.15.6. In *Wireless Communications and Networking Conference (WCNC), 2011 IEEE*, pages 174–178, March 2011.

[79] S. Ullah, M. Chen, and K.S. Kwak. Throughput and Delay Analysis of IEEE 802.15.6-based CSMA/CA Protocol. *Journal of Medical Systems*, 36:3875–3891, 2012.

[80] C. Tachtatzis, F. Di Franco, D.C. Tracey, N.F. Timmons, and J. Morrison. An energy analysis of IEEE 802.15.6 scheduled access modes. In *GLOBECOM Workshops, 2010 IEEE*, pages 1270–1275, Dec. 2010.

[81] S. Rashwand, J. Misic, and H. Khazaei. IEEE 802.15.6 under saturation: Some problems to be expected. *Communications and Networks, Journal of*, 13(2):142–148, Apr. 2011.

[82] B.H. Jung, R.U. Akbar, and D.K. Sung. Throughput, Energy Consumption, and Energy Efficiency of IEEE 802.15.6 Body Area Network (BAN) MAC Protocol. In *Personal Indoor and Mobile Radio Communications (PIMRC), 2012 IEEE 23nd International Symposium on*, pages 600–605, Sept. 2012.

[83] R. de Francisco, L. Huang, and G. Dolmans. Coexistence of WBAN and WLAN in Medical Environments. In *Vehicular Technology Conference Fall (VTC 2009-Fall), 2009 IEEE 70th*, pages 1–5, Sept. 2009.

[84] C. Chen and C. Pomalaza-Raez. Design and Evaluation of a Wireless Body Sensor System for Smart Home Health Monitoring. In *Global Telecommunications Conference, 2009. GLOBECOM 2009. IEEE*, pages 1–6, Dec. 2009.

[85] H. Huo, Y. Xu, C.C. Bilen, and H. Zhang. Coexistence Issues of 2.4GHz Sensor Networks with Other RF Devices at Home. In *Sensor Technologies and Applications, 2009. SENSORCOMM '09. Third International Conference on*, pages 200–205, June 2009.

[86] W. Yuan, X. Wang, J.-P.M.G. Linnartz, and I.G.M.M. Niemegeers. Experimental Validation of a Coexistence Model of IEEE 802.15.4 and IEEE 802.11b/g Networks. *International Journal of Distributed Sensor Networks*, 2010.

[87] W. Yuan, X. Wang, and J.-P.M.G. Linnartz. A Coexistence Model of IEEE 802.15.4 and IEEE 802.11b/g. In *Communications and Vehicular Technology in the Benelux, 2007 14th IEEE Symposium on*, pages 1–5, Nov 2007.

[88] I. Ashraf, A. Gkelias, K. Voulgaris, M. Dohler, and A.H. Aghvami. Co-existence of CSMA/CA and Bluetooth. In *Communications, 2006. ICC '06. IEEE International Conference on*, volume 12, pages 5522–5527, June 2006.

[89] I. Ashraf, K. Voulgaris, A. Gkelias, M. Dohler, and A.H. Aghvami. Impact of Interfering Bluetooth Piconets on a Collocated p-Persistent CSMA-Based WLAN. *Vehicular Technology, IEEE Transactions on*, 58(9):4962–4975, Nov. 2009.

[90] E. Reusens, W. Joseph, G. Vermeeren, D. Kurup, and L. Martens. Real human body measurements, model, and simulations of a 2.45 GHz wireless body area network communication channel. In *Medical Devices and Biosensors, 2008. ISSS-MDBS 2008. 5th International Summer School and Symposium on*, pages 149–152, June 2008.

[91] 15-09-0329-01-0006-medwin-physical-layer-proposal-documentation. Available at: https://mentor.ieee.org/802.15/documents, Nov. 2009.

[92] C. Gezer, C. Buratti, and R. Verdone. Capture effect in IEEE 802.15.4 networks: Modelling and experimentation. In *IEEE International Symposium on Wireless Pervasive Computing, IEEE ISWCP 2010*, pages 204–209, Modena, Italy, May 2010.

[93] Channel Model for Body Area Network. Available at: https://mentor.ieee.org/802.15/documents, Sept. 2010.

[94] 15-10-0245-06-0006-tg6-draft. Available at: https://mentor.ieee.org/802.15/documents, May 2010.

[95] V. Tralli and R. Verdone. Performance characterization of digital transmission systems with cochannel interference. *Vehicular Technology, IEEE Transactions on*, 48(3), May 1999.

[96] M. Maman, F. Dehmas, R. D'Errico, and L. Ouvry. Evaluating a TDMA MAC for body area networks using a space-time dependent channel model. In *Personal, Indoor and Mobile Radio Communications, 2009, IEEE 20th International Symposium on*, pages 2101–2105, Sept. 2009.

[97] R. Rosini and R. D'Errico. Comparing on-body dynamic channels for two antenna designs. In *Loughborough Antenna and Propagation Conference 2012, LAPC 2012*, Nov. 2012.

[98] R. D'Errico et al. Final report on the antenna-human body interactions, around-the-body propagation. WiserBAN Deliverable D3.1, Sept. 2011.

[99] L.J. Chu. Physical limitations of omni-directional antennas. *Journal of Applied Physics*, 19(12):1163–1175, 1948.

[100] M. Goyal, S. Prakash, W. Xie, Y. Bashir, H. Hosseini, and A. Durresi. Evaluating the impact of signal to noise ratio on IEEE 802.15.4 PHY-level packet

loss rate. In *Network-Based Information Systems (NBiS), 13th International Conference on*, pages 279–284, Sept. 2010.

[101] Texas Instruments. Website: http://www.ti.com/product/cc2530.

[102] Wireshark. Website: http://www.wireshark.org.

[103] Freescale. Website: http://www.freescale.com.

[104] Daintree. Website: http://www.daintree.net/sna/sna.php.

[105] D. Stoyan, W.S. Kendall, and J. Mecke. *Stochastic geometry and its applications*. Wiley series in probability and mathematical statistics. J. Wiley, 1995.

[106] M. Haenggi, J.G. Andrews, F. Baccelli, O. Dousse, and M. Franceschetti. Stochastic geometry and random graphs for the analysis and design of wireless networks. *IEEE Journal on Selected Areas in Communications*, 27(7):1029–1046, sept. 2009.

[107] X. Yang and A.P. Petropulu. Co-channel interference modeling and analysis in a poisson field of interferers in wireless communications. *Signal Processing, IEEE Transactions on*, 51(1):64–76, Jan. 2003.

[108] A. Rabbachin, T.Q.S. Quek, Hyundong Shin, and M.Z. Win. Cognitive network interference. *Selected Areas in Communications, IEEE Journal on*, 29(2):480–493, Feb. 2011.

[109] P.C. Pinto, A. Giorgetti, M.Z. Win, and M. Chiani. A stochastic geometry approach to coexistence in heterogeneous wireless networks. *Selected Areas in Communications, IEEE Journal on*, 27(7):1268–1282, Sept. 2009.

[110] F. Xue and P.R. Kumar. On the θ-coverage and connectivity of large random networks. *Networking, IEEE/ACM Transactions on*, 14(4):675–682, Aug. 2006.

[111] J. Orriss and S.K. Barton. Probability distributions for the number of radio transceivers which can communicate with one another. *Communications, IEEE Transactions on*, 51(4):676–681, Apr. 2003.

[112] F. Fabbri and R. Verdone. A statistical model for the connectivity of nodes in a multi-sink wireless sensor network over a bounded region. In *Wireless Conference, 2008. EW 2008. 14th European*, pages 1–6, June 2008.

[113] K. Gulati, A. Chopra, B.L. Evans, and K.R. Tinsley. Statistical modeling of co-channel interference. In *Global Telecommunications Conference, 2009. GLOBECOM 2009. IEEE*, pages 1–6, Dec. 2009.

[114] M.Z. Win, P.C. Pinto, and L.A. Shepp. A mathematical theory of network interference and its applications. *Proceedings of the IEEE*, 97(2):205–230, Feb. 2009.

[115] M. Haenggi and R. K. Ganti. *Interference in Large Wireless Networks*, volume 3. Foundations and Trends in Networking, 2009.

[116] H.Q. Nguyen, F. Baccelli, and D. Kofman. A stochastic geometry analysis of dense IEEE 802.11 networks. In *INFOCOM 2007. 26th IEEE International Conference on Computer Communications. IEEE*, pages 1199–1207, May 2007.

[117] R. Verdone, F. Fabbri, and C. Buratti. Maximizing area throughput in clustered wireless sensor networks. *Selected Areas in Communications, IEEE Journal on*, 28(7):1200–1210, Sept. 2010.

[118] M. Kaynia, F. Fabbri, R. Verdone, and G.E. Oien. Analytical study of the outage probability of ALOHA and CSMA in bounded ad hoc networks. In *Wireless Conference (EW), 2010 European*, pages 544–550, Apr. 2010.

[119] C. Buratti and R. Verdone. Performance analysis of IEEE 802.15.4 non beacon-enabled mode. *Vehicular Technology, IEEE Transactions on*, 58(7):3480–3494, Sept. 2009.

[120] J. Misic, S. Shafi, and V. B. Misic. Maintaining reliability through activity management in an 802.15.4 sensor cluster. *Vehicular Technology, IEEE Transactions on*, 55(3):779–788, May 2006.

[121] S. Pollin, M. Ergen, S.C. Ergen, B. Bougard, L. Van der Pierre, F. Catthoor, I. Moerman, A. Bahai, and P. Varaiya. Performance analysis of slotted carrier sense IEEE 802.15.4 medium access layer. *Wireless Communications, IEEE Transactions on*, 7(9):3359–3371, Sept. 2008.

[122] Z. Chen, C. Lin, H. Wen, and H. Yin. An analytical model for evaluating IEEE 802.15.4 CSMA/CA protocol in low rate wireless application. In *Proc. Int. Conf. Advanced Information Networking and Applications Workshops (AINAW 2007)*, pages 899–904, May 2007.

[123] M. Martalò, S. Busanelli, and G. Ferrari. Markov chain-based performance analysis of multihop IEEE 802.15.4 wireless networks. *Elsevier Performance Evaluation*, 66(12):722–741, Dec. 2009.

[124] C. Buratti. A mathematical model for performance of IEEE 802.15.4 beacon-enabled mode. In *Proc. of Int. Conf. on Wireless Communications and Mobile Computing (IWCMC 2009)*, pages 1184–1190, June 2009.

[125] R. L. Streit. The poisson point process. In *Poisson Point Processes*, pages 11–55. Springer US, 2010.

[126] A. Zanella, M. Stramazzotti, F. Fabbri, E. Salbaroli, D. Dardari, and R. Verdone. Comments on "Probability distributions for the number of radio

transceivers which can communicate with one another". *Communications, IEEE Transactions on*, 57(5):1287–1289, May 2009.

[127] A. Papoulis. *Probability, Random Variables and Stochastic Processes*. McGraw-Hill, New York, NY, USA, 1991.

[128] R.C. Shah, S. Roy, S. Jain, and W. Brunette. Data MULEs: modeling a three-tier architecture for sparse sensor networks. In *Sensor Network Protocols and Applications, 2003. Proceedings of the First IEEE. 2003 IEEE International Workshop on*, pages 30–41, May 2003.

[129] D. Kotz and K. Essien. Analysis of a campus-wide wireless network. *Wirel. Netw.*, 11(1-2):115–133, Jan. 2005.

[130] M. McNett and G.M. Voelker. Access and mobility of wireless PDA users. *SIGMOBILE Mob. Comput. Commun. Rev.*, 9(2):40–55, Apr. 2005.

[131] I. Rhee, M. Shin, S. Hong, K. Lee, and S. Chong. Human Mobility Patterns and Their Impact on Routing in Human-Driven Mobile Networks. In *Proceedings of the Sixth Workshop on Hot Topics in Networks (HotNets-VI)*, Nov. 2007.

[132] M.C. Gonzales, C.A. Hidalgo, and A.-L. Barabasi. Understanding individual human mobility patterns. *Nature*, 453:779–782, Mar. 2008.

[133] S. Isaacman, R. Becker, R. Caceres, S. Kobourov, M. Martonosi, J. Rowland, and A. Varshavsky. Ranges of human mobility in los angeles and new york. In *Pervasive Computing and Communications Workshops (PERCOM Workshops), 2011 IEEE International Conference on*, pages 88–93, Mar. 2011.

[134] N. Eagle. Using Mobile Phones to Model Complex Social Systems. *O'Reilly Network*, June 2005.

[135] A. Chaintreau, P. Hui, J. Crowcroft, C. Diot, R. Gass, and J. Scott. Pocket switched networks: real-world mobility and its consequences for opportunistic forwarding. Technical report, University of Cambridge, Computer Laboratory, Feb. 2005.

[136] P. Hui, A. Chaintreau, J. Scott, R. Gass, J. Crowcroft, and C. Diot. Pocket switched networks and human mobility in conference environments. In *Proceedings of the 2005 ACM SIGCOMM workshop on Delay-tolerant networking*, WDTN '05, pages 244–251, New York, NY, USA, 2005. ACM.

[137] J. Leguay, A. Lindgren, J. Scott, T. Friedman, and J. Crowcroft. Opportunistic content distribution in an urban setting. In *Proceedings of the 2006 SIGCOMM workshop on Challenged networks*, CHANTS '06, pages 205–212, New York, NY, USA, 2006. ACM.

[138] A. Natarajan, M. Motani, and V. Srinivasan. Understanding urban interactions from bluetooth phone contact traces. In *Proceedings of the 8th international conference on Passive and active network measurement*, PAM'07, pages 115–124, Berlin, Heidelberg, 2007. Springer-Verlag.

[139] L. Vu, K. Nahrstedt, S. Retika, and I. Gupta. Joint bluetooth/wifi scanning framework for characterizing and leveraging people movement in university campus. In *Proceedings of the 13th ACM international conference on Modeling, analysis, and simulation of wireless and mobile systems*, MSWIM '10, pages 257–265. ACM, 2010.

[140] S. Gaito, E. Pagani, and G.P. Rossi. Opportunistic forwarding in workplaces. In *Proceedings of the 2nd ACM workshop on Online social networks*, WOSN '09, pages 55–60, New York, NY, USA, 2009. ACM.

[141] D. Karamshuk, C. Boldrini, M. Conti, and A. Passarella. Human mobility models for opportunistic networks. *Communications Magazine, IEEE*, 49(12):157–165, Dec. 2011.

[142] Inmaculada B. Aban, Mark M. Meerschaert, and Anna K. Panorska. Parameter estimation for the truncated pareto distribution. *Journal of the American Statistical Association*, 101, 2006.

[143] K. Lee, S. Hong, S.J. Kim, I. Rhee, and S. Chong. Demystifying levy walk patterns in human walks. Technical report, NCSU, Computer Science Department, 2008.

[144] I. Rhee, M. Shin, S. Hong, K. Lee, and S. Chong. On the levy-walk nature of human mobility. In *INFOCOM 2008. The 27th Conference on Computer Communications. IEEE*, pages 924–932, Apr. 2008.

[145] T. Karagiannis, J.-Y. Le Boudec, and M. Vojnovic and. Power law and exponential decay of intercontact times between mobile devices. *Mobile Computing, IEEE Transactions on*, 9(10):1377–1390, Oct. 2010.

[146] A. Natarajan, M. Motani, and V. Srinivasan. Understanding urban interactions from bluetooth phone contact traces. In *Proceedings of the 8th international conference on Passive and active network measurement*, PAM'07, pages 115–124, Berlin, Heidelberg, 2007. Springer-Verlag.

[147] J. Ghosh, S.J. Philip, and C. Qiao. Sociological orbit aware location approximation and routing (SOLAR) in MANET. *Ad Hoc Networks*, 5(2):189–209, 2007.

[148] Q. Zheng, X. Hong, J. Liu, D. Cordes, and W. Huang. Agenda driven mobility modelling. *Int. J. Ad Hoc Ubiquitous Comput.*, 5(1):22–36, Dec. 2010.

[149] C. Boldrini and A. Passarella. HCMM: Modelling spatial and temporal properties of human mobility driven by users' social relationships. *Computer Communications*, 33(9):1056–1074, 2010.

[150] A. Vahdat and D. Becker. Epidemic routing for partially-connected ad hoc networks. Technical report cs-200006, Duke University, Apr. 2000.

[151] T. Spyropoulos, K. Psounis, and C.S. Raghavendra. Efficient routing in intermittently connected mobile networks: the multiple-copy case. *IEEE/ACM Trans. Netw.*, 16(1):77–90, Feb. 2008.

[152] A. Lindgren, A. Doria, and O. Schelén. Probabilistic routing in intermittently connected networks. *SIGMOBILE Mob. Comput. Commun. Rev.*, 7(3):19–20, July 2003.

[153] L. Vu, Q. Do, and K. Nahrstedt. 3R: Fine-grained encounter-based routing in Delay Tolerant Networks. In *World of Wireless, Mobile and Multimedia Networks (WoWMoM), 2011 IEEE International Symposium on a*, pages 1–6, June 2011.

[154] P. Hui, J. Crowcroft, and E. Yoneki. BUBBLE Rap: Social-Based Forwarding in Delay-Tolerant Networks. *Mobile Computing, IEEE Transactions on*, 10(11):1576–1589, Nov. 2011.

[155] E.M. Daly and M. Haahr. Social Network Analysis for Information Flow in Disconnected Delay-Tolerant MANETs. *Mobile Computing, IEEE Transactions on*, 8(5):606–621, May 2009.

[156] R. Verdone and F. Fabbri. Sociability based routing for environmental opportunistic networks. *Journal of Advances in Electronics and Telecommunications, Poznan University of Technology*, 1, Apr. 2010.

[157] F. Fabbri and R. Verdone. A sociability-based routing scheme for delay-tolerant networks. *EURASIP Journal on Wireless Communications and Networking*, 2011:1–13, Jan. 2011.

[158] Y. Zhu, B. Xu, X. Shi, and Y. Wang. A Survey of Social-based Routing in Delay Tolerant Networks: Positive and Negative Social Effects. *Communications Surveys Tutorials, IEEE*, PP(99):1–15, 2012.

[159] S. Wasserman and K. Faust. *Social Network Analysis – Methods and Applications*. Structural Analysis in the Social Sciences. Cambridge Univeristy Press, 1995.

Acknowledgements

"I would maintain that thanks are the highest form of thought, and that gratitude is happiness doubled by wonder." [G.K. Chesterton]

This works has been possible only thanks to the support of so many people that a second thesis would be necessary to include them all with motivations.

First of all, I would like to express my deepest and sincere gratitude to my supervisor, Prof. Roberto Verdone, for his constant and caring guidance, and to my Tutor, Prof. Oreste Andrisano. Special thanks to the reviewers who were very helpful with their detailed and fruitful comments: Dr. Mischa Dohler and Dr. Alex Gluhak. To the latter, double thanks are owed, because of his really welcoming reception and valuable supervision during my semester at CCSR. I would also like to thank all the researchers I met within WiserBAN project and Cost Actions, especially Raffaele D'Errico and Mickael Maman.

I am thankful towards all my colleagues, the "old" and the "new" ones. Thank you Chiara for your patience with me as your office-mate and collaborator. Thank you Ramona for sharing all these PhD months, the good and the bad moments, inside and outside the office, even remotely, as a true friend does. Thank you Giorgia for your always present smile and because lately you are forcing to care about us also outside work. Thank you Danilo for having been kind and available for suggestions even before becoming my boss. Thank you Riccardo for being our biographies expert. Thank you Andrea for your warming laughs. Thank you Stefan for all your coolest and strangest things ever. Thank you Raffaele for your jokes, I am missing them so much. Thank you Silvia for your help with documents and administrative stuff

Acknowledgements

during the first years, but mainly for being always direct and motivating. Thank you Cengiz for all the chats and the nice walks we had together. Thank you Francesco, Flavio, Andrea, Virginia. Thanks to Davide, Francesca, Gianpiero, Giacomo, and all the people I met within CSITE and the new Telecommunications Labs for being good office neighbours and lunch companions.

I really wish to thank all the people I met in Surrey, everyone contributed to make my semester there an incredible and unforgettable experience. Thanks to CCSR workers and in particular to the volunteers who (more or less freely) agreed on participating to the experiments described in the last chapter of this thesis. Thank you Michele and Amir for having been very friendly and helpful since the beginning. Thanks to the Economy Department, which became my second home: Matteo, Diana, Marco, Apostolos, Marcelo... I will not repeat here the motivations of my deep gratitude towards you all because I do not want to start crying again. Thank you Elisabetta for all the chats we had for a couple of months as if we had known each other for ages. Thank you Pasquale and Lucia for the nice moments we spent together in the always amazing London.

I owe truly sincere thanks to all my friends, who helped me surviving even after so many hours spent in front of the computer or lost in impossible calculus. Chiara, Giulia, and Francesca, you really are the proof that "Whoever finds a friend has found a treasure"; and I am lucky since I have found three. Thank you Valeria for being more than a friend and more than a PhD colleague at the same time, it is nice to reach also this goal with you, but let us promise each other that the PhD will be the last one, ok? Dani, Laura, Milly, Sara, Luca, thank you for being still here (even remotely) after so many years. Thanks to all the Saint Mary's babies (and coaches), because playing with you is always the best way to let off steam. Thanks to my kummi family, to Maciej, and to all the others from Finland: even if distance keeps us physically apart, it is nice to have friends around Europe. Thank you Francesca, Chiara, Silvia, Veronica, Francesca, Den, Enrico, Riqui, Elisa, Roberto, and every other person I am forgetting to cite in this moment.

Last but not least, I would like to thank my family, for the support they have given me during all these years: Mum, Grandma, Grandpa, Dad, Anna, Bibi, Lucio, Elena, and, most important of all, my not-so-little-anymore Edoardo, who, probably unwitting, gave me the best comforting moments during the thesis stress period, always reminding me that Life finds wonderful ways to carry on.